Electronic Thesis and Dissertation Repository

12-6-2017 10:30 AM

Design, Implementation And Control Of A Robotic Platform For Post-Stroke Upper- And Lower-Limb Rehabilitation

Vahid Mehrabi, *The University of Western Ontario*

Supervisor: Patel, Rajni, *The University of Western Ontario*
Co-Supervisor: Talebi, Heidar A., *The University of Western Ontario*
A thesis submitted in partial fulfillment of the requirements for the Master of Science degree in Biomedical Engineering
© Vahid Mehrabi 2017

Follow this and additional works at: https://ir.lib.uwo.ca/etd

Part of the Biomedical Devices and Instrumentation Commons

Recommended Citation

Design, Implementation and Control of a Robotic Platform for Post-Stroke Upper- and Lower-Limb Rehabilitation

Vahid Mehrabi
M.Sc. Thesis, 2017
Biomedical Engineering Graduate Program
The University of Western Ontario

Abstract

Stroke is the primary cause of permanent disabilities worldwide. Hemiparesis and hemiplegia (the most common consequences of stroke) are the decreases in motor-functionality of the brain on one side of the body which will affect the daily life activities of the patient. There are several challenges with the current state of delivering rehabilitation services such as limitations on the number of the clinics, financial resources needed for providing rehabilitation, associated costs of transportation, and human resources. To overcome the issues related to conventional ways of delivering therapy, different robotic systems have been developed to benefit healthcare systems and patient with disabilities. Although various devices have been developed for rehabilitation on either upper or lower extremity, there is no robotic system in the market for physical rehabilitation on both upper and lower limbs. Developing such devices is useful particularly in the case of hemiparesis as the rehabilitation process can be performed on both upper and lower limbs using the same device. This thesis represents the design process, manufacturing, and control of a novel robotic rehabilitation device for delivering post-stroke therapy on both lower and upper extremities. This portable, lightweight, inherently safe robot has five degrees of freedom, and its mechanical characteristics are modifiable to suit different modes of therapy. An ethics application was submitted and approved by the Western University Ethics Board to validate the functionality of the device by performing experiments on healthy participants. The proposed robot has been manufactured, verified through the experimental tests and been tested on the healthy subjects.

Keywords Robotic Rehabilitation, Stroke Rehabilitation, Multi Degrees-of-freedom Robot, Inherently Safe Mechanisms, Mathematical Modeling, Experimental Trial.

Dedicated to:

My lovely parents, my brother and sister for their help and support throughout my life.

Acknowledgements

Contents

List of Figures

List of Tables

Nomenclature and Acronyms

Latin Symbols

C_G	Global coordinate system assigned to the working mat
C_R	Local coordinate system assigned in the centre of the base plate
C_{SL}	Local coordinate system assigned in the centre of the left ADNS sensor
C_{SR}	Local coordinate system assigned in the centre of the right ADNS sensor
F_max	Maximum force applied by each wheel in the design "A"
F_W	Force applied by each wheel in the design "A"
O_S	Location of the ADNS sensors
P_S	Minimum power required
$\vec{r}_S$	The position vector of the local coordinate system of each ADNS sensors
r_w	Radius of the wheels in mobile base
$\vec{R}_k$	Position vector of contact point of wheel "k" in C_R
R_P	Distance between contact point of the wheels and the dome in design "A"
$R(\theta + \phi)$	Rotation matrix of ADNS sensor coordinate systems with respect to C_G
T	Minimum output torque for LE ankle rehabilitation
$\mathbf{T}_k$	Transformation matrix
T_Y	Generated torque in Roll direction

T_X	Generated torque in Pitch direction
v_x	velocity of the robot along "x" in C_R
v_y	velocity of the robot along "y" in C_R
V_{W_k}	Velocity of the wheel "k" in design "A"

Greek Symbols

α	Orientation of sensor
ω	Minimum angular velocity of the ankle rehabilitation
ω_k	Angular velocity of the wheel "k" of the mobile platform
ω_z	Angular velocity of the robot in "z" direction of C_R
$\omega_W k$	Angular velocity of the wheel "k" in design "A"
Ω	Angular velocity of the dome in design "A"
Ω_k	Contribution of the wheel "k" in angular velocity of the dome in design "A"
ψ_S	The angle between each $\vec{r}_S$ and the "x" axis of the C_R
ϕ_S	The angle between "x" axis of each C_S and the "x" axis of the C_R
$\vec{\Delta}_{OS}^S$	Vector of incremental displacement measurements of ADNS sensors
ΔX_{SL}	Incremental displacement measurement of the left ADNS sensor in "x" direction of C_{SL}
ΔX_{SR}	Incremental displacement measurement of the right ADNS sensor in "x" direction of C_{SR}
ΔY_{SL}	Incremental displacement measurement of the left ADNS sensor in "y" direction of C_{SL}
ΔY_{SR}	Incremental displacement measurement of the right ADNS sensor in "y" direction of C_{SR}
Δu	Incremental displacement of the O_R with respect to C_G
θ	Angle between "x" axis of C_R and "x" axis of C_G
θ_k	Angle between $\vec{R}_k$ and "x" axis of C_R
Θ_X	Angular orientation of the dome in Roll direction

Θ_Y Angular orientation of the dome in Pitch direction

Acronyms

2-D   Two-Dimensional

3-D   Three-Dimensional

ADC   Analog to Digital Converter

ADL   Activity of Daily Living

AMHEF/H   Active Mobile End-effector Foot-plate/Handle-grip

CAD   Computer Aided Design

CAN   Controller Area Network

DAQ   Data Acquisition

DOF   Degrees of Freedom

EMG   Electromyography

I2C   Inter-Integrated Circuit

LE   Lower Extremity

LLRR   Lower Limb Rehabilitation Robots

LPU   Local Processing Unit

MMCE   Mathematical Modeling, Control and Experiments

NMT   Network Management

PCB   Printed Circuit Board

PDO   Process Data Object

PTM   Power Transmission Mechanism

PTR   Power Transmission Ratio

ROI   Report Of Invention

RPI   Raspberry PI

SCI   Spinal Cord Injuries

SDO   Service Data Object

SPI   Serial Peripheral Interface

UART   Universal Asynchronous Receiver/Transmitter

UDP   User Datagram Protocol

UI   User Interface

UE   Upper Extremity

WEDM   Wire Electron Discharge Machining

Chapter 1

Introduction

1.1 Introduction

According to the World Health Organization (WHO), stroke is "a clinical syndrome typified by rapidly developing signs of focal or global disturbance of cerebral functions lasting more than 24 hours or leading to death, with no apparent causes other than of vascular origin" [27]. A stroke happens when brain cells die when they do not receive oxygen because of interruption in blood circulation to the brain. The symptoms of stroke are: (a) numbness or weakness, (b) sudden problem in speaking and speech recognition, (c) sudden problem with vision, and (d) sudden issues with walking or loss of balance [28]. It is estimated that about 15 million people suffer from stroke each year worldwide. In addition, five million stroke survivors experience permanent motor disabilities and require therapeutic services [29]. This means that stroke is the leading cause of permanent disability in developed countries [30]. This trend results in a high burden on healthcare systems and families of health care providers [29]. The majority of stroke survivors require assistance in activities of daily living (ADL) and experience different levels of disability [31].

The two major consequences of stroke are hemiplegia and hemiparesis. According to the website of the National Stroke Association (NSA) of the United States,

1

"Hemiplegia is a paralysis that affects one side of the body. It is often diagnosed as either the right or left hemiplegia, depending on which side of the body is affected. As many as 9 out of 10 stroke survivors have some degree of paralysis immediately following a stroke [32]."

Hemiparesis occurs when one side of the body is weakened and is the most common consequence of stroke. According to the website of the NSA,

"Hemiparesis or one-sided ("hemi") weakness (paresis) affects about 8 out of 10 stroke survivors, causing weakness or the inability to move one side of the body. One-sided weakness can affect your arms, hands, legs and facial muscles. If you have one-sided weakness you may have trouble performing everyday activities such as eating, dressing, and using the bathroom. Rehabilitation treatments, exercises at home, and assistive devices can help with your mobility and recovery [32]."

Experiencing weakness in one side of the body will result in: (a) difficulties in grasping objects, (b) loss of balance and walking difficulties, (c) muscle fatigue, and (d) lack of coordination. Although, hemiplegia and hemiparesis are serious disabilities, rehabilitation, physical and occupational therapies can assist patients to regain some of their motor skills and increase their mobility.

1.1.1 Post-Stroke Physical Rehabilitation

A common regime of treatment is through motor rehabilitation therapies where a therapist interacts with a patient to provide various types of kinesthetic exercises. The goal is to initiate neuromuscular recovery in addition to preventing joint stiffening and pain related to the lack of sufficient mobility. It has been shown that these therapy exercises have a desirable effect on the recovery of the patients especially in cases where a therapy procedure is initiated in the first 6 months after paralysis and is delivered for a minimum amount of time [30]. In addition it has been shown that early involvement in rehabilitation therapies can significantly accelerate the recovery procedure [24]. This indicates that to make the therapy process fast and effective for the patient,

the rehabilitation process should start right after the stroke incident. Such therapies include (a) passive movement therapy, (b) interactive kinesthetic therapy, and (c) functional therapy.

The goal of rehabilitation is to prevent joint stiffening and pain through combining the physical self-actuated muscle movement by patients added to the therapist-guided joint movement right after experiencing stroke [30]. This physical rehabilitation process can strengthen the damaged cerebral tissues to regain lost motor functionality of the body after stroke [33, 34]. During the initial stages of therapy, although patients show some improvement in the recovery of motor skills, the gains achieved in motor functionality are limited [35]. It has been shown that the two factors, (a) initiation time of the therapy and (b) focusing on functional tasks such as walking and grasping have significant impact on decreasing the recovery time and more effective recovery of their motor functionality [24, 36, 37].

In physical and occupational therapy, the goal is to increase flexibility, strength, coordination, motor control and endurance of the muscles [38]. During this process the therapist guides the patient in performing movements, doing stretching exercises and teaching movement strategies [39]. The first step of rehabilitation therapy starts within 48 hours of the stroke. As the weakness is severe in the initial stages, the patients are encouraged to change positions frequently to engage in passive and active movement exercises. In passive exercises, the motion is performed by the therapist whereas in active exercises, self-actuation of muscles performed by the patient creates the motion [40]. Depending on the severity of the impairment, the position of the patient while performing the exercises can be a bed, a chair, a standing position or walking with no assistance. The therapist helps the patient to recover faster through sets of simple exercises to more complex ones such as bathing, dressing or walking to be able to perform activities of daily living. This rehabilitation process may take from months to years depending on the level of impairment, timing and duration of therapy sessions, therapist's experience and patient's motivation through out the process.

Rehabilitation movement therapy can be categorized based on the part of the body involved. For the lower limb, the exercises are more towards walking, standing and stretching the leg, while

for the upper limb, reaching and grasping objects are practiced during the therapy sessions. Figure 1.1 shows a therapist practicing with a patient on how to grasp an object. For the case of shoulder and hip, the concept of the exercises is the same since the types of the joint in both cases are similar. This can also be extended to case of wrist and ankle rehabilitation since the movements are flexion/extension, pronation/supination and inversion/eversion [41].

Figure 1.1: Therapy exercise on UE for grasping an object [1]

1.1.2 Conventional Therapy Challenges

There are several challenges with the current state of delivering rehabilitation services such as limitations on the number of the clinics, financial resources needed for providing rehabilitation, associated costs of transportation, and human resources [42]. In addition to that, uneven distribution of resources, lack of knowledge and insufficient insurance coverage limit the access of patients to rehabilitation services [43]. The aforementioned challenges can result in (a) excessive delays in initiating rehabilitation regimes, and (b) limited duration in which a patient can receive supervised therapy. For the case of Lower Extremity (LE) rehabilitation, the situation is even more challenging. For example, due to the relatively high weight and possible excessive rigidity of the lower limb following a stroke, it is sometimes even required to have multiple therapists collaboratively assisting a patient to perform an exercise as shown in Fig. 1.2. This increases the cost of the therapy and may necessitate more manpower. Some other issues associated with performing the

therapy at clinics are the limitation of the clinic facilities and the cost and discomfort related to transportation to clinics [42]. In addition to the above mentioned issues, it has been shown that in order to achieve the best and fastest results from therapy sessions, the rehabilitation process should start in the early stages after stroke. Therefore it is important to overcome the above mentioned challenges as much as possible so patients can have access to therapy sessions and facilities. Apart from various methods such as cortical stimulation, it is suggested that assistive devices can also be used to increase the strength and the control of the movement of an impaired limb.

Figure 1.2: Therapy procedure for gait training performed by three therapists in a manual assistance process [2].

1.2 Robotic Rehabilitation

To overcome the previously mentioned issues associated with the conventional ways of delivering therapy, different robotic systems have been developed to benefit both the healthcare systems and the people with disabilities [44–46]. Several studies have been performed to measure the outcome

of these robotic systems in comparison to that of the conventional therapy methods [47–53].

The most important component for improving the functionality and motor skill learning after stroke is task-specific practices and repetitions, this is where robotic devices play an important role as these systems are ideally suited for repetitive tasks. The main advantages of the robotic application in motor function training are: (a) reducing the cost of the rehabilitation process, (b) enabling home and self training and (c) enabling modification for different therapy applications.

There are four types of robotic configuration for application of upper and lower limbs, (a) end-effector based, (b) programmable foot-plates, (c) exoskeleton and (d) mobile base robots [3]. Various types of robotic systems for the lower and upper limb rehabilitation are shown in Fig. 1.3.

Each of these configurations have some advantages and disadvantages in rehabilitation application. For example, end-effector and mobile types robots provide design simplicity, flexibility in the actuation mechanism and wide range of motion (working volume). However, applying specific isolated movement to a particular joint is difficult in this type of robots as the motion generated by these robots is complex.

To independently and concurrently control the movement of the joints, exoskeleton type of robots are the best option. However, to ensure the proper movement at each joint from patient to patient, the length of the links should be adjustable which adds up to the setting up time and the complexity of the device. Additionally, the complexity of the joint movement in the case of the hip and shoulder, makes the design of the exoskeleton type robots challenging [54]. Additionally, as the exoskeleton robots are attached to the limb of the patient through different points, the control algorithms and mechanical complexity of this type of robots are significantly high to ensure the safety of the patients [46].

For each configuration and concept of operation on upper or lower limbs, several robotic systems have been developed. Some notable examples of the end-effector type robotic systems for the upper-limb application are, (a) MIT-MANUS [4], (b) the ACRE [5], (c) NeReBot [6], and Re-oGo [7]. In comparison to the end-effector type, exoskeleton type robots, such as CADEN-7 [8], PURPERT IV [9], ARMin III [10] and ArmeoPower (commercially available version of ARMin
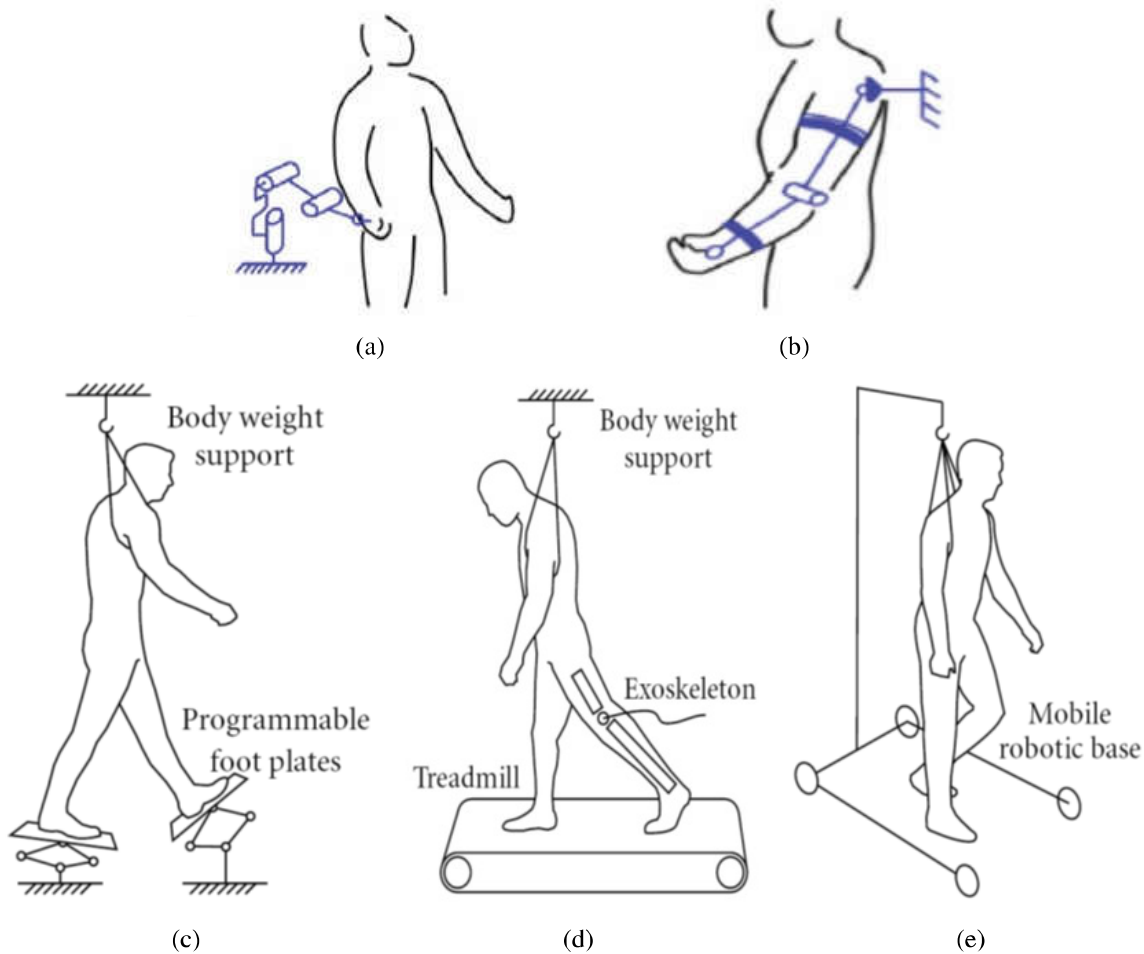
Figure 1.3: Various configuration of the LE and UE robotic systems (a) end-effector type for UE, (b) exoskeleton type for UE, (c) end-effector type for LE, (d) exoskeleton type for LE, and (e) mobile base for LE [3].

for upper extremity applications have attracted more attention in the literature. Fig. 1.4 and Fig. 1.5 show the above mention robotic systems that have been developed for robotic rehabilitation on upper extremity, with the end-effector and exoskeleton structure respectively.

MIT-MANUS is a planar end-effector type robot introduced by Interactive Motion Technologies, Inc. for delivering physical rehabilitation on upper limbs [4]. MIT-MANUS is a two DOF commercially available robot for therapeutic rehabilitation on upper limb as shown in Fig 1.4(a).

Lower Limb Rehabilitation Robots (LLRR) can assist patients and therapist with (a) gait training, (b) various joint movement or (c) exercising leg muscles. Lower limb robotic systems devel-
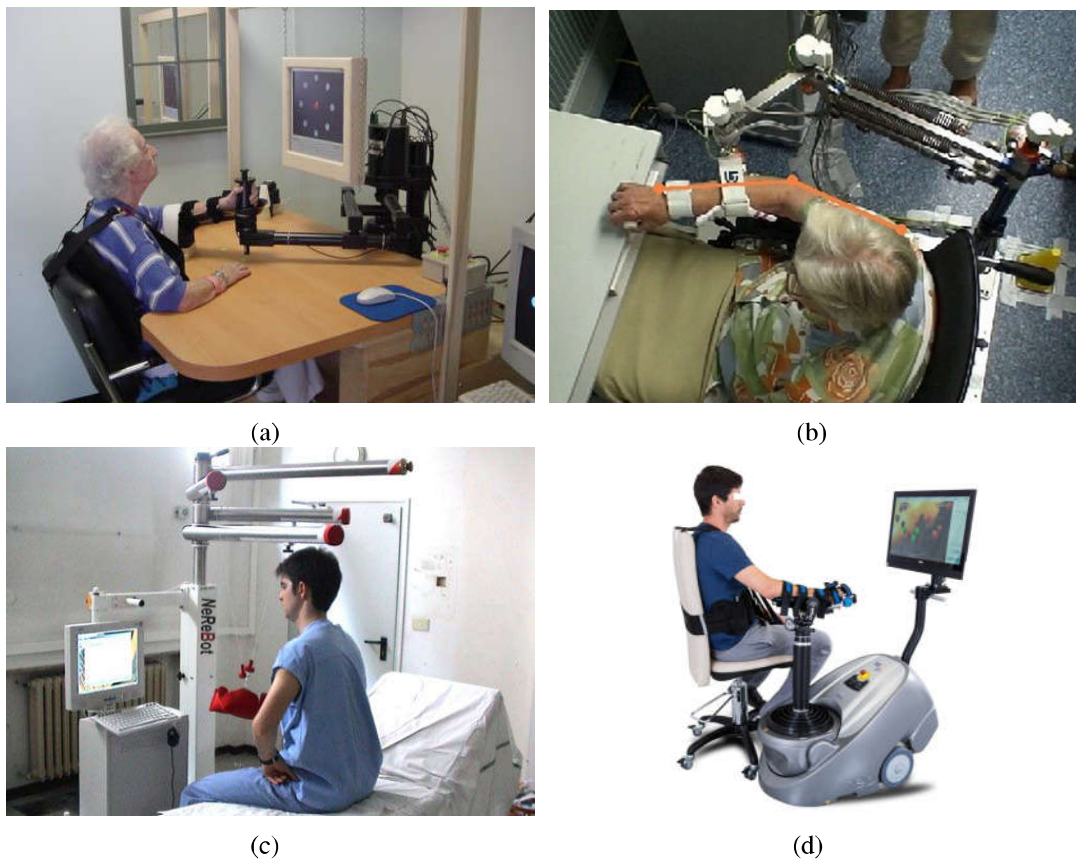
Figure 1.4: End-effector type robots for UE robotic rehabilitation, (a) Commercial version of the MIT-MANUS , the ACRE , (c) NeReBot , and (d) ReoGo [4–7].

oped for rehabilitative purposes can be categorized into three configurations: (a) programmable foot-plate, (b) exoskeleton, and (c) mobile base [3]. In the programmable foot-plate type robotic system, the feet of the patient are placed on the end-effector of a robotic system which simulates the motion required for gait training or other joint movements. In general this type of robots are less bulky, joint specific and have simpler mechanism in comparison to the exoskeleton type robots for gait training. On the other hand, the exoskeleton type of robots are similar to actuated orthosis that can be attached to a patient's limb and can be used for either gait training with the help of a treadmill or specific joint rehabilitation while the patient is stationary. This type of robots can deliver motion directly to a specific joint related to the human biomechanics. Some examples of the robotic rehabilitation devices currently being developed for LE applications are shown in Fig. 1.6 and Fig. 1.7.
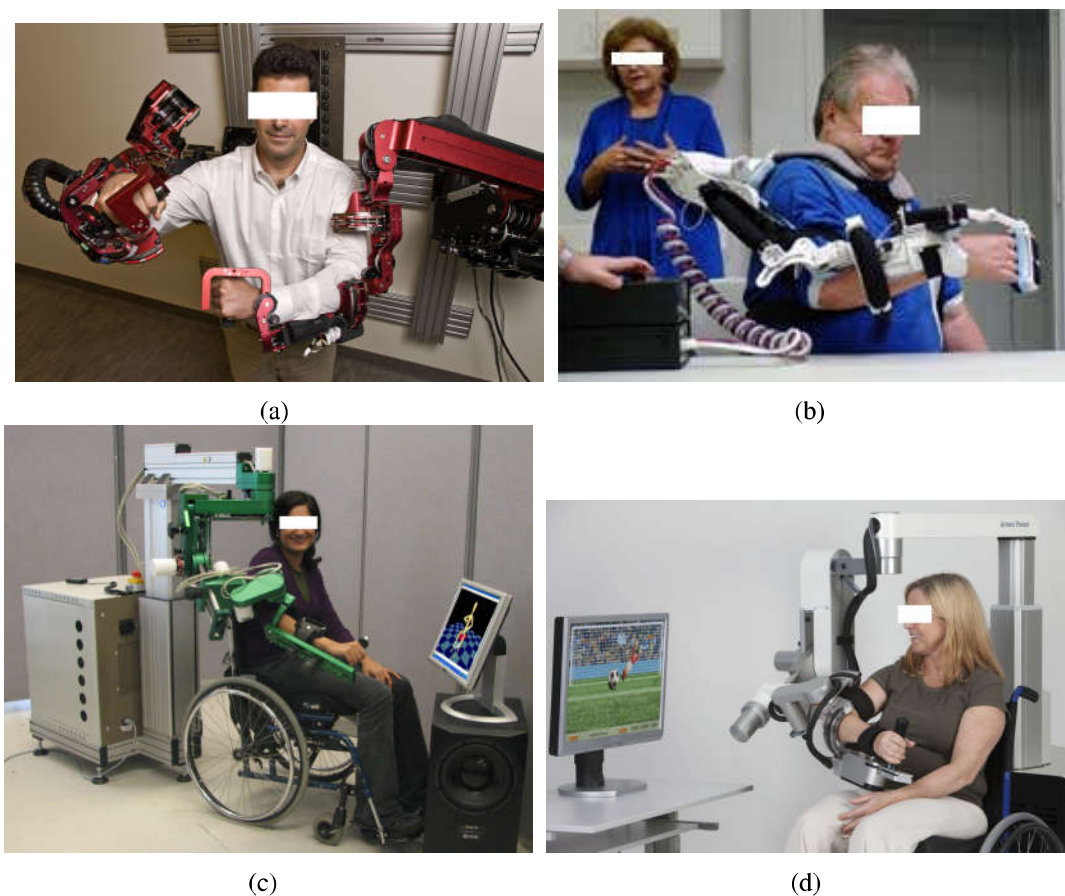
Figure 1.5: Exoskeleton type robots for UE robotic rehabilitation, (a) CADEN-7, (b) PURPERT IV, (c) ARMin III, and (d) ArmeoPower [8–10].

Pedago: Pedago is an end-effector type robotic system developed by the LokoHelp Group for gait training. The studies on the performance and the efficiency of this system show that the improvement in gait training can be achieved similar to the manual locomotor training while providing more assistance to the therapist [55].

Lokomat: This system is a combination of an actuated exoskeleton orthosis, a treadmill and a weight support system developed by Hocoma AG. The speed of the treadmill and the motion of the exoskeleton orthosis (at each hip and knee) is precisely synchronized for accurate rehabilitation on gait training. Lokomat is the most clinically evaluated system for LE rehabilitation [56–58].

Fig. 1.6(d) shows a high performance ankle rehabilitation system developed at the Istituto
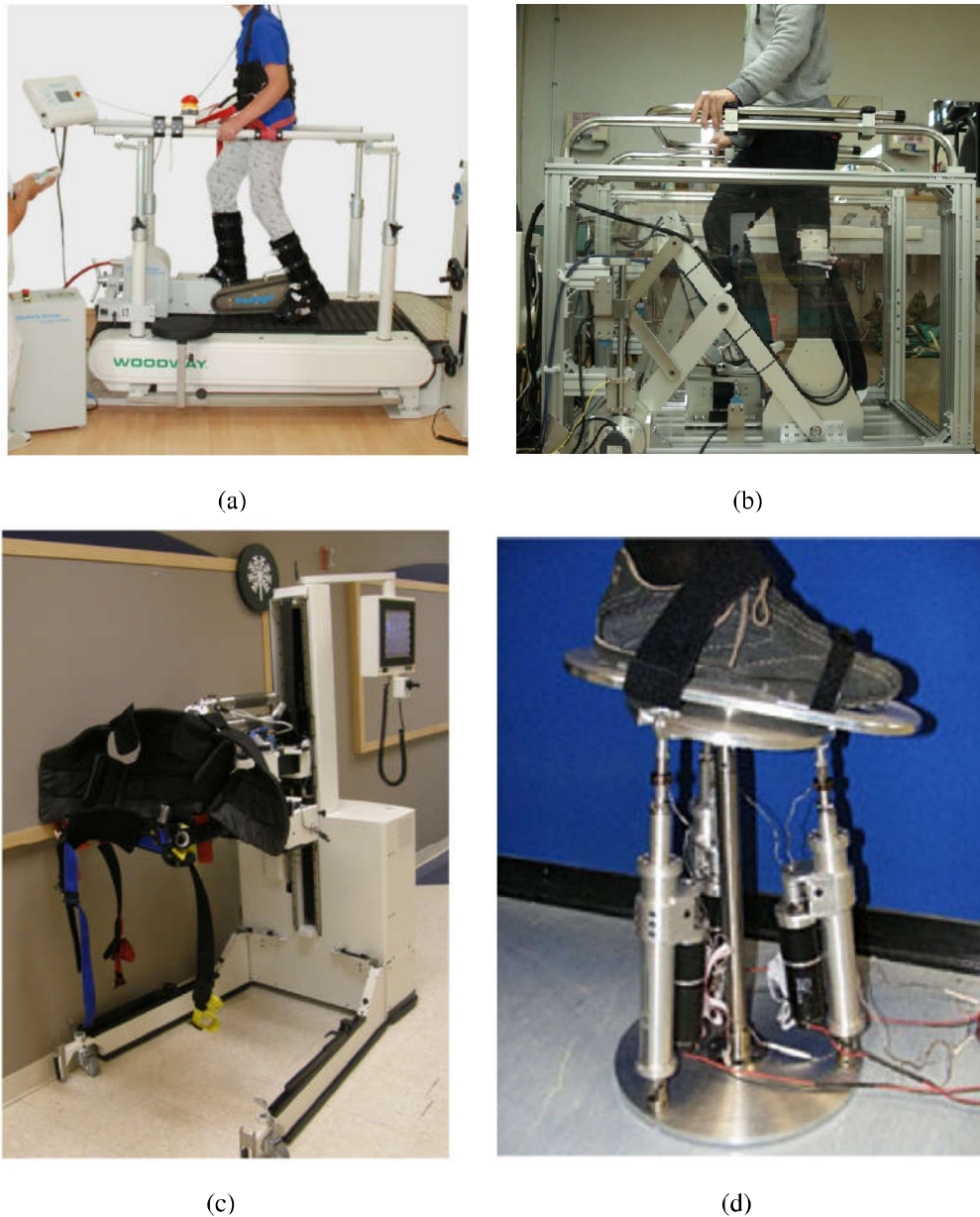
Figure 1.6: Programmable footplate and mobile based type robots for LE rehabilitation, (a) Pedago gait trainer by LokoHelp group, (b) GaitMaster5: a footplate type gait rehabilitation, (c) KineAssist robotic system, and (d) Ankle Rehabilitation Robot [11–14].

Italiano de Tecnologica. This system can generate plantar/dorsiflexion and inversion/eversion motion of the ankle by using a Stewart parallel mechanism similar to the Rutgers Ankle [59].

Most of the systems designed for robotic rehabilitation are still in the research phase and are not commercially available whereas the robots that are commercially available and are accessible

(a)

(b)

(c)

(d)

Figure 1.7: Exoskeleton type robots for gait training or stationary training on LE, (a) ReoAmbulator robotic system (Motorika Ltd.), (b) Lokomat system by Hocoma, (c) MotionMaker (Swortec SA), and (d) ReWalk wearable system (ARGO Medical Technologies Ltd.) [15–18].

in the clinics have not yet been designed for in-home applications. The main reasons behind this are (a) lack of clinical evaluations of the effectiveness of the robots, (b) high cost, (c) need for direct supervision by therapists, and (d) the need for therapy protocol and assessment.

Most of the existing robotic rehabilitation systems have been developed for delivering UE ther-

apy. In comparison to the mechatronic devices designed for UE therapy, LE rehabilitation robots have not attracted the attention they deserve especially for the joint movement rehabilitation. This can be related to the specific difficulties associated with LE rehabilitation.

1.2.1 Drawbacks of current robotic systems

Several robotic systems have been developed for delivering therapeutic rehabilitation in order to overcome the issues related to the conventional methods of delivering therapy. However, some challenges still exist in the current state of rehabilitation robotic technologies such as: (a) relatively higher cost, (b) complex mechatronic design, (c) larger weight and size of the mechanism, (d) portability issues, (e) difficulty in operation, (f) complexity of the systems in the initial stages of therapy, (g) no personalized therapy and need for direct supervision to monitor operation safety, and (h) no robotic system for delivering therapy to both upper and lower limbs. [3].

As mentioned before, the high cost associated with delivering therapy is high and this prevents patients from receiving services within appropriate time or for a sufficient duration. Additionally, most of the commercially available robots are expensive which adds up to the above-mentioned costs. The price-to-performance ratio is also not satisfactory in most of the developed systems when the benefits to clinics and patients are considered [60].

It has been shown that the number of repetitions in performing therapy procedures for neuro-motor recovery is important [61]. One of the factors that limits the number of therapy sessions that the patients can attend is the therapist's and clinic's availability. This eventually increases the cost and decreases the comfort level of patients receiving therapy services. One way to reduce the cost and provide more therapy time to patients is to allow home or personalized therapy to patients through tele-rehabilitation. The benefits of tele-rehabilitation are: (a) decreasing the the travel between rural communities and specialized urban healthcare facilities, (b) better clinical support, (c) delivering rehabilitation technology to rural communities, (d) indirect education to isolated rural clinicians, and (e) improvement in the stability of the services to regions with high clinician turnover [62]. One of the factors that makes robotic tele-rehabilitation more feasible is

the development of robotic systems that are (a) lightweight, (b) easy to operate by patients, (c) transportable, (d) safe to operate, and (e) low cost. Almost all of the systems that are commercially available are either not transportable easily or require direct in-person supervision by the therapist.

Although various devices have been developed for rehabilitation on either upper or lower extremities, there is no robotic system in the market for physical rehabilitation on upper and lower limbs. Developing such devices are useful particularly in the case of hemiparesis (which is the most common consequence of stroke and affects %80 of survivors) where the patients suffer from disability on one side of the body. Developing technologies for this application is useful as the rehabilitation process can be performed on both upper and lower limbs using the same only one robotic system. This multi-functionality feature can significantly decrease the cost of rehabilitation for both patients and the healthcare system as one device can be used for both upper and lower extremity rehabilitation.

Addressing the aforementioned problems can increase the number of facilities that are equipped with the appropriate technology which will increase the availability of these devices for a large number of patients. The ultimate goal for researchers in the field of physical robotics rehabilitation is to provide in-home user friendly robots that can significantly increase the number of hours during which a patient can receive kinesthetic therapies. Additionally, more patients can have access to the equipment at home under the supervision of a therapist in the clinic. This solution will significantly reduce the cost associated with factors such as manpower, transportation and therapy time. In addition, as a result of performing therapy at home, the number of sessions can be increased which should lead to faster recovery.

1.2.2 Control Strategies For Robotic Rehabilitation

The goal of control strategies is to control developed robotic systems in performing the rehabilitation exercises to enhance neural plasticity and increase neuromotor recovery. Overall the high-level control strategies that have been developed for rehabilitation robotics are: (a) assistive,

(b) challenge based, (c) simulate of normal tasks, and (d) non-contact coaching [63]. The most developed mode of control is the assistive one. In this mode the tasks are made easier for the patient to complete with the assistant provided by the robot. This results in more repetitions and faster skill recovery [46]. Significant effort has been made in the past two decades on validating the design and proposed control strategies for robotic rehabilitation and the effect of each strategy on the improvement of patients. Although most of the studies on clinical evaluation of the robotic technologies are sparce, most of the studies show promising result on the developed technologies and the control strategies for faster and more efficient recovery and motor learning skills.

1.3 General Problem Statement

As mentioned earlier, one possible step to address some of the above-mentioned difficulties (in particular, cost and complexity) is to develop devices that are designed specifically for one particular therapy regime and one joint. In other words, the solution could be a simple device that can be used for multiple simple therapy regimes. This will decrease the complexity of each system, increase portability, decrease the cost of the devices and allow for customization of the therapy for each patient [26].

It is worth mentioning that the problems for current LE robots are interlinked in a way that addressing one can improve the others. For example, to target the complexity and the size of the system by making function-specific robots will decrease the cost and the weight of the system.

One of the disadvantages of the devices developed for robotic rehabilitation, especially in LE applications is the relatively high cost of the devices. Also most of the commercially available robots are too complex for movement therapy and are mostly designed for functional therapy like gait training. There are some limitations with the currently existing technology for LE, such as: (a) not providing active hip abduction/adduction therapy that is necessary for maintaining balance during walking [20]. (b) unsuitability for in-home self-performed therapies due to size, price and technical issues.

An other limitation of the current systems is the need for having separate devices for upper-limb and lower-limb rehabilitation when the patient is experiencing hemiparesis. There is currently there is no system that can deliver physical therapy for both UE and LE. Developing such a device is a challenging task as the motions in the two cases are different. Another challenge is related to the range of force and motion required for these two cases which can create complexity in the design.

In recent work in the REACT lab at Western University, a six degrees of freedom (DOFs) rehabilitation robot was designed and implemented for LE rehabilitation [20]. The implemented prototype is an end-effector mobile footplate-type robot that is designed to be used for different therapy tasks such as early-stage motion assistance and ankle training. The robot consists of a mobile base with a parallel Stewart platform mechanism that is used to provide the rotational movements required for plantarflexion/dorsiflexion and supination/pronation of the ankle joint. Initial tests showed the feasibility of the mobile platform in generating the appropriate motions for LE rehabilitation.

Although the Stewart mechanism used in [20] is capable of generating the required range of forces and motions, due to the considerable weight of its linear actuators, the overall weight of the robot is relatively high. In addition, due to the type of lead-screw actuation system, the parallel mechanism has high intrinsic impedance and is not back-drivable (backdrivability is an important feature for rehabilitation robots). More importantly, similar to most of the existing examples, the Stewart platform results in a rigid linkage between the limbs of the patient and the moving parts of the robot. Consequently, the mechanism is not inherently safe.

The only possible safety feature for most of the existing LE devices is to implement software-based limitations on the applied forces. Although, by using software-based safety features, we may be able to limit the transmitted forces, the mechanism can be unsafe if the software fails to properly detect a fault and limit the force or if some part of the sensory system fails to report an adverse event [64]. Considering all of the above-mentioned difficulties associated with the classical design of LE robots, a novel mechanism is proposed in this thesis which addresses several

of the major challenges.

For the UE rehabilitation, various robots have been developed and are available on the market. One of the interesting types of these is the Armotion by Reha-Technologies shown in Fig. 1.8(a) [19]. This is an end-effector mobile-base type robot. This robot has three degrees of freedom, two translation and one rotational, designed for shoulder and elbow motion exercises.

(a)   (b)
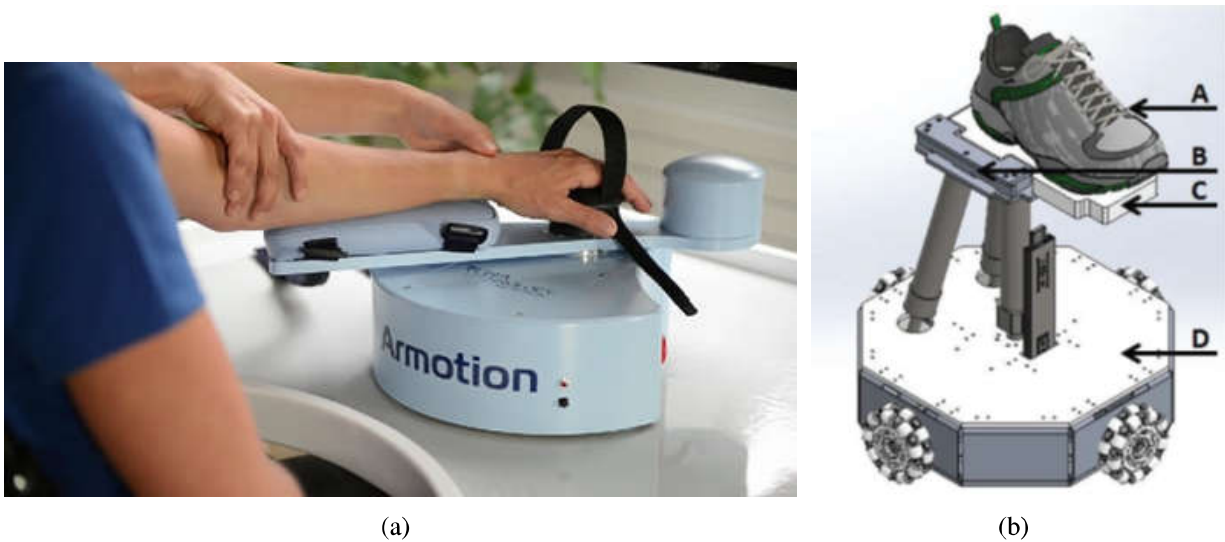
Figure 1.8: (a) Armotion mobile/end-effector type robot for UE rehabilitation and (b) Six DOFs LE rehabilitation platform designed at CSTAR [19, 20].

The purpose of this thesis is to design and implement a novel versatile mobile rehabilitation robot that can be used for both upper and lower limb therapy on patients suffering from neuromuscular trauma such as hemiparesis. The proposed concept for the robot will have the following characteristics: low cost, portability, multi-functionality, simple mechanism, inherently safe mechanisms and home training capability. More details about the concept and the design are described in Chapter 2.

1.4   Overview of the Thesis

In Chapter 2, a set of requirements for LE and UE robotic rehabilitation systems is given. The design procedure, concept generation, detailed design of the system and component selection are

described. In Chapter 3, the system model including the Jacobian and inverse kinematics and the algorithms used for trajectory control are then discussed. In Chapter 4 various experiments are presented to validate the design of the system and the controller algorithms. At the end of Chapter 4 the healthy subject validation including the ethics board form application and trial protocol is explained. Concluding remarks and suggestions for future work are given in Chapter 5.

Chapter 2

System Design

2.1 Introduction

The device described here is a novel Active Mobile End-effector Foot-plate/Handle-grip (AME-F/H) type robot that can be used to conduct motor rehabilitation for both UE and LE limbs. It has several novel features including (a) dual-usability (UE and LE), (b) light-weight, (c) adjustable mechanism for transferring forces and torques, (d) inherent safety and (e) portability.

2.2 Concept Design

Robotic rehabilitation systems designed for Upper-Extremity(UE) and Lower-Extremity(LE) therapy require different specifications and requirements. The range of motion, accuracy in the generated motion, resistance impedance and generated output force/torque are some examples of the requirements that are different for application of UE and LE rehabilitation. This diversity in the specifications presents interesting mechatronic challenges in finding a workable solution to satisfy all these needs.

To initiate the design process, a list of requirements and specifications of the currently developed systems for the UE and LE is presented. Table 2.1 summarizes the list of all requirements

Table 2.1: List of desired requirements and specification of the rehabilitation systems [14,20,24–26]

Type	Requirement	Specification for UE	Specification for LE
Functionality	Range of applied force/torque	40N for planar motion at the end-effector	40Nm for ankle training therapy 400N for translation force
	Range of motion for Inversion/eversion	$\pm 30^o$	$\pm 30^o$
	Positioning and velocity accuracy	$1 deg$ for orientation and $1 deg/sec$ for angular speed	$1 deg$ for orientation and $1 deg/sec$ for angular speed
	Low static and rolling intrinsic impedance	Maximum rotational resistance of 0.5Nm Maximum translation resistance of 2N	No specification
	Low inertia of moving parts	Maximum equivalent moving mass of 5Kg	equivalent mass as low as possible
Safety	Restraining the amount of applied torque to patient	Mechanically and electrically controlling the generated force	
	Preventing pinching and sticking of patients body	Enclosing all the moving parts inside the device	
Cost	Minimizing the cost	Lowest possible cost for in-home end-user under $20k	

and specifications necessary for concept design process initiation.

From the functionality point of view, the key parameters considered for designing the robot are: (a) adequate range of torques and motions, (b) minimum friction, (c) low impedance for back-drivability and (d) minimal overall mass. The values considered for each requirement interpreted from the existing devices in the literature. For example, as given in [14], with the inversion/eversion direction, the required torque for ankle rehabilitation is $40Nm$, and the needed range of motion is $\pm30''$. Also, considering the application, the mechanism should have a small equivalent moving mass and a low intrinsic impedance for UE application, and it should be back-drivable [14,65].

From the safety point of view, as the device is in direct contact with the patient, the amount of force applied by the robot should be restricted. This has been done, as mentioned in the literature, through software limits [66]. However, relying only on a software-based safety feature for inherently unsafe systems can be problematic if the software fails to detect a faulty event or if the sensory system fails to report an unsafe event to the software. The alternative approach proposed in this research is to design and implement an inherently safe mechanical mechanism that can be adjusted to tune the maximum amount of force allowed to be transferred to the patient's limb. This concept is proposed in this chapter and results in a novel and safe mechanical design for UE and LE rehabilitation robots. It is worth noting that to enhance safety, attention should be paid to designing the robot compactly. This is done to ensure that the robot does not pinch or stick to the patient's limb. All moving parts are enclosed in the robot's case. Furthermore, the electrical voltage used in the device is set to be as low as possible to prevent any shocks in case of failure.

Following several brainstorming sessions and a literature review, a mobile footplate /handle-grip end-effector type robot was chosen as the base platform. This concept was chosen as it provides important features such as more simplicity in structure design and actuator type, a wide range of motion(workspace) and its capability for the multi-purpose application. It is important to note that a wide range of motions is achievable as the robot is a mobile platform. It can be said that ground type robots generally provide more simplicity in design than the exoskeleton type.

2.2.1   Concept of Operation

The concept behind the rehabilitation procedure with this novel robot is to perform therapy on patients in the seated position. For the UE therapy case, the robot will be equipped with a handle and will be placed on a table. By attaching the patient's hand or forearm to the handle, various movement therapies can be performed on the UE. To perform therapy on the LE, a small number of adjustments to the robot are needed. First, the handle is replaced by a foot-plate. Second, the gear ratio in the power transmission mechanism is increased to match the requirement of LE rehabilitation. Third, the stabilizer arms are extended to prevent the robot from tilting. The robot is placed on the ground on a specially designed pad. After attaching the patient's foot to the footplate, the rehabilitation exercises on the LE can be started. For a better understanding of the device, Fig. 2.1(a) and Fig. 2.1(b) are provided to show the robot in different modes of operation, one with a grip handle for UE and the other with a footplate and unfolded balancing arms (explained later) for the LE application.

(a)   (b)
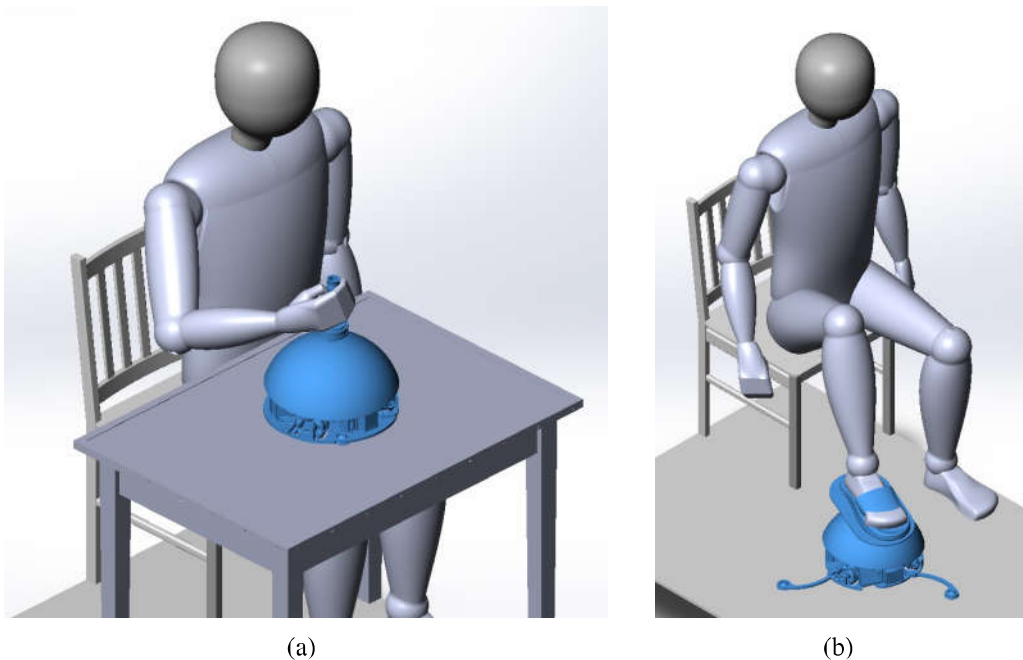
Figure 2.1: The concept of operation for the proposed robot for the (a) UE application; (b) LE application

Device Description: The robot consists of a mobile platform that is driven by three omni-directional wheels. The mobile platform provides two translational degrees-of-freedom in planar motion and one rotational degree-of-freedom for the yaw rotation. Attached to the mobile platform is a mechanism that can provide two decoupled rotational degrees-of-freedom that correspond to the pitch and roll rotations. Overall the end-effector of the system can generate motions in five degrees-of-freedom to control the movement of the patients limb.

Translation Mechanism: For the mobile platform, a three-DOF Omni-directional mechanism is selected which provides a large workspace for translation motion. The platform is capable of generating two linear DOFs in the plane of the mat and one rotational DOF perpendicular to that plane as shown in Fig. 2.2. Using these three DOFs, the robot can activate knee flexion/extension and hip abduction/adduction and internal/external motions in LE and elbow flexion/extension and shoulder abduction/adduction and internal/external in UE.
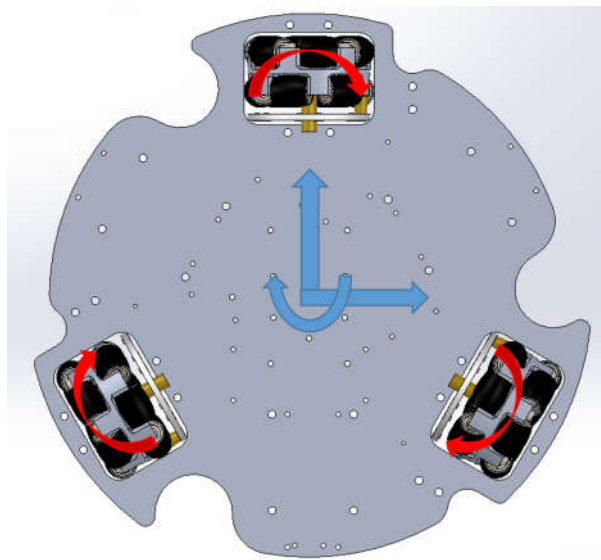
Figure 2.2: The concept of motion generation using the Omni-directional mechanism

Rotation Mechanism: To generate necessary motions corresponding to ankle and wrist, e.g., Dorsiflexion/Plantar-Flexion and Inversion/Eversion motions, two rotational DOFs are needed. After considering different concepts, an omniwheel-based and a cable-based mechanism were selected which will be described here. As mentioned before, having an inherently safe robot

is vital for the rehabilitation purposes and is essential for In-home use where the safety of the patient is the top priority. As a result, in order to limit the amount of transferred forces/torques, the connection between the actuated mechanical elements of the system (e.g. motors) and the part supporting the patient's limb was designed such that it does not use conventional direct mechanical connections (such as linkage power transmission).

The proposed solutions for generating the rotational motion are indirect techniques which utilize tunable friction-based power transmission mechanisms (such as those using the concept of clutches). This will ensure that the forces/torques applied to the patient's limb will not exceed the adjusted power transfer capability of the system. The adjustable design is motivated by the fact that the maximum allowable force in a rehabilitation regime is affected by several factors, such as the state of motor deficits, the biomechanics of the patient's limb, gender, age, the place where the therapy is delivered (clinic versus home). As a result, it is important to make the maximum transferred power of the system adjustable. For this purpose, the proposed designs allow for tuning the maximum inherent power capability (for example by simply adjusting a thumb-nut).

In both mechanisms, there is a rod attached to the center of a base plate using a universal mechanism as shown in Fig. 2.3(a). Using a universal joint with two DOFs at the center of rotation instead of a commonly used three DOFs spherical joint will (a) decrease the friction and (b) eliminate the backlash associated with commercially available spherical joint.

(a) Omni-wheel Based Rotation Mechanism(Concept A): To achieve the other two rotational degrees-of-freedom, a novel friction-based mechanism is used to transfer the power to the rod (as explained below). This friction-based mechanism consists of a dome, a rod, a universal joint and three omni-directional wheels attached to the base as shown in Fig. 2.3(a). The dome is a hemispherical shell that is attached to the rod using a set screw. It is important to mention that in this assembly, the center of the hemispherical dome is coincident with the center of the joint. As a result, the rotation of the dome that is attached to the rod occurs around the center of the joint. The wheels are attached to the base and are in contact with the dome at the inner circumference surface. By driving the wheels, due to the friction in the contact points of the wheels and the

dome, the dome will move. The motion of the dome results in the rotation of the rod around the center of the joint and consequently moving the end-effector of the robot. For power transmission between motors and the wheels for both LE and UE applications, a two-mode gear train power transmission is used which will be described in Section 2.3.2.2 . This power transmission mechanism can be adjusted with two gear ratios which enables different ranges of output forces for different therapeutic applications.

(a)   (b)
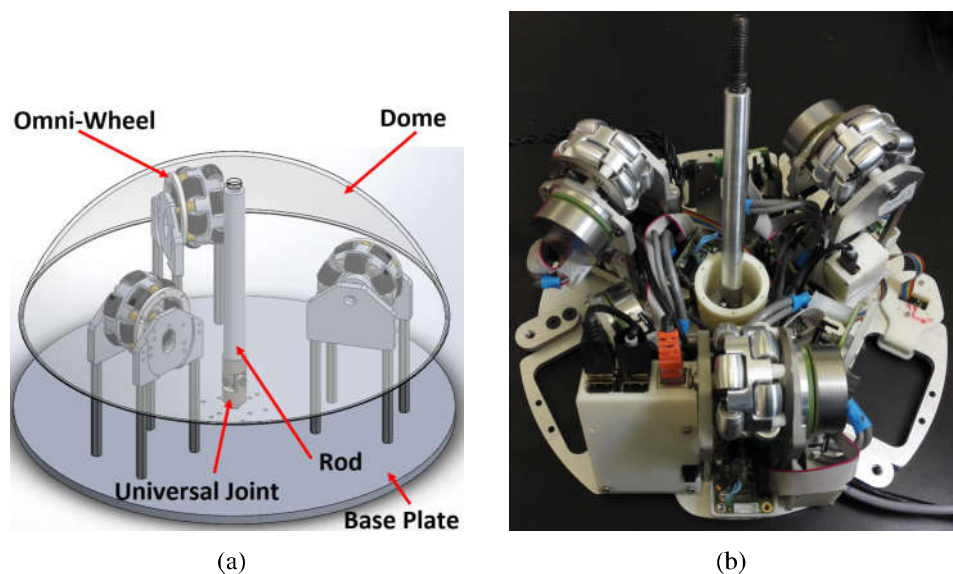
Figure 2.3: (a) Different component of orientation mechanism (b) Manufactured components with the center rod in the middle

(b) Clutch-based Cable Mechanism(Concept B): The other alternative mechanism that can be used to actuate two orientation DOFs of the rod is a novel cable-driven mechanism with configurable output torque. As shown in Fig. 2.4(a), in this mechanism the orientation of the center rod is controlled with tension and length of three cables attached to the rod. These cables are driven by three motors equipped with cable/drum mechanisms. To incorporate the safety feature, a friction clutch is attached to each drum and the motor. This way, by adjusting the maximum capacity of the friction clutch, the maximum amount of the force transferred to the cables can be adjusted and accordingly limited. Fig. 2.4(b) shows the cross section view of the concept design for the proposed cable-driven mechanism.
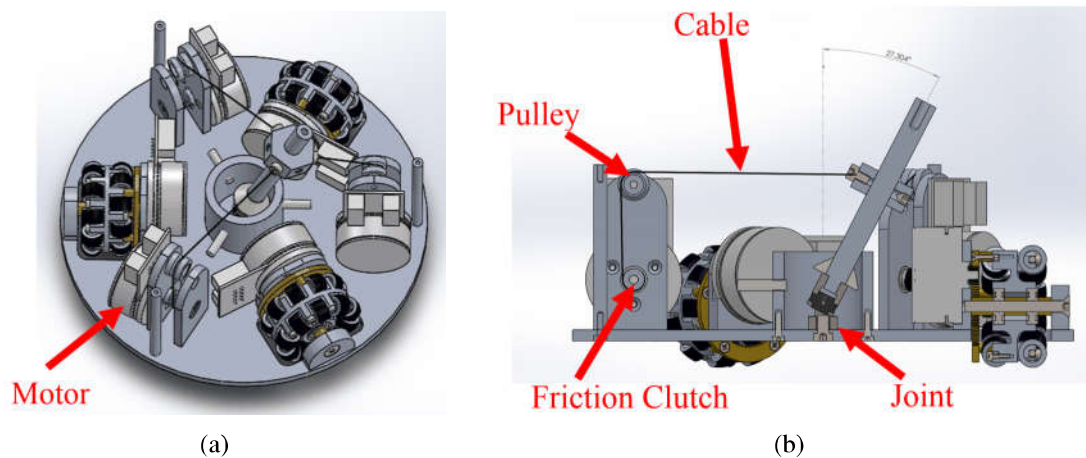
Figure 2.4: CAD model of the concept design for cable driven orientation mechanism (design "B"), (a) the first concept model; (b) different components in the mechanism

2.2.2   Adjustable Force/Torque Mechanism

As mentioned earlier, to ensure the safety of the patient when using the device, the robot should be inherently safe. This means that the mechanism designed and utilized in the system should be mechanically adjustable for power transmission. Both of the concept mechanisms described above for generating orientation DOFs have a unique capability in limiting the transferred force/torque. Using the specific proposed design, it is possible to adjust the amount of force transferred to the rod and accordingly to the user. Here, these features will be described in details for the concept mechanisms A and B.

Adjustable Torque Mechanism A: In this mechanism, the force transferred to the dome is the result of the friction force between the wheels and the dome. Consequently, there is a maximum threshold for the amount of the transferable force that depends on two factors, (a) normal force between the wheels and the dome and (b) friction coefficient of the contact area. If the generated force by the wheels exceeds a particular value (maximum friction force), the wheels will slip and the force transferred to the user will be mechanically limited. To change this specific value (maximum transferable force), the two above-mentioned factors can be modified with two methods. First method is by changing the coefficient of friction of the contact area (e.g. by changing the

material of the wheels and the dome), and the second method is by changing the amount of the normal force between the wheels and the dome. As the friction coefficient is a constant parameter, the amount of the transferred force can not be modified after the materials are selected. The only method that can be used to control the value of the transferred force is by controlling the normal force between the dome and the wheels. The novel mechanism depicted in Fig. 2.5(a) and Fig. 2.5(b) can change the normal force between the dome and the wheels. This mechanism consists of a thumb-nut, a compression spring and a set-screw attached to the middle rod. Turning the thumb-nut around the set-screw (red arrow) consequently changes the compression force in the spring located between the thumb-nut and the dome (green arrow). The force applied to the dome by the spring (green arrow) is transferred to the wheels which consequently changes the normal force between the wheels and the dome (blue arrows). Therefore, by twisting the thumb-nut, the maximum transferred force of the mechanism can be controlled mechanically. Fig. 2.5(b) shows various components of the adjustable torque mechanism A.

(a)   (b)
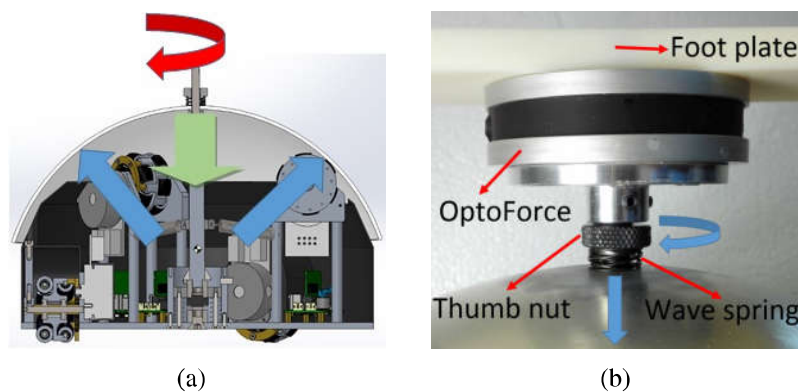
Figure 2.5: (a)) Force transmitted diagram; (b) detailed view of components in the adjustable mechanism.

Adjustable Force/Torque Mechanism B: In this mechanism, as described above and depicted in Fig. 2.4(b), a friction clutch is placed between the motor and the pulley. By adjusting the slippage threshold of the clutch, the maximum torque transferred from the motor to the central rod can be limited and accordingly, the amount of force applied to the user is controlled. It should

be noted that the clutch used here to limit the output torque of the motor can be chosen from any type of clutch such as friction, magnetic, etc.

2.3 Detailed Design

In this section, the concept design is elaborated more, and the process of the design is explained from the power calculation to the component selection and detailed structural design. Like most of the mechatronic systems, the design process followed in this project went through various iteration steps.

2.3.1 Power Analysis

Orientation Mechanism: Based on the required range of force and velocity of movement given in Table.2.1, an estimate of the power required for the orientation mechanism and the actuators was calculated as explained below. Based on the existing research and commercially available devices for ankle rehabilitation training, a rotational speed greater than $\frac{\pi}{2}$ rad/s is not usually expected [14,67]. Also, considering the required output torque given in Table. 2.1, the minimum power of the orientation mechanism can be calculated as

$$P_S = T \times \omega = 40 \, Nm \times \frac{\pi}{2} rad/s = 62.8 \, W \tag{2.1}$$

where P_S is the minimum power required, T is the minimum output torque, and ω is the minimum output velocity of the system. In both of the orientation mechanisms, we have three actuators in the device. This means that by calculating the minimum power required for each actuator in one mechanism, the same actuators with the same power can be used in the other mechanism. In the case of mechanism "A", to calculate the contribution of each wheel on the overall output force, an analysis of the output force is performed under static conditions. As shown in Fig. 2.6, considering the alignment of the omni-wheels, the contribution of each wheel

in generating motion in the roll and pitch directions can be summed up to calculate T_X and T_Y, as

$$\begin{bmatrix} T_X \\ T_Y \end{bmatrix} = F_{W_1} R_P \begin{bmatrix} \frac{-1}{2} \\ \frac{\sqrt{3}}{2} \end{bmatrix} + F_{W_2} R_P \begin{bmatrix} \frac{-1}{2} \\ \frac{-\sqrt{3}}{2} \end{bmatrix} + F_{W_3} R_P \begin{bmatrix} 1 \\ 0 \end{bmatrix}$$

$$-F_{max} < F_{W_k} < F_{max}$$

$$k = \{1, 2, 3\}$$

(2.2)
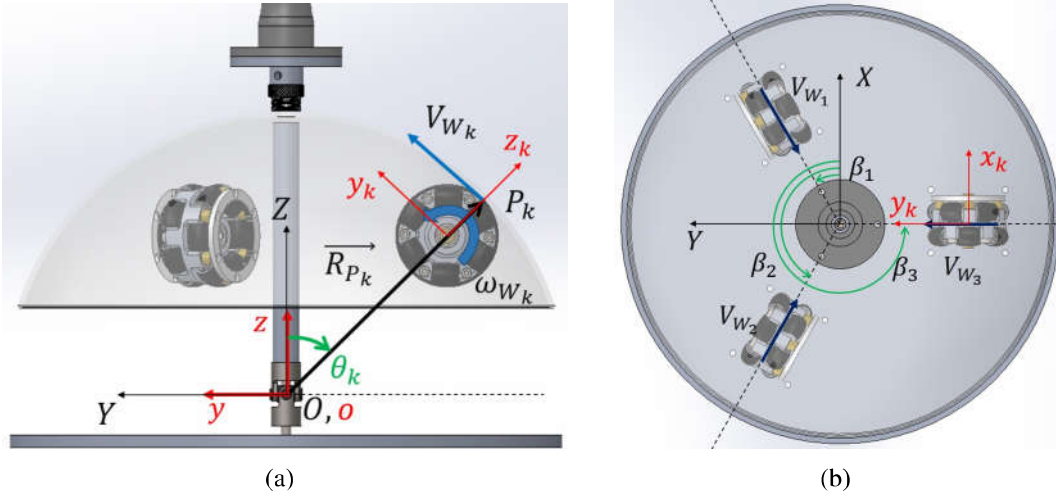
Figure 2.6: Global and local coordinates assigned to describe kinematics: (a) side view, (b) top view

where T_X and T_Y represent the generated torque in the roll and pitch directions, respectively. R_P is the distance between the contact point of each wheel and the center of rotation of the dome. In this mechanism, the value of R_P is same for all of the wheels. F_{W_k}, $k = \{1, 2, 3\}$ are the forces applied to the dome by each wheel. The value of F_{W_k} can vary in the range of $[-F_{max}, F_{max}]$ where F_{max} is the maximum force that each wheel can generate. Using (2.2) the contribution of each actuated omniwheel system, in generating the total output torque, was calculated. To simplify the analysis, this equation was normalized with respect to the geometrical parameters. For this purpose, the normalized value of F_{max} was 1 N and that of the normalized R_P was 1 m. Fig. 2.7

shows all possible values of T_X and T_Y when F_{W_k} varies in the range of $[-1,1]$ N. Changing the values of F_{W_k} generates the torque in the range of $[-2,2]$ Nm and $[-\sqrt{3},\sqrt{3}]$ Nm for T_X and T_Y, respectively.
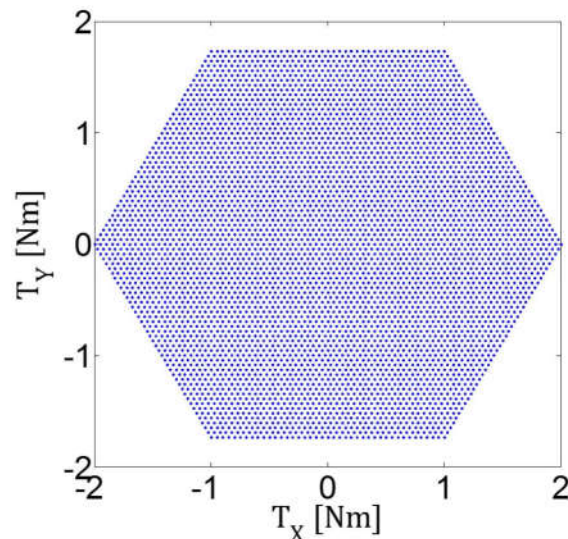
Figure 2.7: Map of possible normalized torques achievable in roll and pitch

Based on the force decomposition shown in (2.2) and visualized in Fig.2.7, the amplitude of the output torque vector $T = \sqrt{T_X^2 + T_Y^2}$ has the least value equal to $\sqrt{3}$ Nm in the "X" direction (pitch). To achieve the minimum required power for the system in the pitch direction, the power of each actuator was calculated to be $\frac{1}{\sqrt{3}}$ of the total required power. This gave us the required value of 36.3 W for each actuator in the orientation mechanism that was used in both designs "A" and "B".

Mobile Base: Similar derivations was made for the mobile base mechanism to compute the minimum power required by the actuators. As mentioned in Table.2.1, for LE application, the maximum force in the planar direction is 400 N. Also for the therapy procedures proposed in Chapter 1, the velocity more than 0.2 m/s is not expected. This means that the minimum power required by the system for the mobile platform is 80 W (product of force and velocity). Using the Jacobian matrix which will be explained in Section3.2.2, the minimum power required by each

actuator in the mobile platform was calculated as $\frac{1}{\sqrt{3}}$ of the total power which is equal to 46 *W*.

2.3.2 Structure Design

2.3.2.1 Mobile Platform:

The mobile base consists of a platform with three actuated mechanisms attached to the omni-wheels. By driving these three omni-directional wheels, the robots base can be moved on a flat surface in two translational directions and one rotational direction (as shown in Fig. 2.2). Also, three balancing arms are designed to be attached to the base of the robot, which can be folded and unfolded as needed (which will be described later). The purpose of the balancing arms is to increase the contact point of the robot with the ground and prevent tilting in LE cases. They can also be folded when the robot is in use for the UE application to reduce the size of the robot. At the end of each arm, there is an eye-ball bearing for enduring normal force and reducing friction in contact points.

As the robot has a mobile platform, to decrease the sizes of actuators, decrease the endpoint impedance and make the device portable, the structure of the system should be as light as possible. For this, all components were attached to a single base plate made from aluminum alloy 7075T6 with thickness of 6.35 *mm* and overall diameter of 290 *mm*. The thickness of the plate is calculated to endure the maximum force of 1000 *N* with safety factor of 4. Finite element analysis was performed using SolidWorks Simulation with static loading conditions. Diameter of 290 *mm* is the minimum size that can fit all components attached and enclosed inside the base plate. Minimizing the diameter of the base decreased the overall size of the robot and increased portability which consequently makes the robot more suitable for UE application. However having a small base for the mobile platform decreased the distance between contact points of the wheels and the ground padding which increased the instability of the robot to tilt specifically in the LE application. To address this issue, a foldable mechanism (balancing arms) was designed on the side of the mobile platform that could be opened in the LE application mode for increasing the contact points of the

device with the ground. It can also be folded inside to decrease the overall size of the device in UE mode. At the end of each arm, an eyeball bearing was attached to minimize the friction at the contact point with the ground padding. Fig. 2.8 depicts the stabilizer arms in different modes of operation. Using these stabilizing arms, the distance between the contact points was increased two times without changing the size of the robot's base.

(a)   (b)   (c)
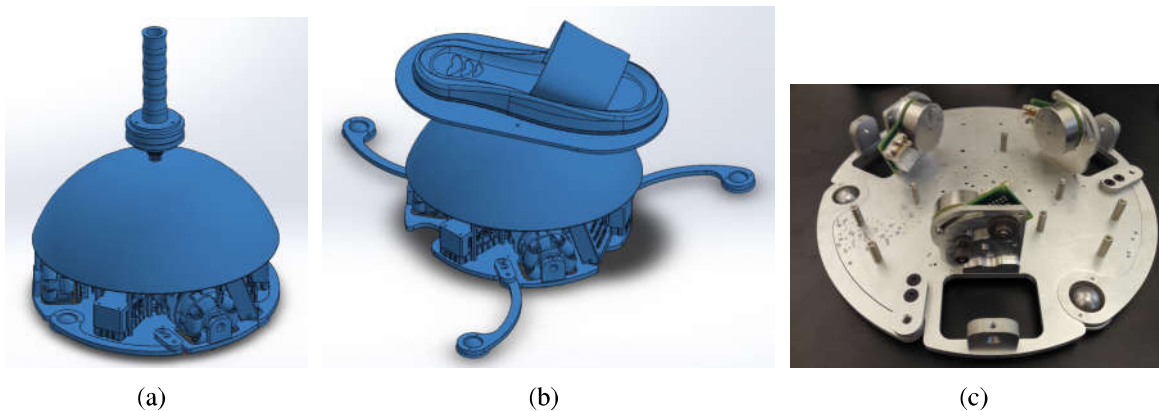
Figure 2.8: Robot in two modes of operation, (a) UE mode with wrapped stabilizer arms, (b) LE mode with stabilizer arms opened and (c) base plate with stabilizer arms wrapped inside

2.3.2.2   Power Transmission Mechanism:

To select the type of power transmission mechanism (PTM), some factors should be considered. For the application of rehabilitation, the accuracy of the motion is of the order of 0.1mm. Additionally, the size of the PTM should be as small and light as possible for the mobile type robot. These requirements suggested the use of gear-type PTM which was custom designed and manufactured using WEDM as shown in Fig. 2.9. One of the important requirements of end-effector type rehabilitation robots, specifically for UE application, is the low intrinsic impedance of the end-effector. This feature is particularly useful in the assistive stages of therapy when the patient tries to move the limb without any help from the robot. At this stage, the motion of the robot should be smooth to the patient's impaired limb as the muscles are still weak. In other words, the robot should have the least possible resistance to the motion. Having this feature in mind requires us

to design the transmission mechanism to be back-drivable and with lowest possible power transmission ratio (PTR). As the application of this robot also includes LE rehabilitation, to satisfy the output force requirements, the power transmission mechanism should provide enough output force. This means that to keep the size and power of the actuators as low as possible, the PTR should be high enough to increase the output torque of the actuator. Keeping PTR low for UE and high for LE applications requires us to have a mechanism with multi PTR that can be adjusted easily. Fig. 2.9 shows the CAD design of the two-stage gear PTM that can be adjusted by sliding the motor to either side of the curved slot. This can be done by turning a thumb-nut attached on the bottom of the robot. To satisfy the output force requirement, the PTR can be adjusted between 5:1 for UE and 25:1 for LE application.

(a)	(b)	(c)

Figure 2.9: Power transmission mechanism at (a) low PTR (5:1); (b) high PTR (25:1) and (c) Custom made omni-wheels, gearbox and MAXON EC45 50W motor for mobile base

Mobile base   Power transmission can be performed using different mechanisms, such as gears, belts, cables and so on. In this robot, to decrease the size of the structure, a set of custom-made gears is used to transmit power, reduce the rotational speed and increase the output torque of motors. The gear-set is designed to have different ratios which are adjustable between two settings, the higher one is designed and implemented for the LE application, and the lower ratio is designed for UE applications. The gear ratio setting can be easily adjusted by the user with

a simple mechanism at the bottom of the robot (explained below). For this purpose, the motors are attached to the power transmission with a sliding mount (shown in Fig. 2.9(c)). By moving the motors from one side of the slider to the other side, the pinion of the motor can be engaged with different gears and the transmission ratio can be changed as shown in Fig. 2.9. To move the motors and change the transmission ratio of all wheels, the three sliders are attached to cables that are connected to a turning nub at the bottom of the robot. By turning the nub, the motors can be moved to the corresponding side of the slide. Having this novel feature, the system can represent low intrinsic mechanical impedance due to the low gear ratio for UE applications while being able to be used for high force and torque LE applications. This is an important feature of the designed rehabilitation robot. Since patients are weak and cannot initiate movements in the initial stages of therapy, having a low intrinsic mechanical impedance is essential to make sure that the patients are engaged in participating in the therapy. That is why for UE, we need to ensure low mechanical impedance. Also, the design mentioned above allows for providing sufficient output forces as a result of the possibility of increasing the gear ratio for LE applications.

Orientation Mechanism, Design "A"   For the design "A", the PTM is a two-stage gear set as shown in Fig. 2.10. In this PTM, the position of the motor's pinion determines the gear-set stages engaged which results in the ratio. Low ratio PTM in this case is $5:1$ as shown in Fig.2.10(a) and high ratio is $10:1$ as depicted in Fig. 2.10(b). Using this PTM for design "A", the maximum achievable output torque for the implemented system is $60\,Nm$ for the roll (X) direction and $52\,Nm$ for the pitch (Y) direction.

Orientation Mechanism, Design "B"   To decrease the size and the capacity of the required clutch in the design, the clutch is located directly after the motor in PTM where the amount of the transferred torque is minimum. In this way, the capacity of the selected clutch would be minimum which consequently minimizes the size of the clutch. After a wide search on different available products in the market, an EAO12 friction clutch by Dynatech Inc was selected. This small clutch,

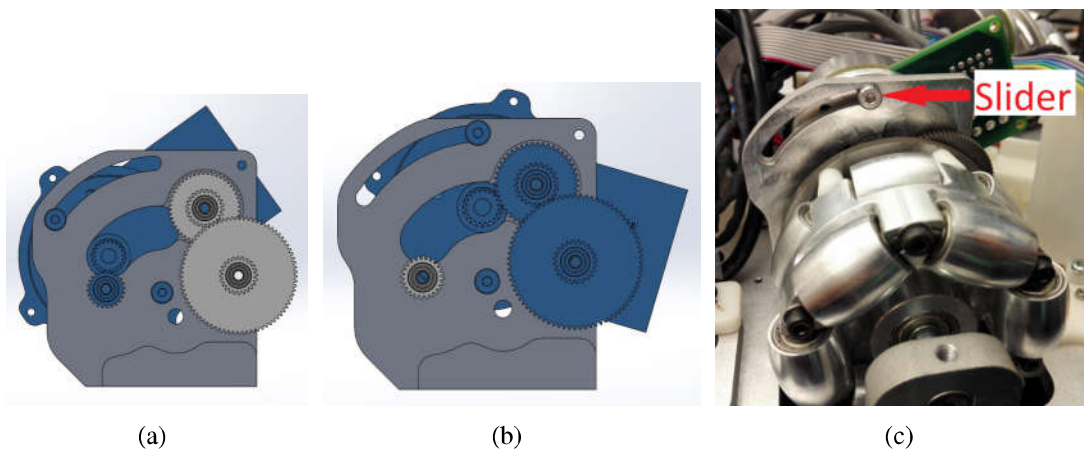(a)   (b)   (c)
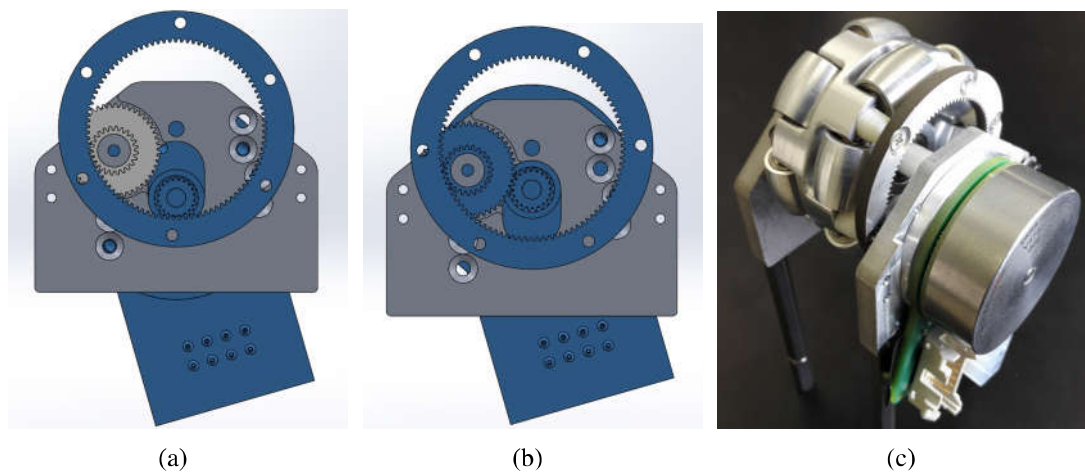
Figure 2.10: Power transmission mechanism at (a) low ratio(5:1); (b) high ratio(10:1) and (c) Custom made omni-wheels, gearbox and MAXON EC45 50W motor for orientation mechanism "A"

as depicted in Fig. 2.12(c), is an adjustable multi-plate friction-based clutch with the maximum torque capacity of 1 *Nm*. By twisting the thumb-nut of the clutch, the compression force in the springs inside the clutch varies which will changes the slippage threshold of it.

To have back-drivability in case of UE and enough output torque for LE, two PTRs are designed for the cable-driven module of design "B" as shown in Fig. 2.11. In this module, by engaging a different set of gears, PTR can increase from 5 : 1 to 16.25 : 1.

In the cable mechanism designed here, the cable passes through the guides and goes around the pulley which is connected to the biggest gear in the gear set shown in Fig. 2.10. It is important to mention that by adjusting the clutch threshold, the amount of the torque transferred to the gear is going to be limited mechanically which consequently limits the maximum tension in the cable and the force transferred to the handle. Fig. 2.12(a) and 2.12(b) depict the CAD and the manufactured models of the module for the design "B" with important components highlighted. The assembled CAD version of three modules with cables attached (and highlighted) of the final orientation mechanism "B" is shown in Fig. 2.13. As can be seen, the cables are attached to the middle rod and by controlling the tension in the cables, the orientation of the middle rod can be controlled.

(a)   (b)
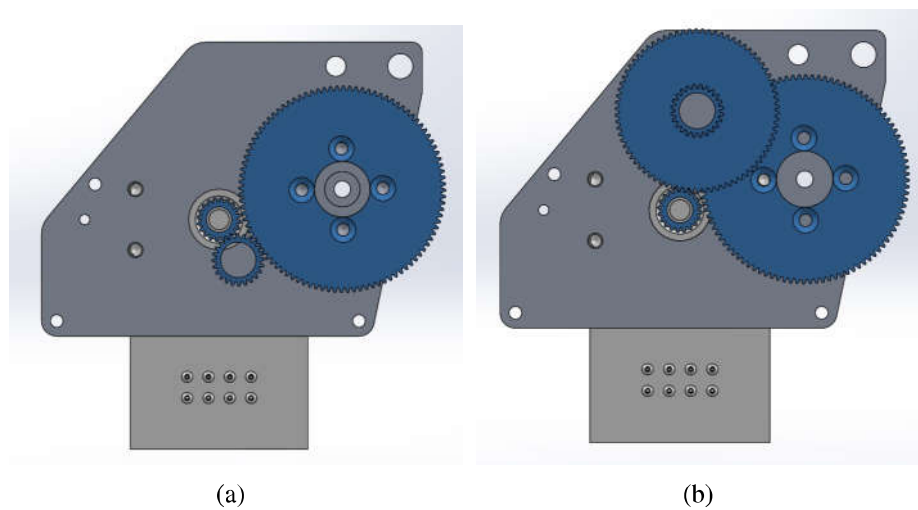
Figure 2.11: Power transmission mechanism for the orientation mechanism design "B": (a) Low PTR and (b) High PTR

(a)   (b)   (c)
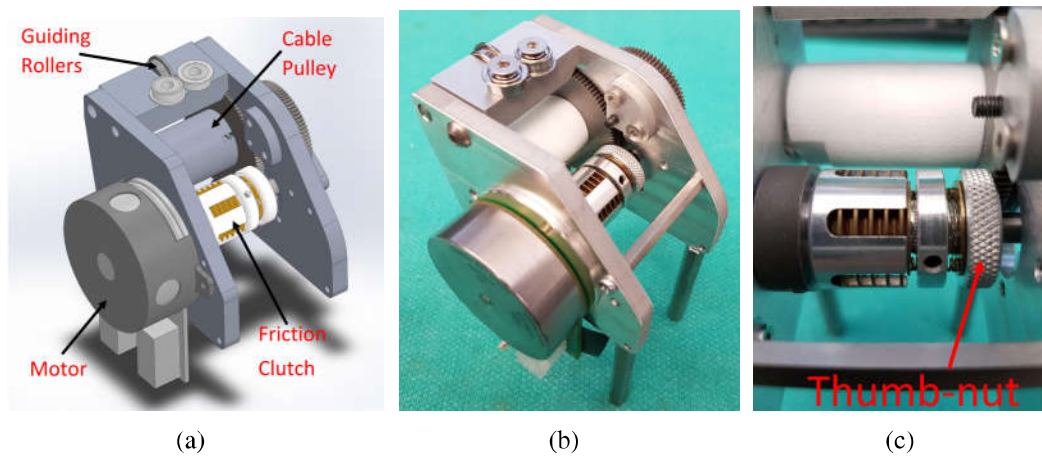
Figure 2.12: Orientation mechanism module "B": (a) CAD model with important elements high-lighted; (b) manufactured model; and (c) friction clutch used in this model

2.3.2.3 Omni-Wheels:

To have the flexibility in the design, decrease the overall size of the robot, provide smooth motion with the lowest friction and maximize the strength of the components, the wheels were specifically designed and manufactured for this robot. Fig. 2.14 depicts the manufactured Omni-wheels for mobile platform and orientations mechanism "A". The size of these wheels is optimized based on the internal spur gear attached to them and the maximum desired strength. Additionally, they
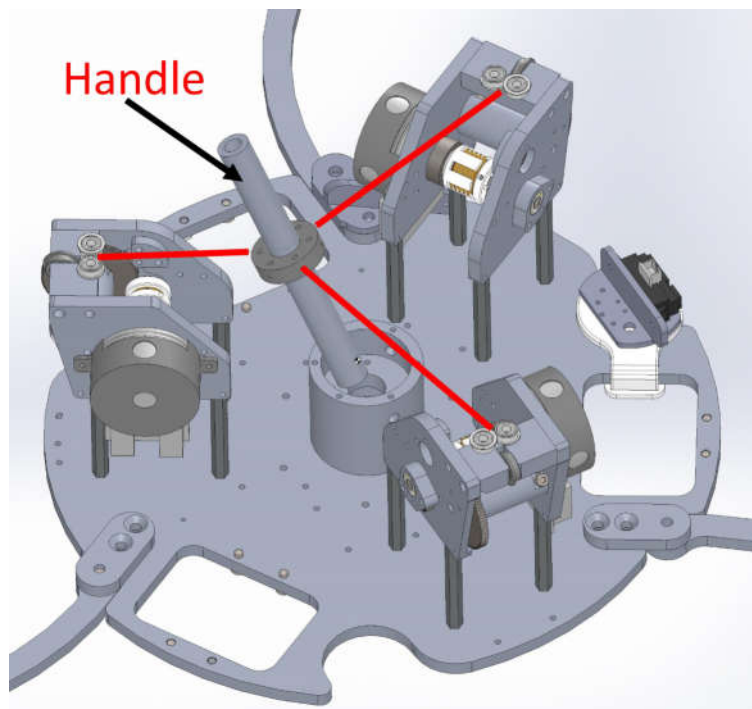
Figure 2.13: Orientation mechanism design "B" with cables highlighted

are designed in a double row so the contact point of the wheels and mat stays as a perfect circle. Having this feature, the mobile platform will not wobble while moving which consequently makes the motion smooth and less noisy.

2.3.2.4 Safety Features:

As mentioned earlier, to ensure the safety in case of sensor failure in detecting the force transferred to the patient's limb, the system should have inherently safe mechanisms to limit the transferred forces or torques. In this robot two main inherently safe mechanisms are implemented in the mobile base and the orientation mechanism. In the mobile base, as the motion is created by omni-wheels on the surface, the amount of the transferable forces/torques can be adjusted in two ways: (a) by changing the PTR, and (b) by changing the type of material of the mat. Modifying the PTR based on the application type (UE or LE) will limit the output force created by the robot. Also changing the material of the mat will change the friction coefficient between the wheels and the

Figure 2.14: Manufactured Omni-wheels for mobile platform and orientations mechanism "A"

mat and limits the output force generated by the robot.

In the case of orientation mechanisms, design "A" or "B", the amount of the transferred torque can be limited by changing the PTR and by adjusting: (a) the normal force between the dome and the wheels in design "A", and (b) by changing the threshold of the friction clutches in design "B". In both mechanisms, the inherently safe implemented features will ensure safe interaction between the robot's end-effector and patient's limb.

2.3.3 Electrical Components Design

To initiate the electrical component design, first, we have to take a look at the necessary elements in the control system. Fig. 2.15 shows the schematic diagram of the elements in the system. For electrical components, the criteria and selection procedure are described in this section. It is important to mention that one of the main criteria considered in selecting and designing the electrical components is to eliminate the need for designing new PCB boards by selecting off-the-shelf products. The reasons for selecting off-the-shelf products are (a) to reduce the number of newly designed components, (b) increase the reliability of the system, (c) reduce the overall price of components, (d) reduce the chance of failure, and (e) decrease the manufacturing challenges

and time.
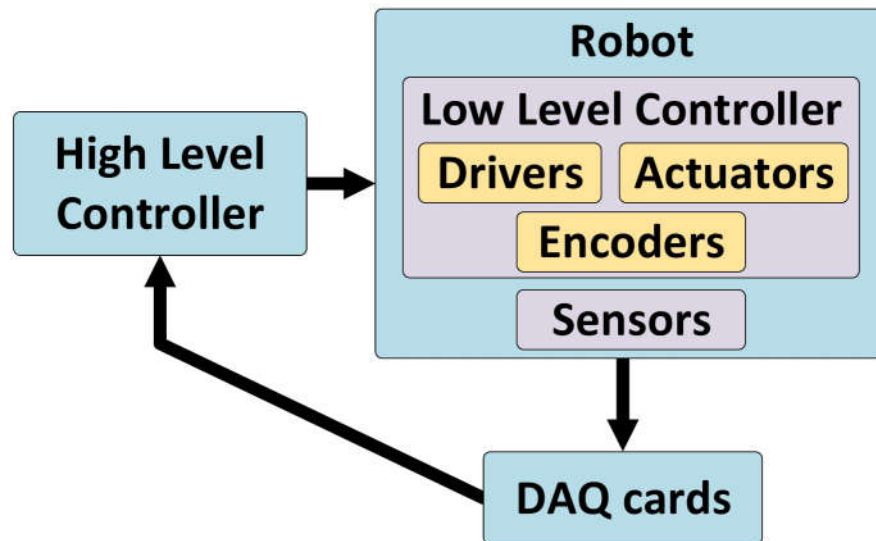
Figure 2.15: Schematic representation of the components in the proposed system

2.3.3.1 Sensor Selection

To allow for different rehabilitation exercises (such as passive movement therapy and kinesthetic interactive therapy), different modes of operation are needed, namely: position, velocity, and current control modes. For each mode, the corresponding feedback is required. The aforementioned feedback modalities are (a) the position, (b) the velocity and (c) the current in the actuators together with (d) the force resulting from the interaction between the patient's limb and the robot.

Localization Sensor: To localize the position of the mobile base on the ground mat, different methods are possible. The previous method used for localization of the first generation of the lower limb robot developed in the REACT lab at Western University [20], is the stereoscopic vision tracking system developed by ClaroNav, a Micron Tracker model BB-BW-S60 stereo camera [68]. Using this technique requires the camera to be installed beside the workspace and the tracking patterns to be attached to the robot while being visible to the camera at all times. This

creates additional difficulties in the calibration process. Additionally, the update rate of the position measured using the tracker is 30 *Hz*, which is very low for the high-quality control required for the therapeutic applications. Adding all of these issues requires us to look for a better method for localization. To achieve proper accuracy in motion and low overall cost, commonly used incremental sensors are selected for this application. Comparison between different incremental sensors, suggests the use of two ADNS-9800 laser motion sensors to measure the relative displacement of the robot's base on the ground mat. The sensors are attached at specific locations on the bottom of the base plate to measure the velocity of the motion in two directions as depicted in Fig. 2.16. Each of these sensors is able to measure the incremental motion in two directions (local x and y coordinates). By fusing the data collected by the two sensors, we can measure the amount of movement in two linear directions (global "X" and "Y") and one rotation (global "Z" direction). For the type of motion expected for rehabilitation therapy applications, the position of the robot can be measured with an accuracy of 0.05mm on the ground mat.

The only problem associated with this type of laser sensor is that as the measurement is incremental, the global position of the robot's base depends on the initial (starting) position. To overcome this issue, three sets of infrared proximity sensors, Sharp GP2Y0A21YK, that can provide global motion measurements are used. These sensors can measure the distance between the robot and the surrounding walls of the workspace with an accuracy of 5 *mm* up to the range of 1.5 *m* and are attached on the side of the mobile base as shown in Fig. 2.17(a). The purpose of using these sensors, despite their low accuracy, is to overcome the above-mentioned problem of laser sensors. By fusing the high accuracy measurements from the incremental laser sensors and the low accuracy data of these absolute proximity sensors, the global position of the robot can be determined.

Orientation Sensor: To measure the orientation and the angular velocity of the handle, two alternative methods are possible, namely, (i) indirect method using the position of the actuators and kinematics calculations, and (ii) direct measurement of the handle's position. It should be

(a) (b)
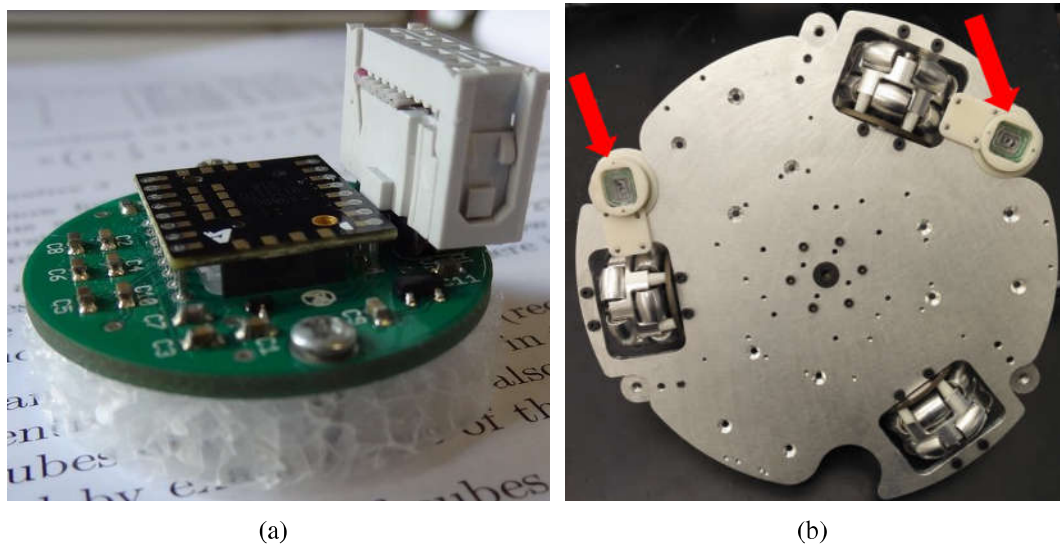
Figure 2.16: (a) ADNS 9800 laser sensor, and (b) location of the two ADNS sensors on the bottom of the Robot.

noted that the indirect method cannot be used as feedback for the position/velocity control loop of the robot. This is because as mentioned earlier, the proposed mechanical safety feature allows the wheels to slip (in design "A") or clutches to slip (in design "B") when the applied force is higher than the adjusted threshold. As a result, it is not possible to calculate the Cartesian motion of the end-effector of the robot (which interacts with the patient's limb), based on the joint space measurements of the actuator position.

The alternative solution is the direct measurement of the orientation and the angular velocity of the handle. For this purpose, one approach is to attach incremental or absolute encoders to the corresponding axes of the spherical joint at the base. However, due to the size limitation of the spherical joint and the cost of small size encoders, this method may not be the best option. Another approach is to attach a gyro sensor to the handle to measure the orientation of the robot's end effector. By integrating the output of the gyro, which is the angular velocity in two DOFs provided in precise interrupt cycles, the relative amount of rotation with respect to the initial position can be measured. The sensor selected for this purpose is the triple axis gyro breakout board MPU6050 with 16bits ADC and the full-scale range of ± 2000 dps. By using this sensor, an accuracy of 3×10^{-2} deg/sec in angular velocity can be achieved which is high enough to

control the orientation of the handle. The sensor is attached to the handle rod and is depicted in Fig. 2.17(c).
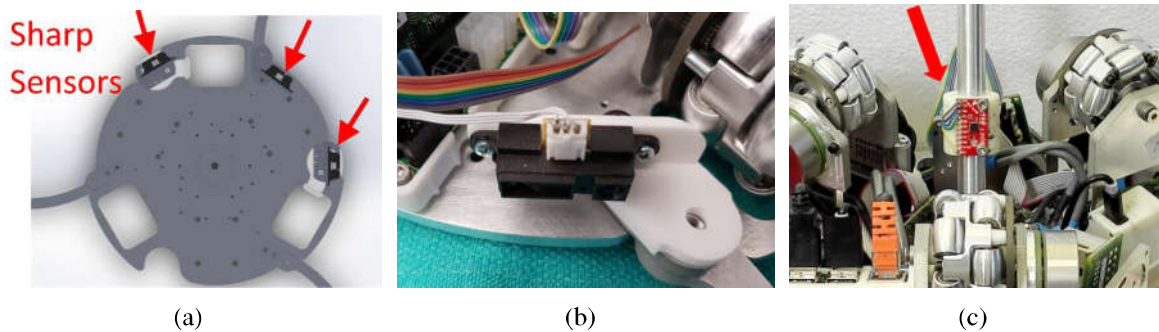
Figure 2.17: (a) Sharp sensor locations on the base plate ; (b) Sharp proximity sensor on the side of the mobile base, and (c) the MPU6050 gyro sensor attached to the handle rod.

However, the estimated position calculated by the indirect method can be used to measure the amount of slippage. This can be done by comparing the position measured with the direct method and the position obtained from the indirect measurement. The slippage calculation is helpful in practice to (a) minimize the power consumed by the actuators during slippage, and (b) prevent excessive wear caused by slippage between the inner surface of the dome and the wheels in design "A" or the clutches in design "B".

Force measurement: To allow for haptics-enabled rehabilitation therapies, the amount of interactive force and torque between the patient and robot should be measured. One method to measure these interaction forces and torques is to install a force sensor at the interface of the robot and the patient's limb. Considering different factors such as the range of forces in LE therapy, the size of the force sensor, the data acquisition technique, and cost, a six-axis HEX-70-CE-2000N OptoForce sensor was selected [69]. The maximum update rate of the sensor data is $1\ kHz$ that can be read through the DAQ module using UART interface. As shown in Fig. 2.5(b), the force sensor is attached to the foot plate and the connecting rod.

2.3.4 Actuator and Driver Selection

There are a variety of motors can be used for the proposed design, namely, EC or DC motors from different manufacturers. Some of the constraints regarding the actuator selection are driver availability, ease of use, high-speed communication, size, weight, operating voltage and technical support of the manufacturer. Among all possible solutions, Maxon EC flat motors were chosen as they can provide high torque at low speed with a reasonable price. This option is suitable for this particular application due to the weight and size constraints and comparably higher output torque on other motors. MAXON EC45 50W 36V motors were selected to drive the Omni-wheels with continuous and stall torque of 0.09 *Nm* and 0.48 *Nm*, respectively. To decrease the amount of wiring to and from the mobile platform, the drivers were designed to be installed inside the mobile base. This way the connection between the motors and drivers would be inside the mobile base and the cabling would be minimized. The process of driver selection was as follow.

2.3.4.1 Electronic Driver Selection

To correctly select the electronic drivers, several design considerations should be considered such as (a) power, (b) operating voltage of the actuator, (c) available space for installation, (d) possible modes of operation (position, velocity or current modes), and (e) communication interface. To deliver various types of rehabilitation exercises (such as passive movement therapy and interactive kinesthetic therapy), it is necessary to control the actuators in position control, velocity control and current control modes of operation. To achieve high-quality force and torque control, the operating frequency of the low-level control loop needs to be high. It has been shown that for general haptic rendering systems, the sampling frequency defines the allowable strength of the force reflection. This is related to the concept of Z-width [70]. In this regard, the capability of the implemented communication interface plays a significant role in the sampling frequency and the speed of the control loop. This is due to the different Baud-rates of the interfaces which directly affects the speed of the control loop.

For the selected actuator, based on different operating voltages and currents, Maxon provides a variety of digital positioning controllers. To minimize the size and the price of the controller, the EPOS2 Module 36/2 was selected which has the required control modes with 1 Mb/sec USB/CANOpen communication interfaces and is depicted in Fig. 2.18. Using this module gives us the opportunity to connect all six drivers in series and control the actuators using USB/CANOpen interface on the first Node.
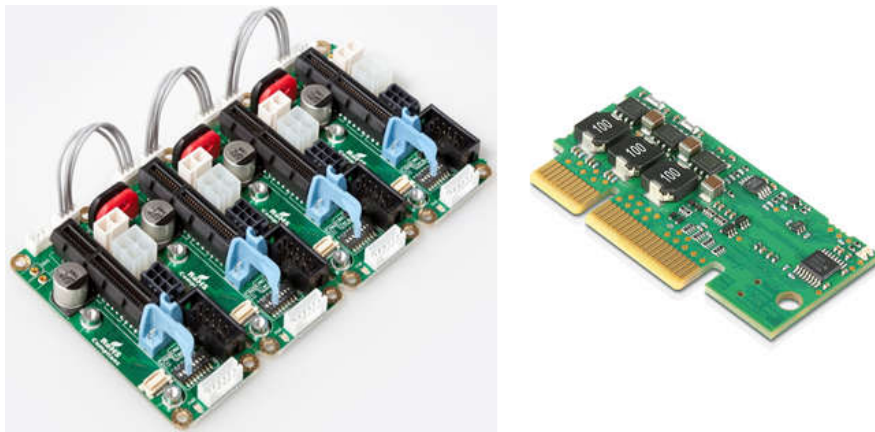
Figure 2.18: Maxon EPOS2 Module 36/2 motherboards connected in series and the EPOS2 driver

2.3.4.2   Processing and Communication Devices

For high-level control, the real-time Quarc library (from Quanser Inc, Markham, ON, Canada) was used in MATLAB/Simulink. The Quarc library provides powerful tools and capabilities such as real-time and multi-threaded control that can easily interact with hardware interfaces such as Ethernet and DAQ cards. To simplify and reduce the amount of wiring and cabling, a local intermediate processing system was utilized as an interface between the robot and Quarc. The task of this processing unit is to receive actuator commands from the high-level controller and send them to the EPOS drivers, while it reads the sensor's data and sends them back to the high-level controller. Based on the computational power and the size required for this processing unit, a Raspberry Pi (RPI) version 3B was selected as the low-level processing unit on the robot.

The data transfer protocol between Quarc and Raspberry Pi is based on the UDP protocol via an Ethernet cable. This communication interface provides fast and real-time (measured transfer time<400 μs for 64-Bytes packet size) data transfer between the high- and the low-level controllers. The schematic diagram of the system and the components involved together with the communication protocol are shown in Fig. 2.19.

It should be noted that to achieve a robust and high-quality force and torque control, the high-level controller loop is suggested to have an update frequency of at least 1000 Hz. This means that the low-level control loop should be able to send command data and receive feedback (position, velocity or current) from all EPOS drivers and the feedback data from OptoForce DAQ and gyro sensor in less than 1 ms for each loop. Based on the communication data-sheet of the Maxon driver, using USB interface an update rate about 2.3 ms can be achieved for each driver. This would result in a total sample time of 13.8 ms to send and receive data to/from the six EPOS drivers. To make the communication between the Raspberry Pi and the EPOS drivers faster, the CANOpen interface was used by attaching a PICAN2.0 shield to the Raspberry Pi. Using the Socket CAN library, the sample time including all EPOS drivers was reduced to 1 ms. This will be described in Section 2.3.5. Fig. 2.19 shows the communication diagram for transferring data between the Raspberry Pi and EPOS drivers.

2.3.5 Programming the PI

Some of the interesting features of the RPI are (a) small size unit with comparably powerful processing power (as small as a mobile phone), (b) wide variety of I/O interfaces such as Universal Asynchronous Receiver/Transmitter(UART), Serial Peripheral Interface(SPI), Ethernet(LAN and WAN), and (c) the Linux operating system environment (Raspbian) for developing the codes and User Interfaces (UI). Having all of these interesting features together was the reason to select RPI for the Local Processing Unit (LPU) as (a) it can be used to read the sensors data locally (eliminates lots of cabling to and from the robot), (b) communicate (send commands and receive feedback from the motors) with the EPOS drivers using Serial or CANOpen protocol, and (c)
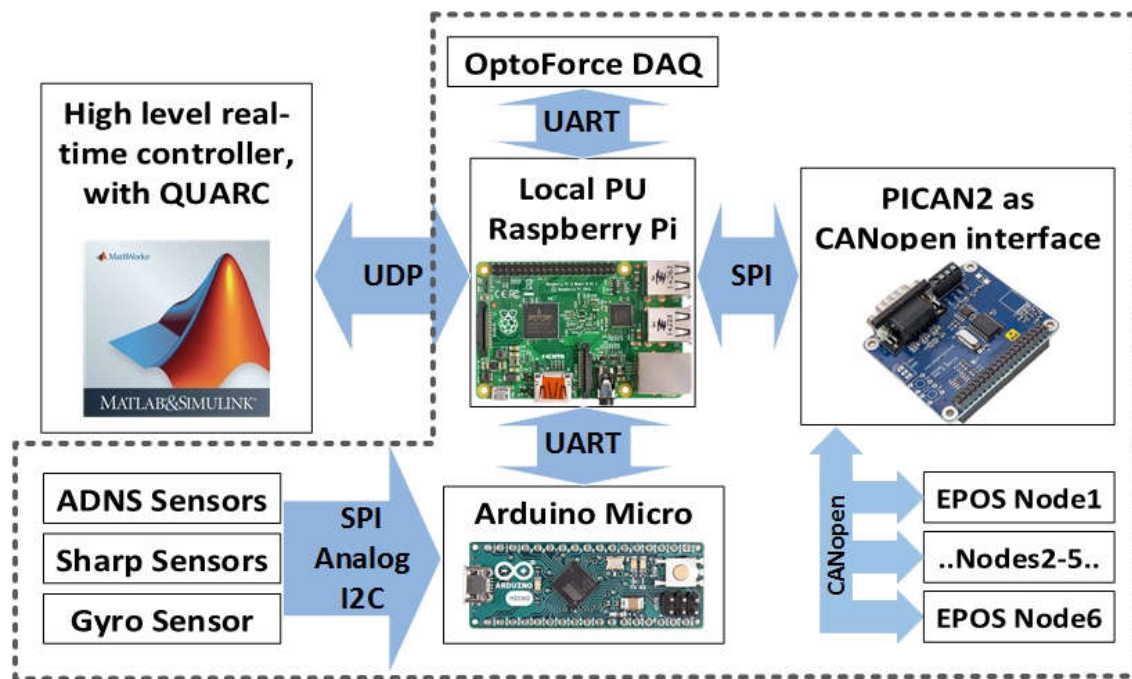
Figure 2.19: Communication protocol between different components of the system; The components inside the mobile base are wrapped with the dashed line

send and receive the control commands to the PC (running MATLAB) using the UDP protocol. Adding all of these features significantly reduces the number of cables attached to the robot which is advantageous as the robot is a mobile platform. To optimize the RPI for running the local control loop, the overall tasks were split into 4 major semi-independent functions: (I) Controlling the EPOS drivers, (II) UDP send and receive, (III) Configuring and reading OptoForce data, and (IV) Reading the sensor data from Arduino through UART. The details of each task are described below.

2.3.5.1 (I) Controlling the EPOS Drivers Using RPI

USB vs CANOpen: To connect the EPOS2 drivers to the RPI, the first interface option of the RPI that was used was the USB. By using the libraries provided by Maxon for Linux systems, a C++ program was developed to control the EPOS drivers in Raspbian by sending and receiving the command to Node1 while measuring the elapsed time. It took 8 *ms* on average to send and

receive the command and feedback to one Node of the EPOS drivers. As in total, the system has 6 actuators (Driver Nodes), it took about 48*ms* to command all actuators in one control loop. This elapsed time would limit the control loop speed to 20 *Hz* which is much lower than the desired value of 1 *kHz* for high-quality digital control of the system. The problem with the slow communication speed was found to be the USB communication interface in the RPI. Based on the Maxon datasheet, to increase the speed of communication, the CANOpen interface on EPOS was suggested. As the RPI does not have CANOpen interface, the PICAN2 shield on RPI for CANOpen communication was used to control the EPOS2 drivers with faster speed.

By using SocketCan libraries, contributed by Volkswagen Research to the Linux kernel, another code was developed to control EPOS2 on Raspbian. Using this method, the elapsed time for sending the command data to each EPOS Node was decreased to 150 *mus*. The elapsed time to communicate with all of the 6 Nodes of EPOS was measured as 900 *mus*. As this elapsed time value is lower than 1 *ms*, having a control loop with the speed of 1 *kHz* was possible.

Modes of Control: Different modes of control can be defined in the EPOS drivers in addition to the different types of feedback. Controlling the drivers in a low-level C++ code in RPI requires defining the mode of operation (profile position, velocity or current) and the type of feedback (actual position, velocity or current) from the EPOS drivers. A summary of the procedure that was followed in setting and operating the drivers in the CANOpen protocol is given in Table. 2.2. To communicate between Simulink and the developed code on RPI for controlling the robot, eight modes of operation for EPOS were defined as summarized in Table. 2.3. There are two main modes of operation in the Simulink code, (a) the Setting Mode with ID "333", and (b) the Operating Mode with the ID starting with "1". In the last version of the developed code as shown in Table 2.3 there are ten operating modes for different commands and feedback.

It is important to mention that in the initial 0.01 *s* of the start of the Simulink code, the Setting Mode would be activated to set the parameters in EPOS drivers, and after that, the specific Operating Mode would be activated. The mode of operation would be sent to the RPI in the initial

stage of the high-level control code in Simulink after the Setting Mode.

2.3.5.2 (II) UDP Send and Receive

UDP Packet Definition: As mentioned before the data transfer between mobile processing unit (RPI) and MATLAB (Simulink on PC) will be via an Ethernet connection using the UDP protocol. This is the fastest way of data transfer using a single Ethernet cable attached to the mobile platform. Having this option, in future phases of the project will be useful as the WiFi module of the RPI can be utilized (by keeping the communication protocol the same as before) to eliminate the need for the Ethernet cable to be attached to the robot. For UDP communication, the Stream Client block provided by Quanser in Simulink was used to send the UDP packets to the RPI and the Stream Server block was used for receiving the UDP packets from the RPI. The packet size for the data transferred from Simulink to the RPI is a nine four-bytes double type packet. The packet contains the structure shown in Table. 2.4.

For the feedback data from the RPI to Simulink, the packet size is twenty-one four-bytes double which is described in Table. 2.5.

The measured elapsed time to send and receive the packets through UDP is $400mus$ that is lower than the $1ms$ loop time in Quarc Simulink.

2.3.5.3 (III) Reading OptoForce Data

There are three options available for communicating to the OptoForce DAQ card, (a) RS232 (b) UART through USB and (c) CANOpen. To have a secure connection, a USB (UART) connection was used to connect the DAQ card to the RPI. A code was also developed and tested to read the data from OptoForce DAQ card at four different update rates, $1 \, kHz$, $333 \, Hz$, $100 \, Hz$ and $33 \, Hz$. For our application, the fastest update rate($1 \, kHz$) was selected. The process of reading the data is as follow: first, in the Setting Mode, the zeroing command would be sent to the DAQ card. Secondly, in the Operating Mode, the data would be read through the UART from the DAQ card.

Table 2.2: EPOS configuration procedure for initialization, enabling and operating

Initialization	• Opening Communication to CAN-network
	
	   – Defining PDO and SDO masks and opening the Socketcan network
	
	• Configuring the each Node
	
	   – Resetting the NMT connection
	   – Entering the Pre-operational Mode
	   – Setting the Operation Mode (Profile Position, Velocity or Current Mode)
	   – Configuring the parameters of each node(for example profile maximum acceleration, maximum velocity, maximum current, PID values and etc)
	   – Setting the PDO configuration, e.g. defining PDO Receive and Transmit type plus setting the number and type of Rx and Tx packages (in other words defining the type of command being sent to the EPOS and feedback like actual position, velocity or current)

Enabling	• Entering the Pre-Operational Mode • Shutting down the drivers • Switching on and enabling • Entering Operational Mode by opening the PDO
Commanding and receiving feedback	• Sending proper PDO command (target position, velocity or current) by writing in SocketCan • Requesting the drivers for sending proper PDO feedback (position, velocity or current)

Table 2.3: Different modes of control defined at the developed code in RPI for EPOS drivers

Mode ID	Definition
111	Profile position mode with actual position feedback
112	Profile position mode with actual velocity feedback
113	Profile position mode with actual current feedback
121	Profile velocity mode with actual position feedback
122	Profile velocity mode with actual velocity feedback
123	Profile velocity mode with actual current feedback
124	Profile velocity mode with No feedback
131	Current mode with actual position feedback
132	Current mode with actual velocity feedback
133	Current mode with actual current feedback
333	Setting Mode

Table 2.4: Sent packet configuration from Simulink to RPI

In the Setting Mode	**[Setting Mode ; Max Profile Acc Dcc ; Max Current ; Max Profile Velocity ; KP PID ; KI PID ; KD PID ; OptoForce Zeroing ; Motor Enable]**
In the Operating Mode	**[Operating Mode ; Node1 desired Command ; Node2 desired Command ; Node3 desired Command ; Node4 desired Command ; Node5 desired Command ; Node6 desired Command ; OptoForce Zeroing ; Motor Enable]**

Table 2.5: Received packet configuration from RPI

Feedback Data Packet:	• Gyro sensor	• 2 doubles
	• Sharp sensor	• 3 doubles
	• ADNS sensor	• 4 doubles
	• OptoForce(Fx,Fy,Fz,Tx,Ty,Tz)	• 6 doubles
	• EPOS feedback	• 6 doubles

2.3.5.4   (IV) Reading Data Through UART From Arduino

Although SPI and I2C are among the available interfaces to attach sensors and read data by RPI, analog sensors cannot be connected to the RPI directly. To overcome this, all of the sensors namely ADNS, Sharp and Gyro were connected to an Arduino Micro with SPI, Analog, and I2C interfaces respectively to configure and read the data. After reading the sensor data using Arduino Micro which takes less than 1 *ms*, the data is sent to the RPI through the serial protocol (UART). A proper code was developed in the RPI to read the data from Arduino.

2.3.5.5   Multi-thread Code on the RPI

Despite all of the advantages of the RPI (small size, a variety of interfaces, etc.), the processing power of the CPU is limited. To make sure that the local control loop on the RPI takes less than 1 *ms* to complete, a multi thread code was developed to run four main semi-independent tasks that were mentioned earlier for the four cores of the CPU. For this purpose, the "pthread" library was used to run four parallel threads for running the four above-mentioned infinite-loop functions. By using this library, we made sure that all functions could complete the functional loop in less than 1 *ms* and were ready for the next command loop that was precisely controlled by Quarc in Simulink.

To prevent data corruption and to synchronize the threads, the UDP thread is in charge of the data transfer between multiple threads. In the code, the UDP thread sends a request to other threads for the data and sets the value of the parameters that are needed for other threads. The pthread library was used for multi-threading and data handling.

Chapter 3

Robot Modeling and Control

3.1 Introduction

In this chapter, the robot model and the data acquisition algorithms for the sensors will be described. Then the therapy and control modes for the different experiments will be discussed.

3.2 Robot Modelling

3.2.1 Localization

As mentioned earlier, for localization of the robot's base on the mat, two types of sensors were selected: (a) high accuracy incremental type ADNS laser sensors and (b) low accuracy absolute type Sharp proximity sensors. To localize the position of the robot, the data from both ADNS sensors and three Sharp sensors is sent to the Simulink model for processing. To obtain the global position of the robot accurately with respect to the global coordinate system defined on the mat, the feedback data of the two sensors is fused. Here, the localization algorithm for each type of each sensor will be described. The data fusion of the two sensors is suggested as one of the future steps of the project in Chapter 5.

51

ADNS localization   The incremental motion captured by the ADNS sensor in the 1 *ms* time step is sent to the Simulink code. The goal is to use the feedback data collected from the two ADNS sensors to measure the amount of motion of the base plate with respect to the initial position of the robot at the start of the program. Using the method provided in [71], the incremental displacement measured by the sensors can be transferred to the global position and orientation of the robot's base plate. As shown in Fig. 3.1, four coordinate systems are assigned: (a) the global coordinate system attached to the ground mat C_G, (b) a local coordinate system on the center of the robot C_R, (c) a coordinate system attached to the position of the right sensor C_{SR} aligned with the direction of the measurement and (d) a coordinate system attached to the position of the left sensor C_{SL} aligned with the direction of the measurement. The location of each sensor, O_S, is determined by the position vector $\vec{r}_S$ with the angle ψ_S with respect to X_R. The angle between X_S and X_R is denoted by ϕ_S. The incremental displacement measured by the sensors can be shown in the vector format $\vec{\Delta}_{OS}^S = \{\Delta X_{SR}, \Delta Y_{SR}, \Delta X_{SL}, \Delta Y_{SL}\}^T$. Here SR is the sensor attached to the right side of the base plate and SL is the one on the left side. To transfer the measurement from the local sensor coordinate frames, C_{SR} and C_{SL}, to the global coordinate frame, the rotation matrix $R_{(\theta+\phi)}$ can be used. The incremental displacement of the O_R in the global coordinate, Δu can be calculated by using (3.1).

$$\Delta u = F^+ b \tag{3.1}$$

where F^+ is the pseudo inverse of F

$$F^+ = (F^T F)^{-1} F^T \tag{3.2}$$

$$F = \begin{pmatrix} 1 & 0 & -r_{SR}sin(\theta + \psi_{SR}) \\ 0 & 1 & r_{SR}cos(\theta + \psi_{SR}) \\ 1 & 0 & -r_{SL}sin(\theta + \psi_{SL}) \\ 0 & 1 & r_{SL}cos(\theta + \psi_{SL}) \end{pmatrix} \tag{3.3}$$
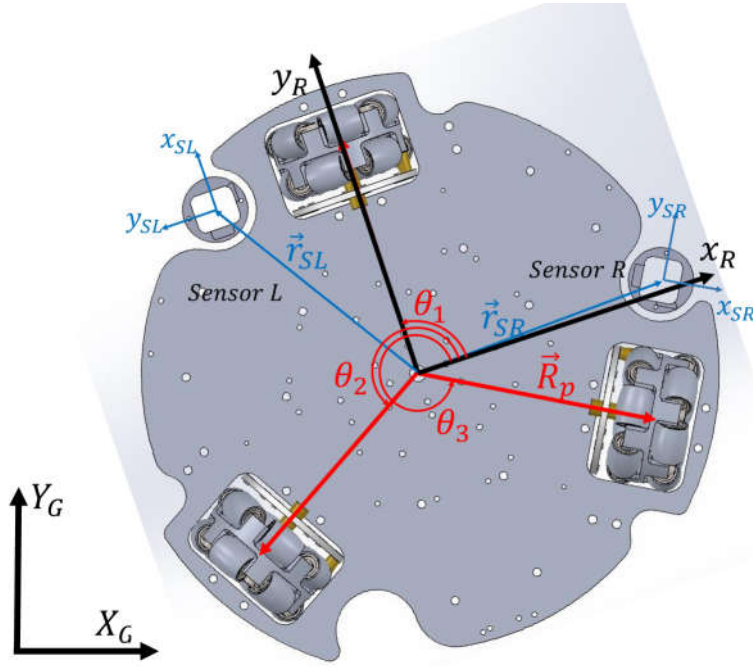
Figure 3.1: Coordinate systems assigned for localization using ADNS sensors

$$
b = \begin{pmatrix} cos(\theta + \phi_{SR}) & -sin(\theta + \phi_{SR}) & 0 & 0 \\ sin(\theta + \phi_{SR}) & cos(\theta + \phi_{SR}) & 0 & 0 \\ 0 & 0 & cos(\theta + \phi_{SL}) & -sin(\theta + \phi_{SL}) \\ 0 & 0 & sin(\theta + \phi_{SL}) & cos(\theta + \phi_{SL}) \end{pmatrix} \vec{\Delta}_{OS}^{S} \qquad (3.4)
$$

By integrating the Δu over time, the position vector of the robot's center O_R at the new step time $t + 1$ can be calculated as $u_{t+1} = u_t + \Delta u$.

3.2.2 Jacobian Model (Planar Motion)

To control the position, and the velocity of the robot, the mathematical relations between the velocity of the robot in local coordinate $\{v_x, v_y, \omega_z\}^T$ and the rotational velocity of the wheels $\{\omega_1, \omega_2, \omega_3\}^T$ is required. As shown in Fig. 3.2(a), the center of the robot is shown with a vector $\vec{R}_k$ to the contact point of each wheel with the mat. The angle between the vectors $\vec{R}_k$ and the

axis x is assigned with angle $\theta_k, k = \{1,2,3\}$ as depicted in Fig. 3.2(a). The relation between the robot's velocity in local coordinates $\{v_x, v_y, \omega_z\}^T$ and the wheel's rotational velocity can be represented as (3.5) [72]. In this equation, r_w is the radius of the wheels, and R_P is the distance between the center of the robot and the contact point of the wheels with the mat.

$$
\begin{pmatrix} \omega_1 \\ \omega_2 \\ \omega_3 \end{pmatrix} = \frac{1}{r_w} \begin{pmatrix} -sin\theta_1 & -cos\theta_1 & 1 \\ -sin\theta_2 & -cos\theta_2 & 1 \\ -sin\theta_3 & -cos\theta_3 & 1 \end{pmatrix} \begin{pmatrix} v_x \\ v_y \\ R_P\omega_z \end{pmatrix} \tag{3.5}
$$

(a)	(b)
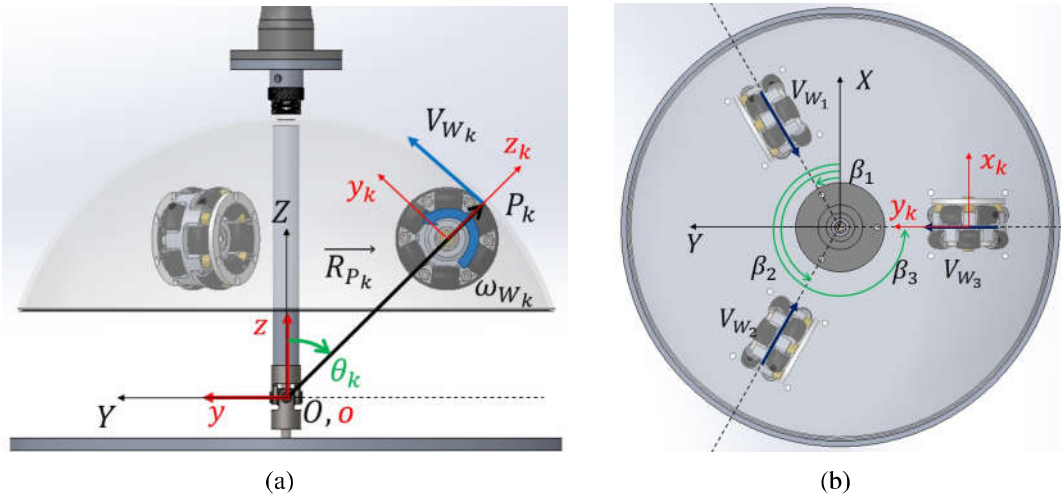
Figure 3.2: Global and local coordinates assigned to describe the kinematics: (a) side view, (b) top view

Using (3.5) and having the desired robot's velocity in the local coordinate system, we can calculate desired rotational velocity of the wheel that can be sent as the command to the drivers.

3.2.3 Jacobian Model (Orientation Design A)

The method used here to derive the inverse kinematic model of the system uses the velocity-based kinematics approach in [73]. As shown in Fig. 3.2(a), two coordinate systems are defined with origins O and o, both at the center of the universal joint. The axes of the Global coordinate system C_G are fixed at the base plane while those of the rotating coordinate system C_l are fixed with

respect to the dome. Another set of coordinate systems C_k are defined in the center of each wheel shown in Fig. 3.2(a). Starting from the velocity of the point P_k (the contact point of wheel k and the dome, on the wheel) we can calculate this velocity vector in the local coordinates of the wheels as

$$\mathbf{v}_{P_k} = \omega_k \times \mathbf{r}_k = [\omega_k, 0, 0]^T \times [0, 0, r_W]^T = [0, -r_W \omega_k, 0]^T$$

$$k \in 1, 2, 3$$

(3.6)

Here, $\mathbf{v}_{P_k}$ is the velocity of the point P_k in the local coordinates of C_k, ω_k is the rotational velocity of the wheel "k". Moreover, $\mathbf{r}_k$ and r_W are position vector of the point P_k and the radius of the wheel, respectively. Using the transformation matrix $\mathbf{T}_k$ which maps the local coordinate of C_k to the global coordinates of C_G, after two rotations with respect to x_k and z_k, the velocity in C_k can be mapped to that in C_G as shown in (3.7).

$$\mathbf{V}_{P_k} = \mathbf{T}_k \mathbf{v}_{P_k}$$

(3.7)

where

$$\mathbf{T}_k = \mathbf{R}_z(\beta_k)\mathbf{R}_x(\theta_k) = \begin{bmatrix} -s\beta_k & -c\beta_k c\theta_k & c\beta_k s\theta_k \\ c\beta_k & -s\beta_k c\theta_k & s\beta_k s\theta_k \\ 0 & s\theta_k & c\theta_k \end{bmatrix}$$

(3.8)

In this equation, "c" and "s" denote the cosine and sine of the variables, respectively. Knowing the velocity of the point of contact between the wheels and the dome in C_G, the angular velocity of the dome can be calculated as

$$\Omega_k = \frac{\mathbf{R}_k \times \mathbf{V}_{P_k}}{||\mathbf{R}_k||^2}$$

(3.9)

In this equation, $\mathbf{R}_k$ is the radial vector which connects the origin of C_G to the contact point P_k and $||\mathbf{R}_k||^2$ is the second norm of that vector. Also, Ω_k is the angular velocity of the dome generated by the kth omni-wheel, when other wheels are in free motion. Summing up the three angular velocity vectors generated by each omni-wheel, the total angular velocity vector of the dome can be calculated as $\Omega = \sum_{k=1}^{3} \Omega_k$. As a result, the Jacobian matrix can be obtained from the relation between the angular velocities of the wheels and the angular velocity of the dome as

$$\Omega = \mathbf{J}\omega = \frac{r_W}{||\mathbf{R}_k||^2} \begin{bmatrix} J_{11} & J_{12} & J_{13} \\ J_{21} & J_{22} & J_{23} \\ J_{31} & J_{32} & J_{33} \end{bmatrix} \begin{bmatrix} \omega_1 \\ \omega_2 \\ \omega_3 \end{bmatrix} \tag{3.10}$$

where

$$J_{11} = -R_{1Y}s_{\theta_1} - R_{1Z}s_{\beta_1}c_{\theta_1} \ , \ \ J_{12} = -R_{2Y}s_{\theta_2} - R_{2Z}s_{\beta_2}c_{\theta_2}$$

$$J_{13} = -R_{3Y}s_{\theta_3} - R_{3Z}s_{\beta_3}c_{\theta_3} \ , \ \ J_{21} = R_{1X}s_{\theta_1} + R_{1Z}c_{\beta_1}c_{\theta_1}$$

$$J_{22} = R_{2X}s_{\theta_2} + R_{2Z}c_{\beta_2}c_{\theta_2} \ , \ \ J_{23} = R_{3X}s_{\theta_3} + R_{3Z}c_{\beta_3}c_{\theta_3}$$

$$J_{31} = R_{1X}s_{\beta_1}c_{\theta_1} - R_{1Y}c_{\beta_1}c_{\theta_1} \ , \ \ J_{32} = R_{2X}s_{\beta_2}c_{\theta_2} - R_{2Y}c_{\beta_2}c_{\theta_2}$$

$$J_{33} = R_{3X}s_{\beta_3}c_{\theta_3} - R_{3Y}c_{\beta_3}c_{\theta_3}$$

In (3.10), R_{1X}, R_{1Y} and R_{1Z} are the three components of the radial vector $\mathbf{R}_k$. As can be seen from (3.10), the Jacobian is time-invariant and depends only on the geometrical parameters of the system. Consequently, if the constants can be chosen such that $\mathbf{J}$ is non-singular, the angular speed of each omni-wheel ω_k can be obtained using the desired angular velocity of the dome Ω_{des}. Based on the singularity calculation performed in [73], internal singularities occur only in impractical cases when the radius of the wheels becomes zero $r_W = 0$ or the radius of dome tends to infinity $R \to \infty$. Boundary singularities still exist at the limits of the working volume of the mechanism, for example, when the connecting rod touches one of the wheels. Considering boundary singularities, the safe working volume of the robot is a cone with a tip angle of 30 deg. The tip of the cone is at the center of rotation, and the main axis is along the Z axis of C_G.

3.3 Therapy Modes and Control

3.3.1 Therapy Modes

The goal of the robotic systems developed for post-stroke rehabilitation purposes is to enable patients to regain their movement ability by providing various training and therapy exercises. Different stages of recovery of the patient, requires different passive or active robot-assisted therapy modes suggested by the therapist. As an overview, various therapy modes provided by robot-assisted rehabilitation can be categorized as: (i) the passive mode, (ii) active mode, (iii) active assist mode, and (iv) active resist mode [45]. For example, in the early stages of therapy due to the weakness of muscles and inability of the patient in performing voluntary motions, the passive mode should be used. In this stage, the goal is to decrease muscle atrophy and increase the movement range. By regaining muscle strength and recovering after more therapy sessions, active modes can be used to engage the patient in the process of the rehabilitation. In this phase, the voluntary motion of the patient modifies the trajectory of the robot in performing the tasks, so this stage of the therapy is referred to as the "patient in charge" phase.

Active modes can be assistive in the initial stages to increase self-initiation of the patient in performing the tasks or they can be resistive to increase the strength of the muscles. The former mode is similar to a "therapist in charge" phase in conventional therapy and the later is referred to as an "active constrained" mode.

In this project, to test the performance of the designed system, various control strategies are implemented for passive, active-assist and active-resist therapy modes. Each therapy mode was tested in a study involving healthy subjects before future experiments involving patients.

3.3.2 Control Strategy

Several control strategies have been developed to utilize different feedback data such as position, force or bio-signals to provide appropriate therapy procedure and to control the interaction

between robotic systems and patients [45]. The four main control strategies for robotic-assisted rehabilitation are: (a) position control, (b) force and impedance control, (c) EMG-based control and (d) adaptive control. For this project, to validate the designed system, only the position and force control strategies are implemented as the other methods of control are more sophisticated and outside the scope of this project.

3.3.2.1 Position-based Tracking Control (Robot-in-Charge Phase)

Mobile Base As needed in initial stages of therapy, the robot should be controlled in position modes. The commonly used position control loop is a closed PID control loop as shown in Fig. 3.3. Here a desired global position is the input of the control loop.

The error between the desired and actual positions is sent to a well-tuned PID controller and the output of the controller is transferred to the velocity of the robot in the local coordinate system using the rotation matrix. The tuning process of the PID controller was done using MATLAB toolboxes. The model of the robot is unknown in this closed-loop PID controller and it contains the disturbance load applied by the environment. The PID controller was tuned in the presence of some disturbance load by a user assuming that the maximum force capability of the system is applied by the robot. Applying the maximum force capability of the system to the robot during PID tuning ensures the stability of the system under various therapy procedures. The load applied by the environment during the therapy procedure is mainly due to the weight of the limb and the static force applied by the muscles. The force capability of the robot and the PID controller ensure a proper performance of the robot under various working conditions. It is important to mention that only quasi-static loads (due to the nature of the rehabilitation process) were applied to the robot during the PID tuning process. Using the Jacobian calculated in Eq. 3.5, the desired rotational velocity of the wheels is calculated. By knowing the PTR, the desired velocity to the EPOS drivers is sent using the UDP protocol through the Ethernet cable to the robot.
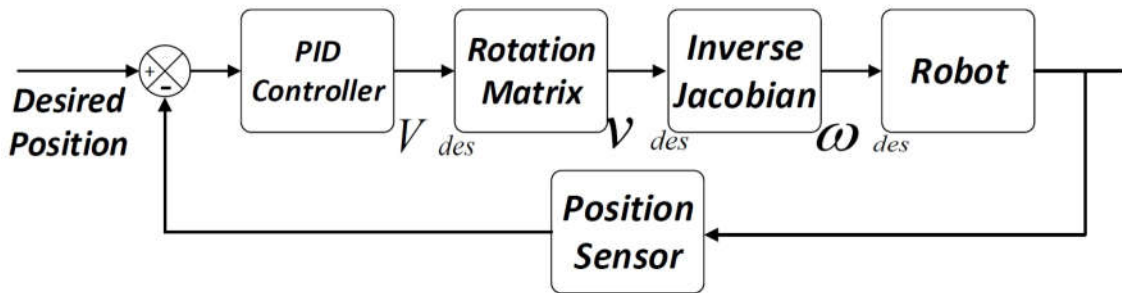
Figure 3.3: PID control loop used for trajectory control of the mobile base

Orientation Mechanism   To evaluate the performance of the mechanism in generating the required motion, first, a trajectory controller was developed in MATLAB/Simulink which uses the orientation feedback obtained from the gyro sensor. A schematic of the implemented control loop is shown in Fig. 3.4. As can be seen, after applying a PID controller, a velocity-based control signal is calculated which is then used to generate the desired angular velocity of the motors utilizing the robot's inverse Jacobian. It is important to mention that the control loop implemented in this experiment is only meant to show the performance of the robot in providing the expected motion and safety feature corresponding to the adjustable transferred force.
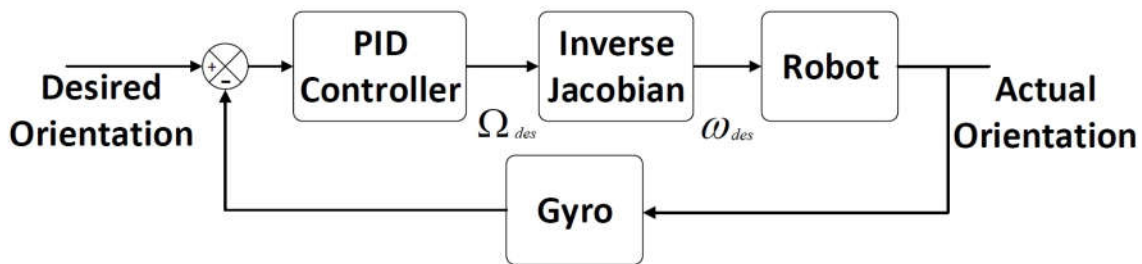
Figure 3.4: PID control loop used for trajectory control of the handle orientation base

3.3.2.2   Force and Admittance Control (Patient-in-Charge Phase)

To control the interaction force between the robot and the patients limb, a PID controller has been designed and implemented in MATLAB/Simulink. This controller uses the interaction force measured by the force sensor (OptoForce) as feedback. The difference between the desired value and the measured feedback is used to calculate the desired velocity that is commanded to the robot. In this controller, the output of the PID block is fed to the admittance control model of the

system. This model calculates the proper command to the robot (in velocity format) to achieve the desired force. A schematic of the implemented PID force control loop is shown in Fig. 3.5
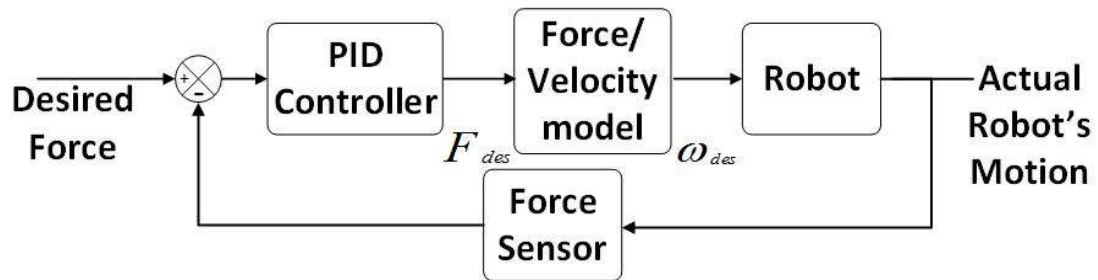
Figure 3.5: PID control loop used for force control of the robot

Chapter 4

Experimental Results

In this chapter, various experimental tests for device validation are presented. These experiments consist of the evaluation of the mechanisms, the algorithm used for data acquisition of feedback data from the sensors, and testing the robot on healthy subjects to ensure the safety and performance of the robot before future experiments involving patients.

4.1 Experimental Results

In this section, different mechanisms in the robot are tested and the algorithms for sensor data analysis described in Chapter 3 are validated. First, the robot's base was commanded to move in different circular trajectories and the desired trajectory was compared to the actual trajectories measured using two different sensors, one of which is the ADNS sensor implemented in the robot and the other is the Motion Tracker stereo camera system. An experimental testbed was then implemented to test the output force of the robot's base and the orientation mechanism. In these experiments, the actuators were commanded to generate force in a specific direction and the output force exerted by the robot was measured.

4.1.1 Trajectory Control In Free Motion

Mobile Base To perform a trajectory motion, the robot was commanded to move in a specific trajectory using the control loop shown in Fig. 3.3. To validate the position measured by the ADNS position sensors, a Micron Tracker model BB-BW-S60 stereo camera was used to track the position of the robot. For this purpose, a marker was attached at the end-effector of the robot to measure the position of the end-effector with respect to the camera as shown in Fig. 4.1. In this setup, the Micron Tracker stereo camera was installed above the robot as depicted in Fig. 4.1(b). Using the trajectory controller in MATLAB as shown in Fig. 3.3, three different desired circular trajectories were commanded to the robot. In this experiment, the measurement of the ADNS sensor was used as the feedback for the closed-loop controller shown in Fig. 3.3. Fig. 4.2 shows the actual measurement by ADNS sensor, Micron tracker camera, and the commanded trajectories. The maximum error between the measurement of the ADNS and Micron Tracker was 4*mm* for the 100*mm* radius circular trajectory (4% error).

(a)   (b)
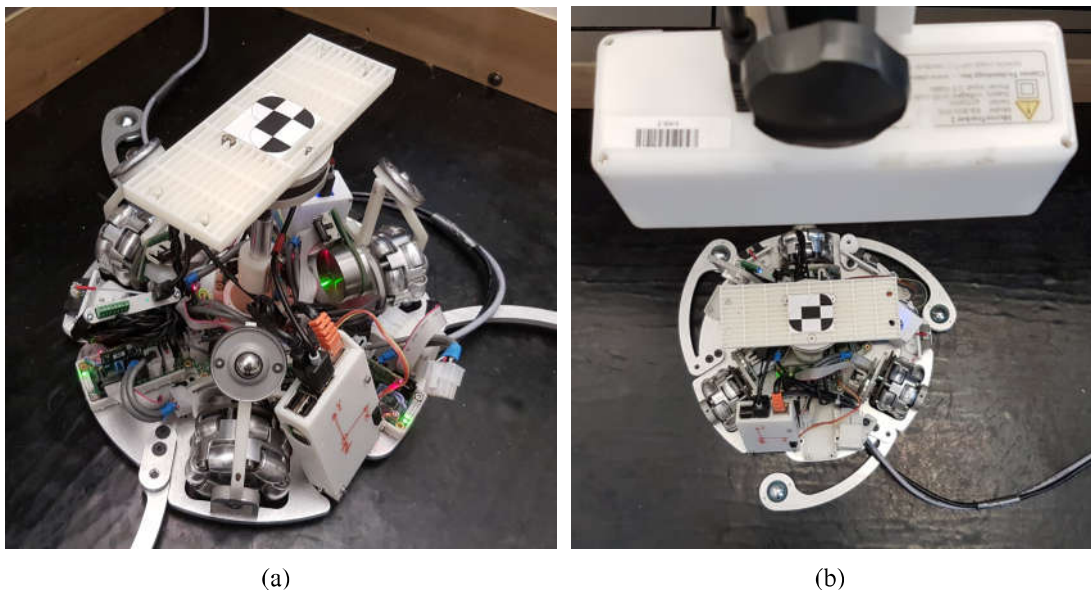
Figure 4.1: Free motion trajectory test on the mobile base using the Micron Tracker: (a) marker attached on top of the robot, and (b) the Micron Tracker camera above the robot

In this experiment, the data obtained from the Motion Tracker stereo camera was used as the
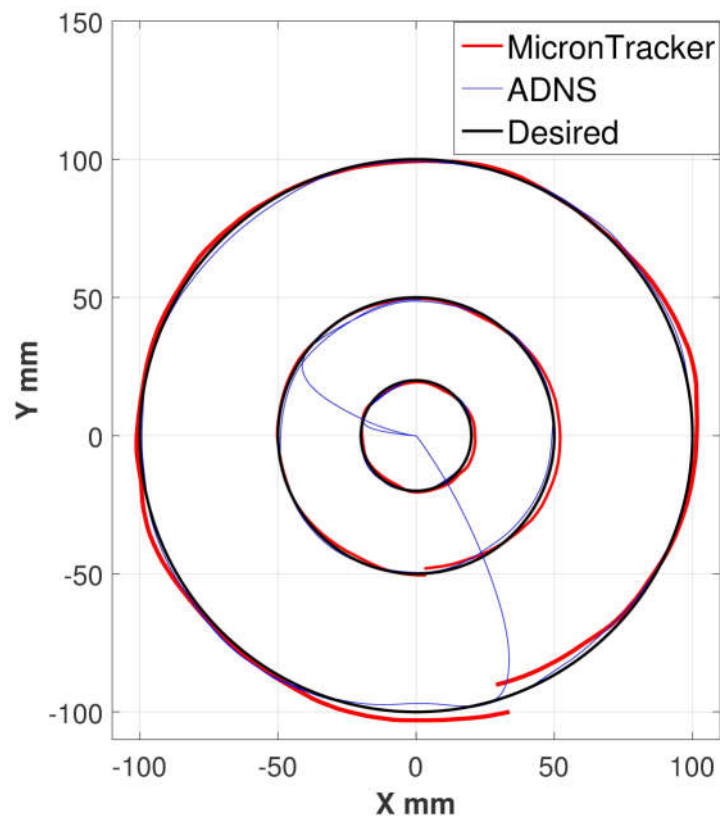
Figure 4.2: Circular Trajectories commanded and followed by the robot and measurement by ADNS sensors and Micron Tracker stereo camera.

reference for comparison. This tracking sensor is calibrated by the manufacturing company and the accuracy of the measurement is $0.25mm$ [68]. As shown in Fig. 4.2 the error between the measurement of the ADNS sensor and the Micron Tracker increases as the trajectory becomes bigger in size. This error is the result of the integration method used in the ADNS acquisition algorithm and could be corrected using a more precise integration loop. Another alternative method for correcting this error is by calibrating the algorithm and the ADNS data using the data obtained from the absolute global measurement of the Sharp proximity sensors. This sensor data fusion will be done in future steps of the project.

Orientation Mechanism To test the performance of the orientation mechanism design "A" under free-motion conditions, a circular trajectory in θ_X-θ_Y plane was considered as the desired

motion to be tracked by the device. In this experiment, the actuators were controlled in the velocity mode and the orientation feedback measured by using the gyro sensors attached to the end-effector (middle rod). The angular velocity feedback obtained from the gyro sensor was used to calculate the orientation of the middle rod in roll and pitch directions. The amplitude of the desired trajectory, for both θ_x and θ_y was 10° and the frequency was 0.5Hz. Fig. 4.3 shows the desired and the actual trajectories generated by the orientation mechanism. As can be seen, the robot was capable of tracking the commanded trajectory under free motion, and the maximum error was 0.06^o.
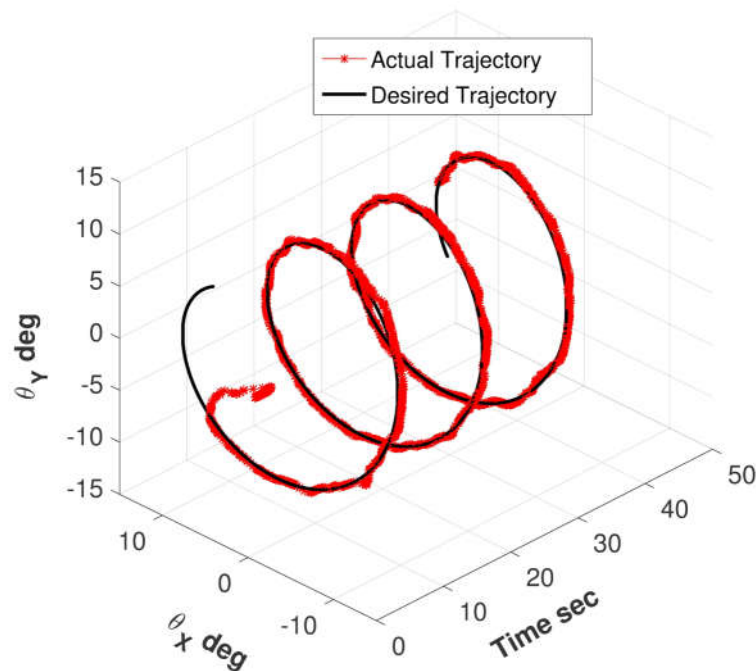
Figure 4.3: The actual and desired trajectory in roll and pitch DOFs commanded and followed by the handle

Although the results obtained for trajectories with 10° in amplitude shown high accuracy in motion, increasing the amplitude of the motion resulted in non-smooth trajectories with errors greater than 10% of the desired value. This significant error is due to errors in manufacturing the wheels and the inner surface of the dome. To clarify, as mentioned before the center of the spherical surface of the dome was designed to coincide with the center of rotation of the middle

rod around the spherical joint. Although in practice, due to manufacturing errors, there is an error between the location of the two centers. This error resulted in uneven motion of the dome while rotating around the center of the spherical joint. Additionally as the motion created by the wheels in contact with the inner surface of the dome significantly changes by the amount of the normal force between the dome and the wheels, any small uneven motion generated by the wheels results in a large disturbance in the motion of the dome. Consequently, any motion generating greater than 10° in value resulted in uneven motion of the dome and denoted the effect generated by the error in manufacturing.

Another issue associated with this mechanism was the aluminum debris created by slippage between wheels and the dome. After performing the experiments mentioned above, three drivers broke (burned MOSFETs) because of electrical shortcut made by the aluminum debris. As a result of the above-mentioned issues with this design, for the orientation mechanism, design "B" was used for the final version of the robot.

4.1.2 Safety Feature On Transmitted Force

Mobile Base To test the safety feature of the robot in limiting the output force, the robot was tested in the setup shown in Fig. 4.5. Here the end effector of the robot is fixed in the XY directions, and the robot (mobile base only) was commanded to generate a sinusoidal force in X and Y directions with the amplitude of $20N$ and frequency of $0.5rad/sec$. In this experiment, the desired force was mapped to the current of the motors using the dynamic model of the system. After that, the calculated currents were sent to the RPI to be commanded to the EPOS drivers. Meanwhile, the generated force by the robot was measured by the force sensor attached between the end-effector and the fixed structure. The test was performed on top of three different types of mats (two wooden and one rubber), and the generated force was measured as shown in Fig. 4.4.

As can be seen, by changing the material of the mat (i.e., changing the coefficient of friction), the amount of the transferred force to the end-effector is changed. The result obtained from this experiment can be used to select a proper mat based on the maximum force requirement of the
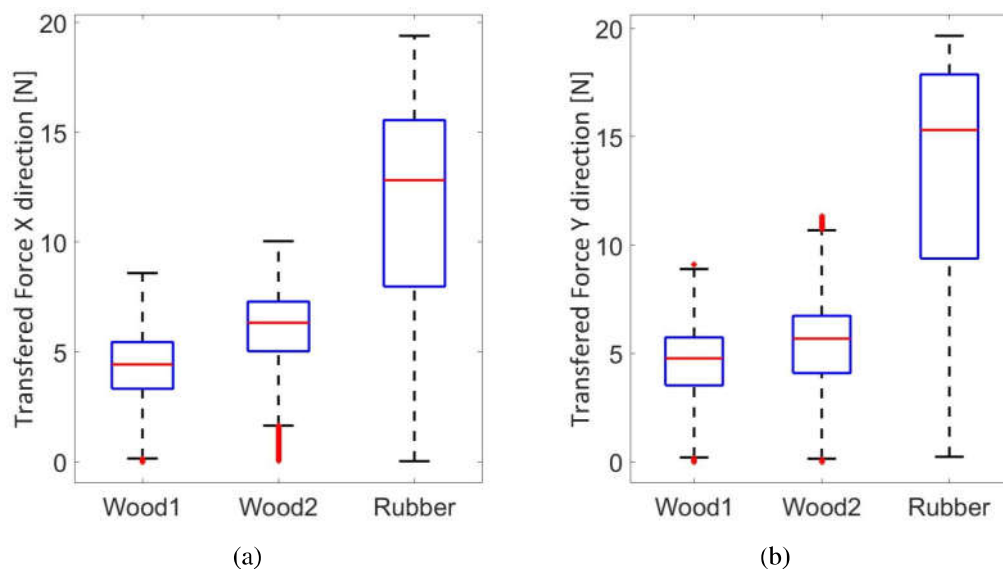
Figure 4.4: Transferred force for three types of mat measured in: (a) *X* direction, (b) in *Y* direction system during each therapy procedure.

Orientation Mechanism   In this experiment, the goal was to evaluate the proposed safety feature implemented by the adjustable force modification of the orientation mechanism (which limits the transmitted forces and torques of the robot to the patient's limb). As mentioned earlier, by tuning the mechanism proposed in this project, it is possible to adjust the amount of transmitted forces/torques. A particular testbed that is shown in Fig. 4.5 was developed to conduct this experiment. In the implemented testbed, the base plate and the foot plate were both fixed to a table. The motors were commanded to generate force in specific direction and the interaction force was measured by the force sensors. A sinusoidal force with an amplitude of 28 N and a frequency of 1 Hz in the "X" direction were generated by the motors.

By using the Jacobian of the system, the desired current of each actuator was calculated and sent to the EPOS drivers. In this experiment, the drivers of the motors were controlled in the current mode. During this experiment, the tightness of the wave spring on top of the dome was changed in six steps from the lowest tightness (i.e. "state-1") to the highest tightness (i.e. "state-6").
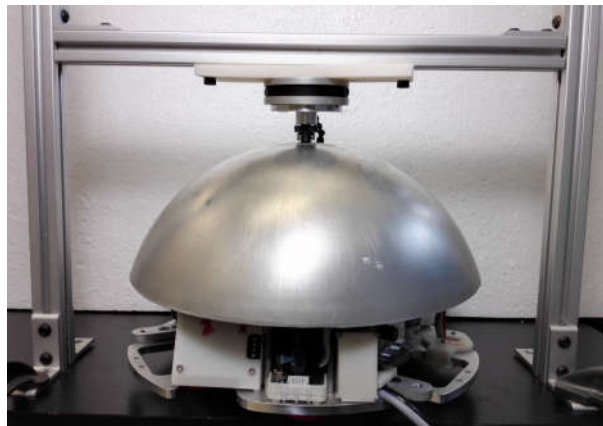
Figure 4.5: Experimental setup used for the slippage test.

For all states of tightness, the actuators applied similar sinusoidal torques. By tightening the wave spring, the amount of the normal force between the dome and the wheels was increased. In Fig. 4.6(a), the distribution of the transferred forces is compared to the 6 states of the experiment. As a result, as can be seen in Fig. 4.6(a), the transferred force during State-1 was limited to a value of 3.35 N. This is due to the activation of the designed slippage mechanism. Increasing the tightness from State-1 to State-6, the maximum amount of the transferred force increases from 3.35 N to 27.3 N. As shown in the Fig. 4.6(a), the saturated sinusoidal force has the maximum values of 3.35 N, 9 N, 11.7 N, 17.6 N, 25.2 N and 27.3 N for the six states of tightness.

The results obtained from this experiment validates the proposed system in limiting the amount of the applied force to the end-effector by using the designed mechanically adjustable mechanism.

4.2 Experimental Test Involving Healthy Subjects

4.2.1 Ethics Preparation

To determine the effectiveness of the device for rehabilitation purposes, several experiments were performed with healthy participants. During the tests, various types of data such as interaction force, EMG signals of the targeted muscle groups and the position of the robot were collected for
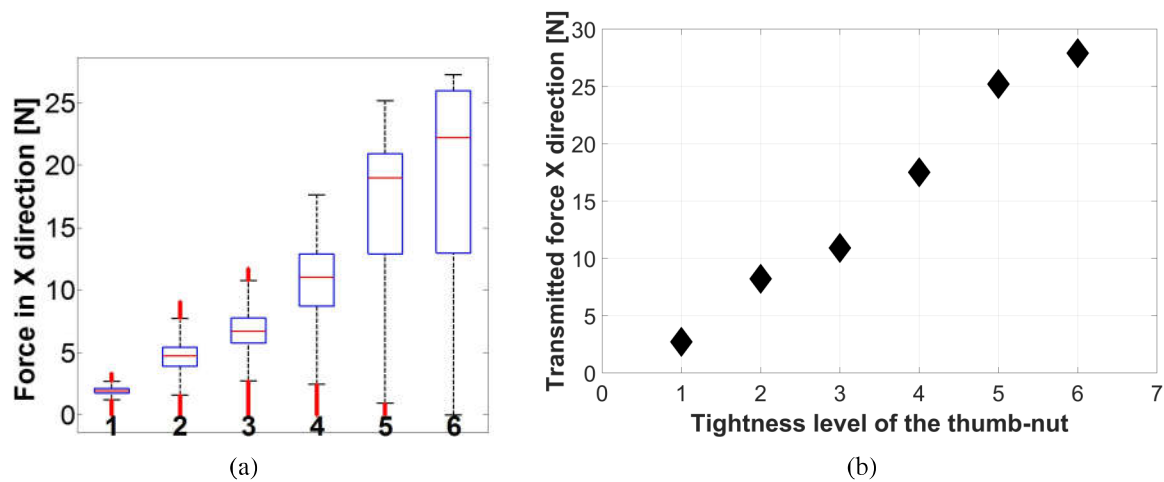
Figure 4.6: Measured force for different adjusted (tightness) states: (a) Boxplot distribution, (b) maximum value of the measured force.

further analysis. These experiments were conducted on healthy participants and investigated the functionality of the robot with respect to several parameters in order to optimize its design. The goal was to investigate the following functionalities: (1) Comfort level of the participant when using the device in various modes of operation such as passive, active, active-assistive mode and active-resistive; (2) Ergonomic design of the interface between the patient's limb and the robot's end effector; (3) Level of motivation and engagement of the participants using the robot; (4) Performance of the device under different body geometries, limb weight, and muscle power. Since the strength of healthy subjects would, in general, be more than that of patients suffering from hemiparesis or other types of paralysis, performing these experiments will ensure that the device has enough power to achieve the therapy goals in the initial stages of rehabilitation; (5) Specifying exercises to specifically target various sets of muscle groups. The purpose of this experiment was to measure the correlation between actuation of different muscle groups and corresponding movement trajectories of the robot during the therapies. This was done by measuring the EMG signals of the muscles and comparing them to the motion of the limb and the robot; (6) Generating maps of forces and torques for different positions of the limb. This information will enable objective assessments of the impairment levels of limbs in future studies involving patients. For now, this phase was performed on healthy participants.

The data obtained from healthy subjects will be incorporated in fine-tuning therapy formats for patients. As the designed device is a novel rehabilitation robot, new methods will be needed to measure the level of impairment of a patient's limb. This measurement will be useful since, during the therapy procedure, the progress of the patient will be monitored by measuring the ability of the patient in controlling limb movement. Additionally, to have a better understanding of the impairment level and corresponding muscles, a guide map will be generated. In this guide map, the amount of the force that can be applied to the limb of a healthy participant in different orientations of the limb will be measured. Generating this map for healthy subjects will help the therapist to compare the progress of patients throughout the rehabilitation process.

4.2.2 Methodology

The study is an experimental study to measure the capability of the system in performing therapy tasks. Participants were picked from healthy volunteers at CSTAR who were not suffering from osteoarthritis or a previous history of stroke, SCI (Spinal Cord Injuries) or paralysis. Additionally, participants were eligible based on the inclusion criteria regarding height and weight. For this study, the participants were asked to test the device and give their opinion about different aspects of the design. The tasks were performed by participants while they were provided with visual feedback of the tasks and trajectory that the robot follows to help them with performing the tasks. To calculate the level and type of each muscle activation, a set of wireless Trigno EMG sensors by Delsys Inc. [21], were attached to the participants hand or leg to measure the EMG signals of the corresponding muscle groups. The Trigno wireless EMG sensors are depicted in Fig. 4.7. It is important to mention that the sensors are small and wireless so they did not interfere with the users motions and performance.

The inclusion criteria for the participants were as follows: healthy subjects 18 years of age or older from the following range of body weight and height: (a) height (160cm-200cm) and (b) weight (50kg-120kg). Additionally, for the exclusion criteria, subjects suffering from osteoarthritis, having a previous history of stroke, SCI or paralysis were not recruited.
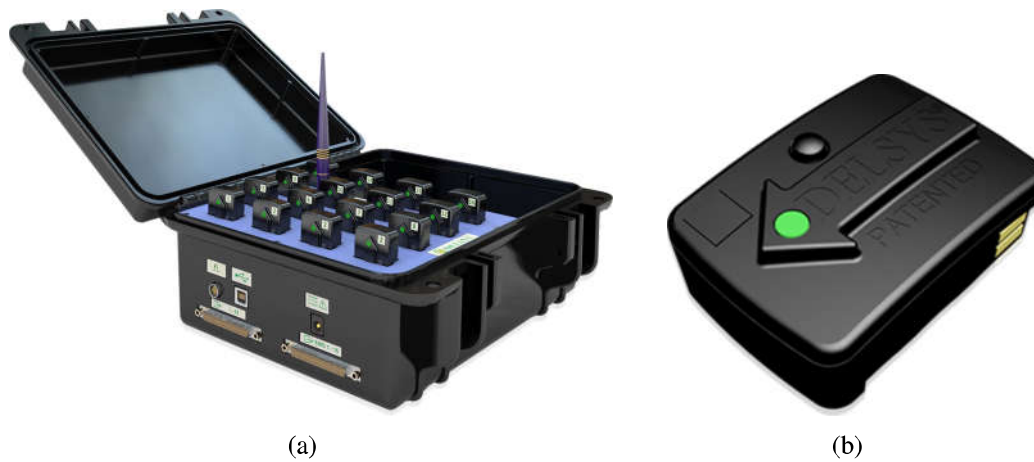
Figure 4.7: (a) Trigno Wireless System, (b) Trigno EMG Flex Sensor. [21]

4.2.3 Study Procedure

The subjects were scheduled to participate in the experiments based on their availability. The Trigno EMG sensors were attached to the limb to be tested for each subject before the experiment to measure EMG signals of the muscles of that limb. The EMG sensors are passive sensorized instruments with electrodes that measure the muscles contraction level. The data is used to measure the level of muscle activity during each task. After attaching the EMG sensors and collecting the data for their limbs at rest configurations, the subjects were asked to sit on a chair behind a table or sit beside a ground-level mat as shown in Fig. 4.8. As depicted, the EMG sensors are attached to the participant's leg at specific locations and the trial is performed on the mat while the participant is sitted on a chair. For this study, the dominant arm (either left or right arm) and dominant leg were tested for each subject. This means that each subject was asked to participate in the study in two sessions, one for the arm and the other for the leg. For the upper limb therapy, the robot was placed on a table, and the subjects were asked to grasp the handle of the robot. For the lower limb therapy, the robot was placed on a specific mat on the level and the subject's foot was placed on the footplate on top of the robot. The subjects then were asked to perform different tasks according to the therapy modes - passive, active, active-assistive and active-resistive modes. For example, one task was to move the end-effector of the robot freely using their hand or foot

to measure the corresponding muscle actuation for various limb movements. The position of the robot and the target point are depicted in the virtual-reality display as shown in Fig. 4.9. Here the position of the robot is indicated by the white square, the yaw angle by the orange rectangle and the destination location by the green square. In all of the tasks of the robot, the goal is to reach the green square in a straight line and in the minimum possible time.

Figure 4.8: Setup configuration for the LE experiments with healthy participants.

The sequence of the experiment all procedure was as follow:

- Running the virtual-reality display

- Assigning a secure ID to the participant and keeping it in the Master List

- Asking the participant to fill out the information section of the questionnaire and reading and signing the consent form

- Attaching the EMG sensors to specific locations on the patient's arm or leg based on the
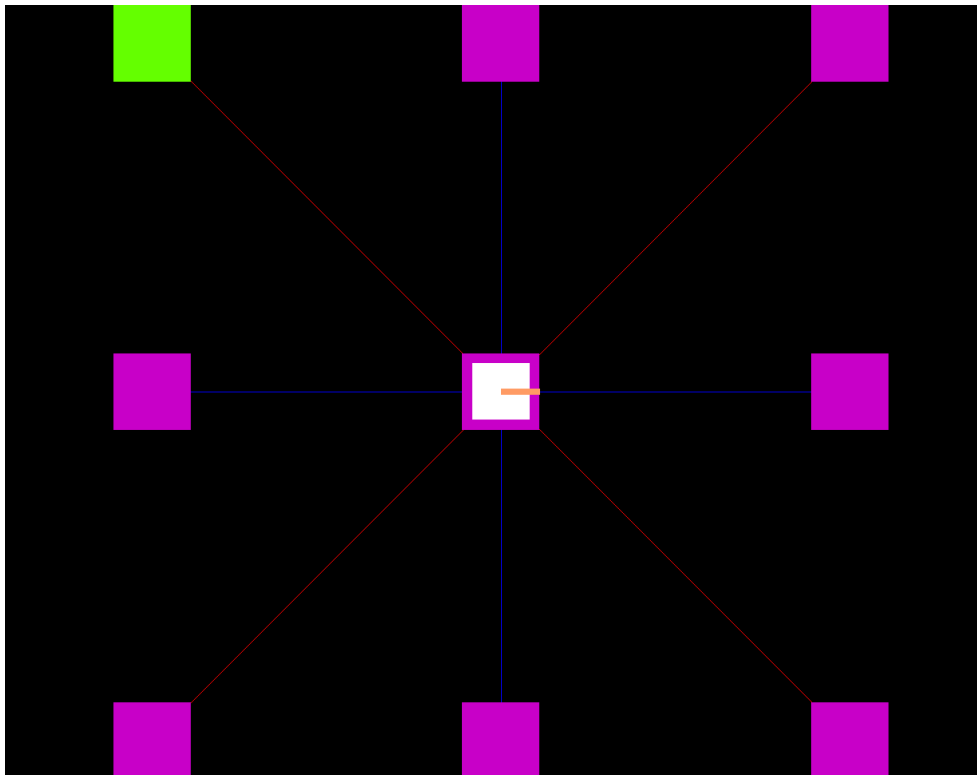
Figure 4.9: Virtual Environment used for the study trial involving healthy participants.

Test Protocol document

- Familiarizing the participant with the tasks and the process of the experiment

- Running the Trigno Control Utility to see the active sensors

- Running the EMG-MVC code for testing the signals and then closing it

- Running the Data Collection code for EMG, Browsing, Initializing, Starting Acquisition, Recording the Data

- Running the proper Simulink code for each task

To collect data for all of the main muscle groups in LE and UE cases, a guide map was created for the locations and places to attach the EMG sensors. For each UE and LE experiments, 16 EMG sensors were put in the locations as shown in Fig. 4.10 and Fig. 4.11. The location of the sensors denoted by with the yellow marker in each figure.
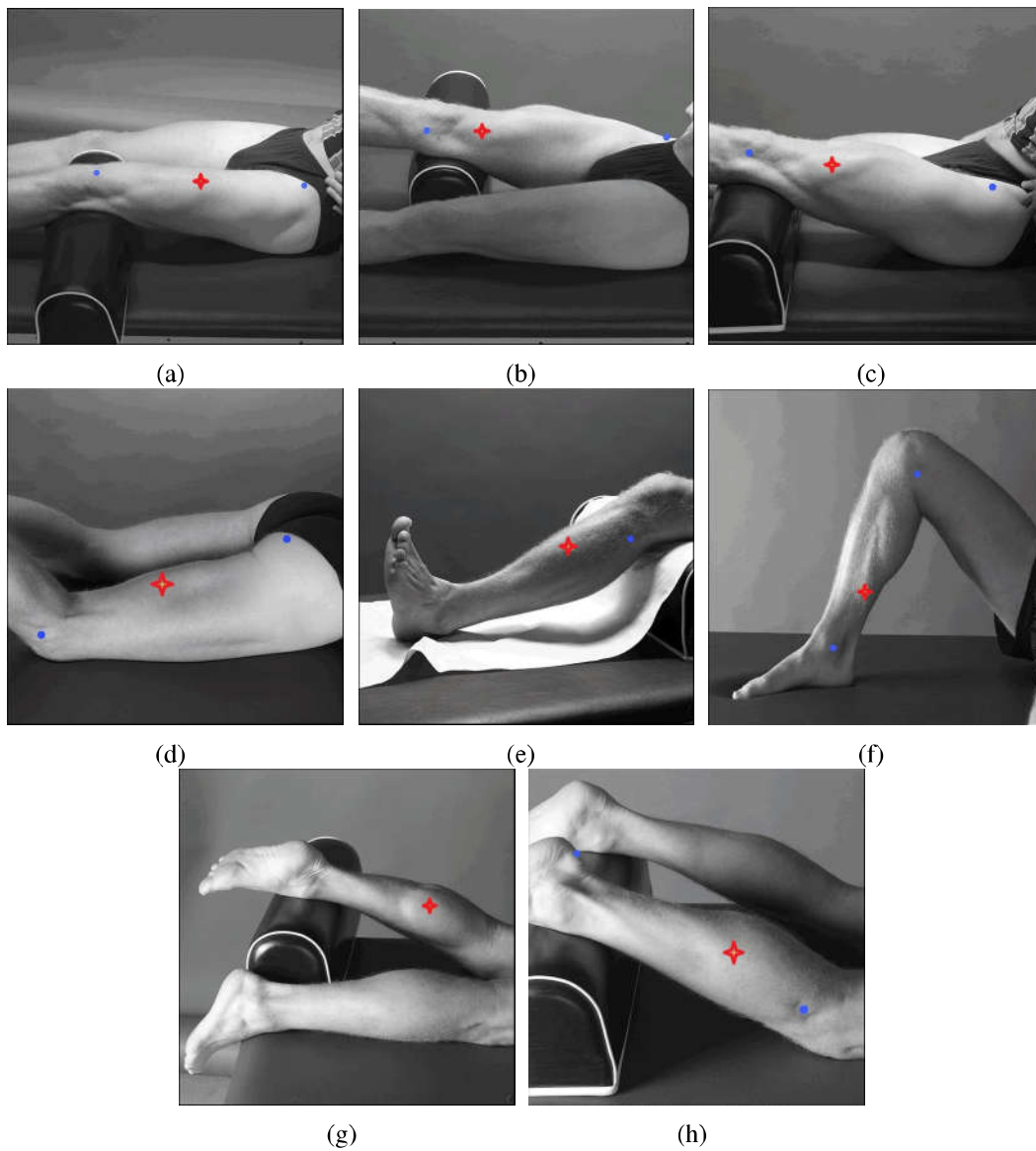
Figure 4.10: EMG sensor placement for the LE experiment marked with red points (a) Quadri-ceps Femoris, (b) Quadriceps Femoris , (c) Quadriceps Femoris vastus lateralis, (d) Biceps femoris, (e) Tibialis anterior, (f) Soleus, (g) Gastrocnemius Medialis, and (h) Gastrocnemius Lateralis [22]
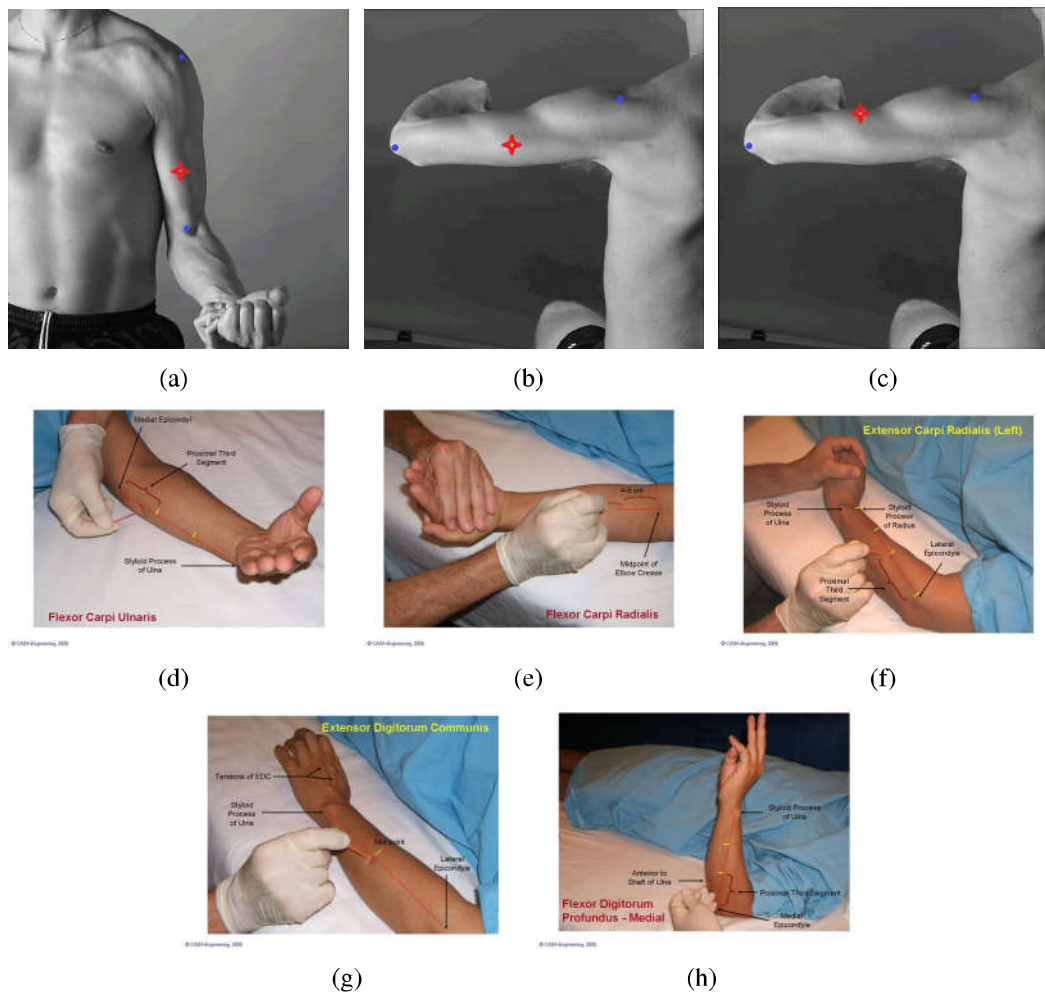
Figure 4.11: EMG sensor placement for UE experiment marked with red points (a) Bicep, (b) Triceps long head , (c) Triceps short head, (d) Flexor Carpi Ulnaris, (e) Flexor Carpi Radialis, (f) Extensor Carpi Radialis, (g) Extensor Digitorum Communis, and (h) Flexor Digitorium Profundus [22, 23]

Similar to each mode of therapy, a MATLAB Simulink code was prepared. The details of the tasks that participants were asked to perform in these experiments are as follows:

Testing Mode   Specific trajectories were shown to the subject on a monitor in a virtual reality environment and the subject was asked to follow the trajectories generated by the robots motion. They were asked to apply as much voluntary motion as they wanted.

Passive Mode   In this task, the subjects were asked to relax the muscles of the specified limb and the robot moves along the trajectories defined in the previous step. The goal of this step was to measure the amount of the force generated by the robot without the contribution of the subject.

Assistive Mode   In this step, the participants were asked to perform the same task as the Passive mode while they are in charge of the motion. The robot assisted them in performing the task by magnifying their applied force.

Idle Mode   In this step, the participants were asked to perform the same task as in the Assistive Mode while they are again in charge of the motion. The robot did not assist them in performing the task. By comparing the results from this mode and Assistive Mode, we can measure the amount of assistance the robot provides to the patients during the therapy procedure.

Resistive Mode   In the last step, the subject was asked to resist the motion provided by the robot as shown in the virtual environment. The purpose of this step was to measure the capability of the robot in following the desired trajectories in the presence of the output disturbance and resistance.

At the end of the trial session, the subjects were asked to fill out a questionnaire that included task-related questions in order to evaluate the perception of the subjects. The questionnaire included the following questions: (a) rate your comfort level when using the device in terms of safety, interaction force, ergonomics with regard to the footplate and handle, (b) rate the resistance of the robot in its non-actuated mode, (c) rate the force applied by the robot compared to the maximum force capability of the subject, and (d) rate the tasks in order of the need for accuracy of muscle control. The entire trial session took a maximum of 2 hours over 2 sessions. The trials were completed by 15 participants.

4.2.4 Study Results

As mentioned before the study was performed with healthy participants on both upper and lower limbs. One of the goals of the study was to validate the operation of the robot in performing various therapy procedures. Another goal was to have feedback on different features of the robot from the participant's perspective. The participant's height and weight were 172.1 ± 10 cm and 75.4 ± 20.2 kg (mean $\pm$ standard deviation [SD]) respectively. 66% of the participants were in the 20-25 years of age and 93% had previous experience with robotic systems. After the trial sessions, the questionnaire was filled by each participant and the summary of the answers is reported in Table. 4.1 and Fig. 4.12. As can be seen, the features relating to the setup of the trials (such as comfort level, clarity of the trial and concern regarding the robot's operation) are acceptable and the procedures can be used to perform the experiments on patients in the future. For the features related to the performance of the system, some issues were mentioned by the participants about some mode of therapy that will be considered in future work involving testing with therapists and patients.

Fig. 4.12 shows the results obtained from the questionnaires regarding the participant's assessments of the performance of the system. As mentioned before, Level 1 represents the worst condition in that category and Level 5 corresponds to the best. For example, Level 5 in power perception means that the robot is extremely powerful with respect to the participant's muscle power. As a summary, 63% of the participants mentioned that the motion of the robot during the idle mode is either slightly resistant or not resistant at all. This indicates that the robot's impedance in the in-active mode is low and the back-drivability is achieved properly. 90% of the participants found the force output of the system powerful or very powerful and 82% mentioned that they performed the motion through the experiment accurately. As a result, the performance of the system was determined to be satisfactory and the evaluation could proceed to the next stage. The comfort level of the participants was noted in the study to have some feedback from the user side and modify and improve the interface (footplate/handle) and the whole set-up in future studies.

The results obtained from the study will be used to determine the effect of previous expe-

Table 4.1: Participant's answers regarding the performance of the robot

General opinion of participants about the trial setup and the experiment					
Previous experience with robotic systems	No previous experience 15%	Previous experience 85%			
Concerns while using the robot	No 93%	Yes 7%			
Clarity in descriptions of the tasks	Not clear at all 0%	Slightly confusing 15%	Clear 85%		
Level of control in performing the tasks	No control 0%	Moderate control 61%	Full control 39%		
Level of comfort on foot-plate	Not comfortable at all 0%	Slightly comfortable 0%	Comfortable 32%	Very comfortable 61%	Extremely comfortable 7%
Level of comfort on whole setup	Not comfortable at all 0%	Slightly comfortable 0%	Comfortable 24%	Very comfortable 61%	Extremely comfortable 15%
Level of motivation in performing the tasks	Not motivated at all 0%	Slightly motivated 7%	Motivated 15%	Very motivated 54%	Extremely motivated 24%
Hardware related opinion of participants about the device					
Robot's resistance in idle mode motion	Extremely resistant 0%	Very resistant 0%	Resistant 32%	Slightly resistant 61%	No resistance at all 7%
Robot's force exertion compared to the subject's strength	Not powerful at all 0%	Slightly powerful 15%	Powerful 46%	Very powerful 17%	Extremely powerful 23%
Participant's motion accuracy while using the robot	Not accurate at all 0%	Slightly accurate 23%	Accurate 46%	Very accurate 23%	Extremely accurate 7%

rience on the performance of the system and the responses obtained from the participants. As in this study, the percentage of experienced users was greater that of inexperienced users, more inexperienced participants will be required for the comparison in the future stages of the study.
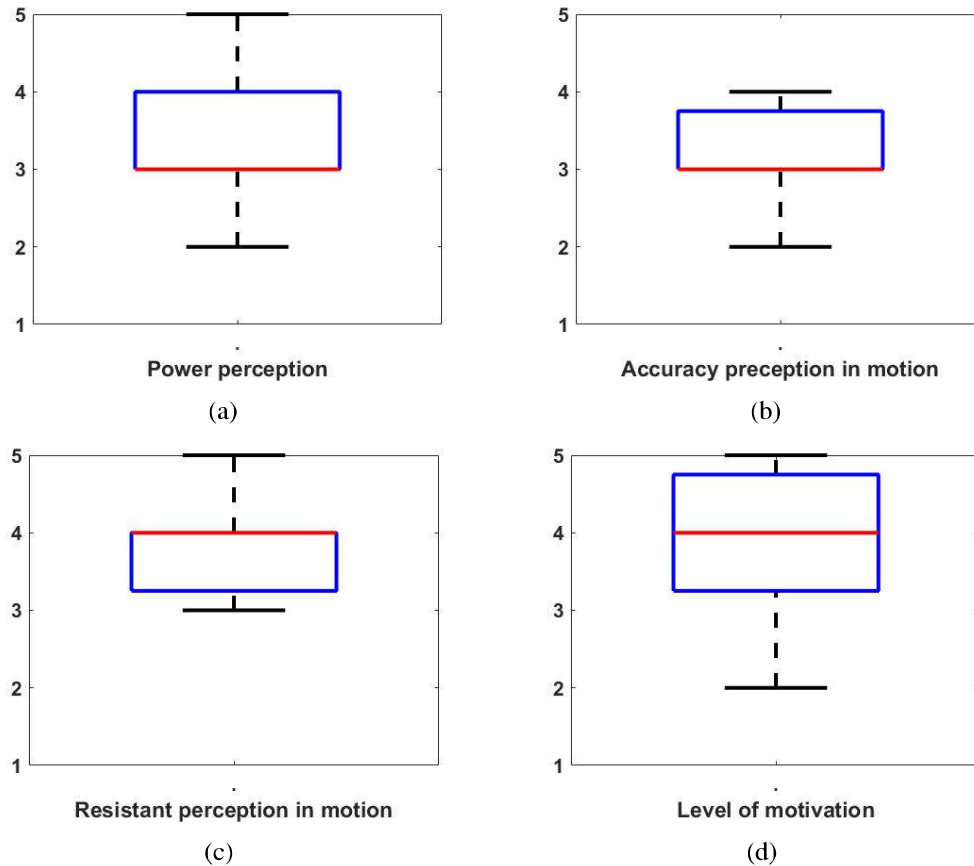
Figure 4.12: Questionnaire results for (a) power perception, (b) level of accuracy in motion, (c) level of resistance in motion during the non-actuated mode and (d) level of motivation while performing the tasks. Here the y axis represents the qualitative level which is described in Appendix A

Initial analysis of the data shows that both the mean and maximum value of the EMG measurement for all eight muscles monitored during the experiments is higher in the non-actuated mode (Task3) versus the assisted mode of therapy (Task2). Fig. 4.13 represents the EMG measurement of one of the participants for Task 2 and Task 3 of the experiment. As shown, both mean values and the maximum values of the measurement are higher in Task 3. This means that the robot's

assisted mode decreased the muscle activity during the same therapy task.

4.3 Report of Invention (ROI) Submission

To protect the novel idea of dual usability of the device and inherently safe mechanisms, a report of invention was submitted to Western's business office (WorlDiscoveries)and a PCT application was filled on October 2017 to protect the intellectual property for the proposed technology. Further evaluation of the device involving therapists and stroke patients planned in the next few months.
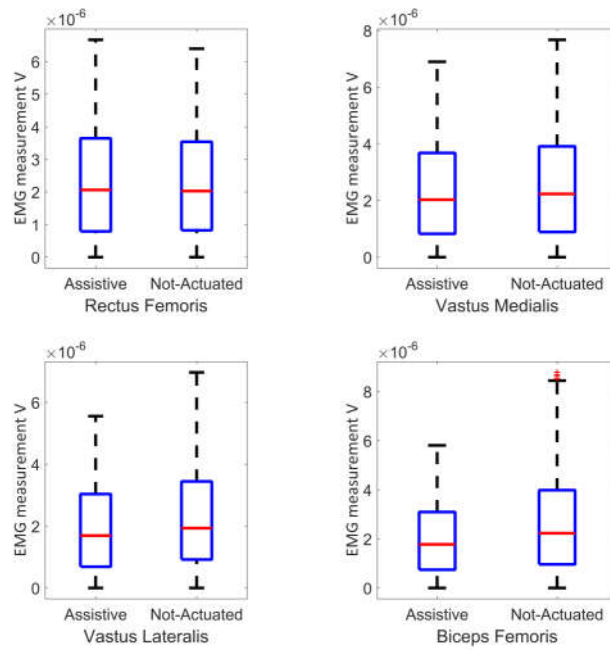
(a)
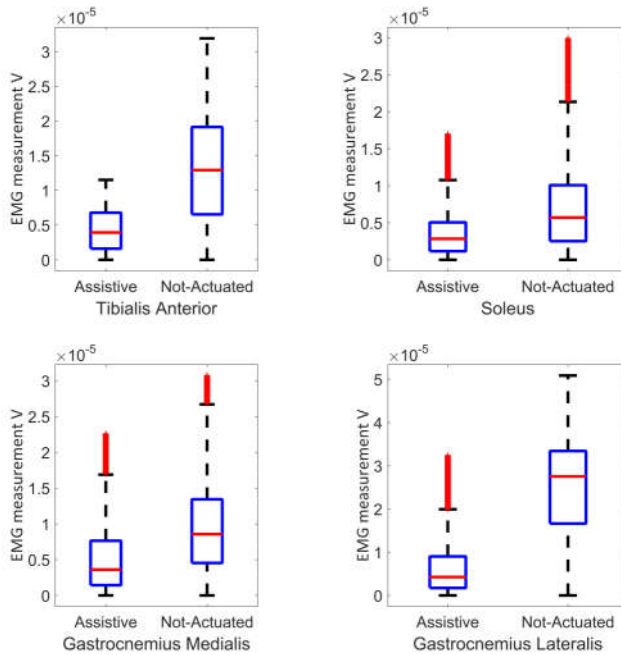
(b)

Figure 4.13: EMG measurement *V* for assisted mode of therapy (Task2) and non-actuated mode (Task3) for (a) upper leg and (b) lower leg muscle groups of healthy participant HP113.

Chapter 5

Conclusion and Future Work

In this project, a novel inherently safe robotic system was developed that is suitable for delivering robotic rehabilitation on both upper extremities (UE) and lower extremities (LE). Through the design process, in addition to the engineering requirements of the project, specifications related to the end-user were also considered. The end-user could be a therapist or a patient. The design process started with developing conceptual designs and selecting the best two concepts for the detail design phase. A list of requiring the UE and LE rehabilitation was used during the concept design selection. The end-effector type robot was selected as it can provide more simplicity in the design process, more flexibility in the actuator selection and a novel dual application idea (LE and UE). For the orientation mechanism, two concepts ideas were selected, modeled and implemented.

Through the design process, various components were prototyped to ensure the functionality of the mechanisms prior to the main manufacturing process. Additionally, most of the components that did not require accurate tolerance and high strength were manufactured with the 3D-printing process. All of the mechanical components that required high accuracy machining and needed to be made out of high strength materials were made by the wire EDM method.

For the electrical components of the system, the idea to use off-the-shelf products such as Maxon drivers and Raspberry Pi (RPI) (to implement the low-level control loop inside the robot's module) was successful. Using off-the-shelf products decreased the overall cost of the electrical

components and the time required to assemble and implement the system. Additionally, placing all drivers in the mobile platform and communicating to the robot by using the RPI decreased the number of wires attached to the robot which increased the reliability, portability and working volume of the robot.

The low-level control loop in the RPI is developed and implemented to read the sensor data, command the Maxon drivers and send/receive the data to/from the Simulink model in the PC through UDP. In the current version of the system, there are 10 modes of control based on the control strategy and the speed of the loop is set to be $1kHz$ and is controlled precisely in QUARC.

After manufacturing the components, the system was assembled and its functionality was tested. A mathematical model of the system and algorithms for localization of the robot using various sensors were derived and implemented in the Simulink model.

Various experiments were conducted to validate the performance of the control algorithm, data acquired from novel localization ADNS sensor and the algorithm used to fuse the feedback data. The results showed proper performance of the system in following specified trajectories in the passive mode of therapy which is related to the position control mode of operation. The developed code was a velocity-based method for trajectory planning followed by a PID controller for position control. The results showed good accuracy for the application of rehabilitation. Although some errors in the localization algorithm have been observed because of the integration error, these errors can be decreased in the future versions of the Simulink model by fusing the feedback data obtained from the Sharp sensors.

The force generated by the mobile platform was tested on different types of working mats. It has been shown that changing the mat type can change the friction coefficient which consequently changes the maximum allowed transferable force. The results also showed that there was good symmetry in the force generated by the end-effector in the x and y directions. This indicates that the Simulink model of the system was able to compensate for any unsymmetrical structure of the wheels in motion generation in x and y directions.

The orientation mechanism design "A" was capable of limiting the applied force/torque to

the end effector and could provide motion with high accuracy in ranges smaller than $10degs$. However, the motion generated by this mechanism was not smooth for a range greater than $10degs$ and the range of motion did not meet the expected value in the design phase ($30degs$). For this reason, the orientation mechanism design "B" was used and provided the two degrees of freedom corresponding to roll and pitch motions.

To validate the performance of the system for therapy procedures, an experimental tests were designed and performed involving healthy participants. Preliminary analysis of the data collected based on questionnaires filled by the participants showed that the device was capable of generating accurate motion and could exert forces in the range required for both LE and UE therapy applications. Some concerns were reported by participants about the setup, clarity of the tasks and comfort level of the footplate. For future studies, the comments provided by participants will be addressed and increased the comfort level of the patients while using the device.

Regarding other modes of operation such as the assistive mode of therapy, the developed code in the Simulink model was tested in the experiments on healthy participants. The feedback collected from participants showed that the assistive mode of the device clearly helped them in performing the tasks with less muscle activation compared to the non-actuated mode of the device. For future steps of the project, more attention should be given to developing more advanced modes of therapy like fusing EMG sensors data to command the robot in the assistive mode of therapy.

Further evaluation of the device involving therapists and stroke patients is needed to fully validate its applicability for LE and UE post-stroke rehabilitation therapy.

There are some limitations regarding the application of this robot for Lower and Upper limb rehabilitation. This is due to the simplicity of the designed structure and the number of degrees of freedom of the system. For example, this device cannot be used for active shoulder abduction/adduction exercises which due to the lack of the Z direction DOF. the same limitation exists for lower extremity case and can be addressed with various configuration of the working mat.

The major contributions of this thesis can be summarized as follows:

- A novel robotic system has been developed that is suitable for physical rehabilitation on

both upper and lower extremities.

- The designed device is lightweight, portable, low-cost, inherently safe to operate and can be used for in-home training.

- Various novel mechanisms have been used in the design of this device that provide the aforementioned features.

5.1 Future Work

5.1.1 Further Analysis and Evaluation

In the current stage of the project, the data collected from the study on healthy participants has not been fully analyzed. No analysis has been done yet to achieve goals (5) and (6) in the study on healthy participants mentioned in Chapter 4. Further analysis is required on the collected results to create a map between actuated muscle groups and the corresponding movements of the device. Additionally, the data collected from EMG sensors and the feedback data from various sensors in the robot can be used to guide the therapist in commanding the robot and planning therapy procedures.

5.1.2 Study involving Therapists and Patients

The next step after fine-tuning to resolve any issues arising from the study involving healthy participants is to perform a usability study involving professional therapists to get their feedback prior to undertaking a study involving stroke patients. For this purpose, a more sophisticated sitting setup (containing an adjustable chair and larger working mat) will be used to perform the experiments. This setup will provide more space for the robot to move and more range of motion for the patient's leg. This way we can compensate the difference in patient's limb length to make the rehabilitation process identical among all subjects. For this purpose, a special sitting place

will be designed with height adjustment so the robot can have more working volume.

To increase the level of motivation and engagement of the participants (therapists and patients) in future studies, a 3D virtual reality environment could be developed to visualize the motion of the robot and the participant's body in the virtual environment. This will increase the motivation and can be used to demonstrate the performance of the robot in a better way.

5.1.3 Second Generation

As the goal of this project and the first version of the device was to validate the initial idea proposed for therapy, the design process was focused on minimizing the time and effort on manufacturing and implementation. For the next generation of the device, the main goal could be to reduce the cost of the system and to address the issues associated with the first generation. For this purpose, the second generation will be designed to have less expensive commercially available actuators as the main cost associated with the current system is because of the expensive Maxon motors and drivers. Secondly, the mobile platform could be replaced with a more robust three DOF mechanism so eliminate issues related to tilting and uneven force generation.

5.1.4 Other Possible Applications

One of the possible applications of the current system could be measuring the rate of recovery (range of motion and force capability) of patients after arthroplasty surgeries. Another possible application could be as an assessment tool for monitoring the effect of medication or other treatment on change in limb stiffness and movements of Parkinson disease patients. As the robot is equipped with various sensors for localization and force measurement, these evaluations can be done by measuring the performance of the patient while performing redefined movements over time. These evaluations can be recorded and quantified for assessment.

References

[1] "National stroke audit reveals shortfall in community assessments — the chartered society of physiotherapy," http://www.csp.org.uk/news/2014/08/20/ national-stroke-audit-reveals-shortfall-community-assessments#comment-form, (Accessed on 08/28/2017).

[2] P. M. Nair and A. L. Behrman, "Spinal cord injury: Role of ankle foot orthoses," *Spinal cord*, 2010.

[3] I. Díaz, J. J. Gil, and E. Sánchez, "Lower-limb robotic rehabilitation: literature review and challenges," *Journal of Robotics*, 2011.

[4] H. I. Krebs, M. Ferraro, S. P. Buerger, M. J. Newbery, A. Makiyama, M. Sandmann, D. Lynch, B. T. Volpe, and N. Hogan, "Rehabilitation robotics: pilot trial of a spatial extension for mit-manus," *Journal of NeuroEngineering and Rehabilitation*, vol. 1, no. 1, p. 5, 2004.

[5] M. Schoone, E. Dusseldorp, M. van den Akker-van Marle, A. J. Doornebosch, R. Bal, A. Meems, M. P. Oderwald, and R. van Balen, "Stroke rehabilitation in frail elderly with the robotic training device acre: a randomized controlled trial and cost-effectiveness study," *Journal of Robotics*, vol. 2011, 2011.

[6] G. Rosati, P. Gallina, and S. Masiero, "Design, implementation and clinical tests of a wire-based robot for neurorehabilitation," *IEEE Transactions on Neural Systems and Rehabilitation Engineering*, vol. 15, no. 4, pp. 560–569, 2007.

[7] S. Faran, O. Einav, D. Yoeli, M. Kerzhner, D. Geva, G. Magnazi, S. van Kaick, and K.-H. Mauritz, "Reo assessment to guide the reogo therapy: Reliability and validity of novel robotic scores," in *Virtual Rehabilitation International Conference, 2009.* IEEE, 2009, pp. 209–209.

[8] J. C. Perry, J. Rosen, and S. Burns, "Upper-limb powered exoskeleton design," *IEEE/ASME transactions on mechatronics*, vol. 12, no. 4, pp. 408–417, 2007.

[9] S. Balasubramanian, R. Wei, M. Perez, B. Shepard, E. Koeneman, J. Koeneman, and J. He, "Rupert: An exoskeleton robot for assisting rehabilitation of arm functions," in *Virtual Rehabilitation, 2008.* IEEE, 2008, pp. 163–167.

[10] T. Nef, M. Guidali, and R. Riener, "Armin iii–arm therapy exoskeleton with an ergonomic shoulder actuation," *Applied Bionics and Biomechanics*, vol. 6, no. 2, pp. 127–142, 2009.

[11] S. Freivogel, J. Mehrholz, T. Husak-Sotomayor, and D. Schmalohr, "Gait training with the newly developed lokohelp-system is feasible for non-ambulatory patients after stroke, spinal cord and brain injury. a feasibility study," *Brain Injury*, vol. 22, no. 7-8, pp. 625–632, 2008.

[12] H. Yano, N. Tanaka, K. Kamibayashi, H. Saitou, and H. Iwata, "Development of a portable gait rehabilitation system for home-visit rehabilitation," *The Scientific World Journal*, vol. 2015, 2015.

[13] M. Peshkin, D. A. Brown, J. J. Santos-Munné, A. Makhlin, E. Lewis, J. E. Colgate, J. Patton, and D. Schwandt, "Kineassist: A robotic overground gait and balance training device," in *Rehabilitation Robotics, 2005. ICORR 2005. 9th International Conference on*. IEEE, 2005, pp. 241–246.

[14] J. A. Saglia, N. G. Tsagarakis, J. S. Dai, and D. G. Caldwell, "A high performance redundantly actuated parallel mechanism for ankle rehabilitation," *The International Journal of Robotics Research*, 2009.

[15] R. G. West, "Powered gait orthosis and method of utilizing same," Feb. 10 2004, uS Patent 6,689,075.

[16] G. Colombo, M. Joerg, R. Schreier, and V. Dietz, "Treadmill training of paraplegic patients using a robotic orthosis," *Journal of rehabilitation research and development*, vol. 37, no. 6, p. 693, 2000.

[17] C. Schmitt and P. Métrailler, "The motion maker: a rehabilitation system combining an orthosis with closed-loop electrical muscle stimulation," in *8th Vienna International Workshop on Functional Electrical Stimulation*, no. LSRO2-CONF-2006-011, 2004, pp. 117–120.

[18] A. Goffer, "Gait-locomotor apparatus," Dec. 26 2006, uS Patent 7,153,242.

[19] "Armotiontm - the latest advancement in occupational therapy." [Online]. Available: https://www.rehatechnology.com/en/products/armotion

[20] A. Yurkewich, S. F. Atashzar, A. Ayad, and R. V. Patel, "A six-degree-of-freedom robotic system for lower extremity rehabilitation," in *2015 IEEE International Conference on Rehabilitation Robotics (ICORR)*, 2015, pp. 810–815.

[21] "Trigno emg systems," delsys, Inc. [Online]. Available: http://www.delsys.com/products/wireless-emg/

[22] "Welcome to seniam," the SENIAM project. [Online]. Available: http://seniam.org/

[23] "Electronic myoanatomic atlas for clinical emg," muscle Anatomy. [Online]. Available: http://www.netemg.com/pictsv1/

[24] B. Katherine Salter, B. Mark Hartley, and B. Norine Foley, "Impact of early vs delayed admission to rehabilitation on functional outcomes in persons with stroke," *J Rehabil Med*, vol. 38, no. 113Á/117, 2006.

[25] K. Luttgens and K. F. Wells, *Kinesiology: Scientific Basis of Human Motion.* Saunders College Pub., 1982.

[26] H. I. Krebs and N. Hogan, "Therapeutic robotics: A technology push," *Proceedings of the IEEE*, vol. 94, no. 9, pp. 1727–1738, 2006.

[27] W. Stroke, "Recommendations on stroke prevention, diagnosis, and therapy. report of the who task force on stroke and other cerebrovascular disorders," *Stroke*, vol. 20, no. 10, pp. 1407–1431, 1989.

[28] "Stroke information page — national institute of neurological disorders and stroke," https://www.ninds.nih.gov/Disorders/All-Disorders/Stroke-Information-Page, (Accessed on 08/28/2017).

[29] D. Mozaffarian, E. J. Benjamin, A. S. Go, D. K. Arnett, M. J. Blaha, M. Cushman, S. R. Das, S. de Ferranti, J.-P. Després, H. J. Fullerton *et al.*, "Heart disease and stroke statistics-2016 update," *Circulation*, vol. 133, no. 4, pp. e38–e360, 2016.

[30] G. Kwakkel *et al.*, "Effects of augmented exercise therapy time after stroke a meta-analysis," *Stroke*, vol. 35, no. 11, pp. 2529–2539, 2004.

[31] T. Truelsen and R. Bonita, "The worldwide burden of stroke: current status and future projections," *Handbook of clinical neurology*, vol. 92, pp. 327–336, 2008.

[32] "National stroke association." [Online]. Available: http://www.stroke.org/

[33] M. A. Dimyan and L. G. Cohen, "Neuroplasticity in the context of motor rehabilitation after stroke," *Nature Reviews Neurology*, vol. 7, no. 2, pp. 76–85, 2011.

[34] B. Kolb, J. Cioe, and P. Williams, "Neuronal organization and change after brain injury," pp. 13–37, 2011.

[35] H. S. Jørgensen, H. Nakayama, H. O. Raaschou, and T. S. Olsen, "Recovery of walking function in stroke patients: the copenhagen stroke study," *Archives of physical medicine and rehabilitation*, vol. 76, no. 1, pp. 27–32, 1995.

[36] R. Zorowitz, B. Bates, J. Choi, J. Glasberg, D. Graham, R. Katz, K. Lamberty, and D. Reker, "Management of adult stroke rehabilitation care: a clinical practice guideline," *Stroke*, vol. 36, pp. 100–143, 2005.

[37] L. W. Forrester, L. A. Wheaton, and A. R. Luft, "Exercise-mediated locomotor recovery and lower-limb neuroplasticity after stroke," *Journal of rehabilitation research and development*, vol. 45, no. 2, p. 205, 2008.

[38] "Physical therapy - types of physical therapy." [Online]. Available: http://www.webmd.com/pain-management/tc/physical-therapy-types-of-physical-therapy#1

[39] "Hope: The stroke recovery guide," 2011. [Online]. Available: http://www.webmd.com/pain-management/tc/physical-therapy-types-of-physical-therapy#1

[40] "Post-stroke rehabilitation fact sheet — national institute of neurological disorders and stroke," https://www.ninds.nih.gov/Disorders/Patient-Caregiver-Education/Fact-Sheets/Post-Stroke-Rehabilitation-Fact-Sheet, (Accessed on 08/28/2017).

[41] "Stroke rehabilitation information — national institute of neurological disorders and stroke," https://www.ninds.nih.gov/Disorders/All-Disorders/NINDS-Stroke-Information-Page/Stroke-Rehabilitation-Information.

[42] R. D. Zorowitz, E. Chen, K. Bianchini Tong, and M. Laouri, "Costs and rehabilitation use of stroke survivors: a retrospective study of medicare beneficiaries," *Topics in stroke rehabilitation*, vol. 16, no. 5, pp. 309–320, 2009.

[43] F. Lowry, "Stroke rehabilitation services inadequate, experts say," 2010.

[44] M. Hillman, "Introduction to the special issue on rehabilitation robotics," *Robotica*, vol. 16, no. 5, pp. 485–485, 1998.

[45] W. Meng, Q. Liu, Z. Zhou, Q. Ai, B. Sheng, and S. S. Xie, "Recent development of mechanisms and control strategies for robot-assisted lower limb rehabilitation," *Mechatronics*, vol. 31, pp. 132–145, 2015.

[46] P. Maciejasz, J. Eschweiler, K. Gerlach-Hahn, A. Jansen-Troy, and S. Leonhardt, "A survey on robotic devices for upper limb rehabilitation," *Journal of Neuroengineering and Rehabilitation*, vol. 11, no. 1, p. 1, 2014.

[47] F. J. Valero-Cuevas, V. Klamroth-Marganska, C. J. Winstein, and R. Riener, "Robot-assisted and conventional therapies produce distinct rehabilitative trends in stroke survivors," *Journal of neuroengineering and rehabilitation*, vol. 13, no. 1, p. 92, 2016.

[48] H. M. Van der Loos, D. J. Reinkensmeyer, and E. Guglielmelli, "Rehabilitation and health care robotics," in *Springer Handbook of Robotics*. Springer, 2016, pp. 1685–1728.

[49] M. Gilliaux, A. Renders, D. Dispa, D. Holvoet, J. Sapin, B. Dehez, C. Detrembleur, T. M. Lejeune, and G. Stoquart, "Upper limb robot-assisted therapy in cerebral palsy: a single-blind randomized controlled trial," *Neurorehabilitation and neural repair*, vol. 29, no. 2, pp. 183–192, 2015.

[50] K. Goto, T. Morishita, S. Kamada, K. Saita, H. Fukuda, E. Shiota, Y. Sankai, and T. Inoue, "Feasibility of rehabilitation using the single-joint hybrid assistive limb to facilitate early recovery following total knee arthroplasty: A pilot study," *Assistive Technology*, pp. 1–5, 2016.

[51] A. C. Lo, P. D. Guarino, L. G. Richards, J. K. Haselkorn, G. F. Wittenberg, D. G. Federman, R. J. Ringer, T. H. Wagner, H. I. Krebs, B. T. Volpe *et al.*, "Robot-assisted therapy for long-term upper-limb impairment after stroke," *New England Journal of Medicine*, vol. 362, no. 19, pp. 1772–1783, 2010.

[52] G. Kwakkel, B. J. Kollen, and H. I. Krebs, "Effects of robot-assisted therapy on upper limb recovery after stroke: a systematic review," *Neurorehabilitation and neural repair*, vol. 22, no. 2, pp. 111–121, 2008.

[53] B. R. Brewer, S. K. McDowell, and L. C. Worthen-Chaudhari, "Poststroke upper extremity rehabilitation: a review of robotic systems and clinical results," *Topics in stroke rehabilitation*, vol. 14, no. 6, pp. 22–44, 2007.

[54] K. Kiguchi, K. Iwami, M. Yasuda, K. Watanabe, and T. Fukuda, "An exoskeletal robot for human shoulder joint motion assist," *IEEE/ASME transactions on mechatronics*, vol. 8, no. 1, pp. 125–135, 2003.

[55] S. Freivogel, D. Schmalohr, and J. Mehrholz, "Improved walking ability and reduced therapeutic stress with an electromechanical gait device," *Journal of rehabilitation medicine*, vol. 41, no. 9, pp. 734–739, 2009.

[56] G. Colombo, M. Wirz, and V. Dietz, "Driven gait orthosis for improvement of locomotor training in paraplegic patients." *Spinal cord*, vol. 39, no. 5, 2001.

[57] M. Wirz, D. H. Zemon, R. Rupp, A. Scheel, G. Colombo, V. Dietz, and T. G. Hornby, "Effectiveness of automated locomotor training in patients with chronic incomplete spinal cord injury: a multicenter trial," *Archives of physical medicine and rehabilitation*, vol. 86, no. 4, pp. 672–680, 2005.

[58] T. G. Hornby, D. H. Zemon, and D. Campbell, "Robotic-assisted, body-weight–supported treadmill training in individuals following motor incomplete spinal cord injury," *Physical therapy*, vol. 85, no. 1, pp. 52–66, 2005.

[59] J. E. Deutsch, J. Latonio, G. C. Burdea, and R. Boian, "Post-stroke rehabilitation with the rutgers ankle system: a case study," *Presence: Teleoperators and Virtual Environments*, vol. 10, no. 4, pp. 416–430, 2001.

[60] Z. Qian and Z. Bi, "Recent development of rehabilitation robots," *Advances in Mechanical Engineering*, 2015.

[61] C. R. Carignan and H. I. Krebs, "Telerehabilitation robotics: bright lights, big future?" *Journal of rehabilitation research and development*, vol. 43, no. 5, p. 695, 2006.

[62] M. R. Schmeler, R. M. Schein, M. McCue, and K. Betz, "Telerehabilitation clinical and vocational applications for assistive technology: research, opportunities, and challenges," *International Journal of Telerehabilitation*, vol. 1, no. 1, p. 59, 2009.

[63] L. Marchal-Crespo and D. J. Reinkensmeyer, "Review of control strategies for robotic movement training after neurologic injury," *Journal of neuroengineering and rehabilitation*, vol. 6, no. 1, p. 20, 2009.

[64] M. Vasic and A. Billard, "Safety issues in human-robot interactions," in *Robotics and Automation (ICRA), 2013 IEEE International Conference on*. IEEE, 2013, pp. 197–204.

[65] J. W. Wheeler, H. I. Krebs, and N. Hogan, "An ankle robot for a modular gait rehabilitation system," in *Intelligent Robots and Systems, 2004.(IROS 2004). Proceedings. 2004 IEEE/RSJ International Conference on*, vol. 2. IEEE, 2004, pp. 1680–1684.

[66] M. Lee, M. Rittenhouse, and H. A. Abdullah, "Design issues for therapeutic robot systems: results from a survey of physiotherapists," *Journal of Intelligent and Robotic Systems*, vol. 42, no. 3, pp. 239–252, 2005.

[67] M. Girone, G. Burdea, M. Bouzit, V. Popescu, and J. E. Deutsch, "A stewart platform-based system for ankle telerehabilitation," *Autonomous Robots*, vol. 10, no. 2, pp. 203–212, 2001.

[68] "Company," claroNav. [Online]. Available: http://www.claronav.com/company/

[69] "Optoforce ltd." [Online]. Available: https://optoforce.com/

[70] J. E. Colgate and J. M. Brown, "Factors affecting the z-width of a haptic display," in *Robotics and Automation, 1994. Proceedings., 1994 IEEE International Conference on*. IEEE, 1994, pp. 3205–3210.

[71] M. Cimino and P. R. Pagilla, "Optimal location of mouse sensors on mobile robots for position sensing," *Automatica*, vol. 47, no. 10, pp. 2267–2272, 2011.

[72] R. Rojas and A. G. Förster, "Holonomic control of a robot with an omnidirectional drive," *KI-Künstliche Intelligenz*, vol. 20, no. 2, pp. 12–17, 2006.

[73] J. Robinson, J. Holland, M. Hayes, and R. Langlois, "Velocity-level kinematics of the atlas spherical orienting device using omni wheels," *Transactions of the Canadian Society for Mechanical Engineering*, vol. 29, no. 4, pp. 691–700, 2005.

Appendix A

Study Protocol

A.1   Letter Of Information and Consent Form

Here the letter of information, consent form, questionnaire and study protocol are represented. The instructions in the study protocol are used while performing experiments invloving healthy subjects.
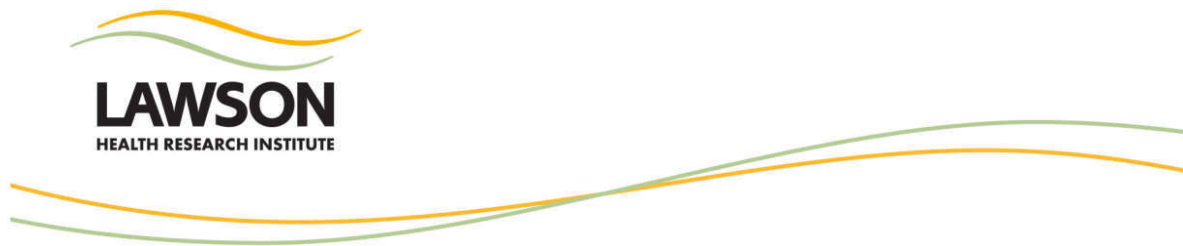
Project Title: A Novel In-home Robot-Assisted Platform for Physical Tele-Rehabilitation and Enhancing Musculoskeletal Function in Upper and Lower Limbs

Principal Investigator: Dr. Rajni V. Patel, Ph.D.

Department of Electrical and Computer Engineering & Department of Surgery
Thompson Engineering Building, Room TEB 379
Western University
and CSTAR (University Hospital - Room B7-218

Other Project Member Info:

Mahya	Shahbazi	Postdoctoral
Seyed Farokh	Atashzar	Postdoctoral
Karen	Siroen	Staff (CSTAR)
Vahid	Mehrabi	PhD Student

Funding Information:

Letter of Information

1. **Invitation to Participate**

   You are being invited to participate in a research study. It is important that you carefully read this letter of information describing the purpose of the study, what it will involve and your role in it should you decide to participate. You are being asked to participate in this study as you are a healthy volunteer and either employee or student of UWO.

2. **Purpose of the Letter**
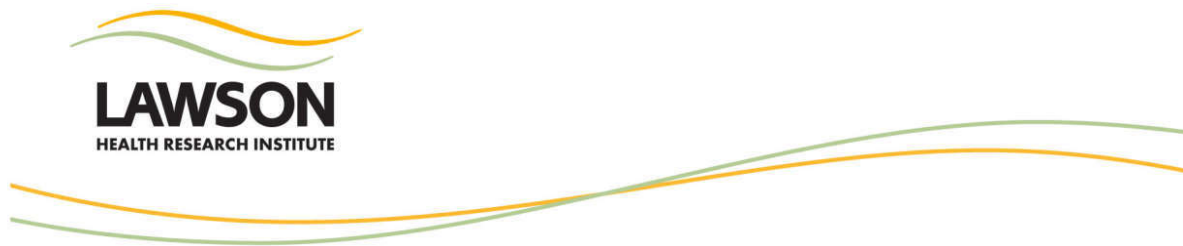
The purpose of this letter is to provide you with the information required for you to make an informed decision regarding participation in this research study.

3. Purpose of the Study

The purpose of this study is to design and develop a versatile mobile rehabilitation robot that can be used for both upper and lower limb therapy on patients suffering from neuromuscular trauma such as hemiparesis. Toward this end, a prototype of the robot has been designed and implemented. The next phase of the study is to conduct pilot user trials involving healthy participants to collect quantitative measurements and qualitative feedback on various aspects of the device such as the level of comfort, ease of use, responsiveness, computer interface, etc. The data collected in the pilot phase will be used to optimize the robot design for further studies involving patients.

4. Inclusion Criteria

You may participate in this study if:

1. You are a healthy subject greater than or equal to 18 year of age with a body weight of 50 kg to 120 kg and a height of 160 cm to 200 cm, and;
2. You give written informed consent.

5. Exclusion Criteria

You may not participate in the study if you are suffering from osteoarthritis, have a previous history of stroke, Spinal Cord Injuries or paralysis.

6. Study Procedures

If you agree to participate, you will be scheduled based on your times of availability. A MYO band will be attached to your limb (arm or leg) prior to the experiment to measure EMG signals of the muscles in that limb. The MYO band is a passive sensorized band (similar in size to a runner's elastic armband used to attach cell phones to their arms) with electrodes used by athletes and measures the muscle's contraction level. The data will be used to measure the level of muscle activity during each task. It should be noted that the MYO band is a passive device (with no actuation) and measures EMG signals of muscles and the acceleration of the limb. After attaching the MYO band, you will be asked to seat
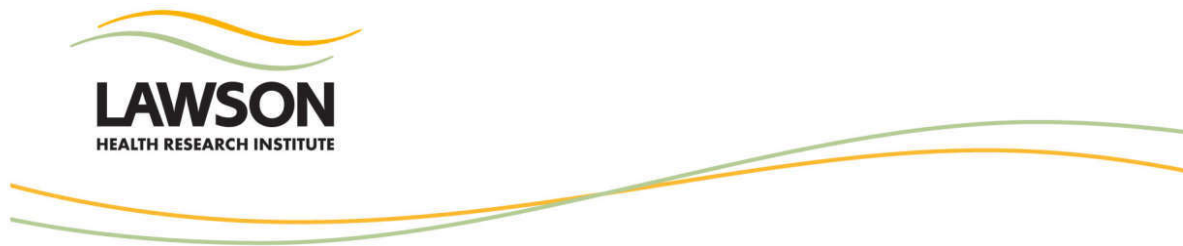
on a chair behind a table or near a ground-level mat. For the upper limb therapy, the robot will be placed on a table and then you will be asked to grasp the handle of the robot. For the lower extremity therapy, the robot will be placed on a specific mat on the ground level and your foot will be placed on the footplate on top of the robot.

Then you will be asked to perform different tasks according to the therapy modes-passive, active, active assistive and active resistive modes. For example, one task could be to move the end-effector of the robot freely using your hand or foot to measure the corresponding muscle actuation for various limb movements.

Later you will be asked to fill out a questionnaire that includes task-related questions to evaluate the perception of the subjects. The questionnaire will include the following questions: (a) How would you rate your comfort level when using the device in terms of safety, interaction force, ergonomics with regard to the footplate and handle? (b) How would you rate the resistance of the robot in its non-actuated mode? (c) How would you rate the force applied by the robot compared to your maximum force capability? (d) How would you rate the tasks in order of the need for accuracy of muscle control?

It is anticipated that the entire task will take a maximum of 2 hours over 2 sessions. The task(s) will be conducted on the 8th floor of CSTAR, University Hospital. There will be a total of 30 participants

7. Possible Risks and Harms

There are no known or anticipated risks or discomforts associated with participating in this study.

8. Possible Benefits

You may not directly benefit from participating in this study. Although, as this project focuses on the design of advanced application-oriented systems for post-stroke rehabilitation based on the latest developments in robotics, human-in-the-loop haptics, and multi-modal sensorimotor integration, this will benefit to society as a whole.

9. Compensation

You will not be compensated for your participation in this research.

10. Voluntary Participation

Participation in this study is voluntary. You may refuse to participate, refuse to answer any questions or withdraw from the study at any time with no effect on your status with CSTAR or Western University.

11. Confidentiality

The data provided by you will be kept confidential. Data will be stored and locked in a cabinet at CSTAR and will only be viewed by the research team. To protect your privacy, a unique study number will be assigned to your experimental data. A list linking your study number with your name will be kept by the Principal Investigator in a secure place, separate from the experimental data. No information that discloses your identity will be collected. Representatives of the Lawson Health Research Institute and the University of Western Ontario Health Sciences Research Ethics Board may contact you or require access to your study-related records to monitor the conduct of the research.

12. Contacts for Further Information

If you have any questions or concerns regarding participation in this study, please contact Dr. Rajni V. Patel, Principal Investigator, at

If you have any questions about your rights as a research participant or the conduct of this study, you may contact The Office of Research Ethics   , email:
                        . You may also contact Dr. David Hill, Scientific Director, Lawson Health Research Institute at

A copy of this letter of information and consent form is yours to keep for your personal records.

13. Publication

If the results of the study are published, your name will not be used. If you would like to receive a copy of any potential study results, please provide your name and contact number on a piece of paper separate from the Consent Form.

14. Commercialization

Please note that Western University and the PI intend to claim sole ownership of any research results consistent with this consent. By signing this consent, you agree that Western University and the PI can apply for patents and you will not receive any financial benefit that might result from the outcome of this research.

15. Consent

<u>Written Consent</u>

This letter is yours to keep for future reference.

<u>**Consent Form**</u>

Project Title: A Novel In-home Robot-Assisted Platform for Physical Tele-Rehabilitation and Enhancing Musculoskeletal Function in Upper and Lower Limbs

Study Investigator's Name: Dr. Rajni V. Patel

I have read the Letter of Information, have had the nature of the study explained to me and I agree to participate. All questions have been answered to my satisfaction.

Are you willing to be contacted regarding participation in future studies?

☐   Yes   ☐   No

Participant's Name (please print):   _____

Participant's Signature: _____

Date: _____

Person Obtaining Informed Consent (please print):   _____

Signature: _____

Date: _____

Project Title: A Novel In-home Robot-Assisted Platform for Physical Tele-Rehabilitation and for Enhancing Musculoskeletal Function in Upper and Lower Limbs

Questionnaire

Pre-task Questions:

I.   What is your level of experience in interaction with robotic systems?

1	2
No previous experience	Previous experience

II.   How old are you?

1	2	3	4	5
< 20 years	20-25 years	25-30 years	30-35 years	>35 years

III.   How much do you weigh?

Weight	kg
	lb

IV.   How tall are you?

Height	cm
	ft

V.   Which is your dominant hand (right/left/ambidextrous)

1	2	3
right	left	ambidextrous

VI.   Do you have pain or discomfort in your muscles or joints?

1   2   If yes, please explain:
Yes   No

Post-task Questions:

VII.   How would you rank your level of comfort with the handle?

1   2   3   4   5
not comfortable   slightly   comfortable   very   extremely
at all   comfortable   comfortable   comfortable

Suggestions to increase the comfort level of the handle:

VIII. How would you rank your level of comfort with the footplate?

1   2   3   4   5
not comfortable   slightly   comfortable   very   extremely
at all   comfortable   comfortable   comfortable

Suggestions to increase the comfort level of the footplate:

IX.   How would you rank your level of comfort with the setup in general?

1   2   3   4   5

| not comfortable at all | slightly comfortable | comfortable | very comfortable | extremely comfortable |

X. How would you rank your level of motivation in performing the tasks?

| 1 | 2 | 3 | 4 | 5 |
| not motivated at all | slightly motivated | motivated | very motivated | extremely motivated |

XI. How was your level of control over the device while performing the tasks?

| 1 | 2 | 3 |
| No control | Moderate control | Full control |

XII. Did you have any concern when using the robot?

| 1 | 2 | If yes, please explain: |
| Yes | No | |

XIII. How clear were the descriptions of the tasks?

| 1 | 2 | 3 |
| Not clear at all | Slightly confusing | Clear |

If unclear or confusing, please explain:

XIV. How much resistance from the robot did you feel during the non-actuated mode of operation?

| 1 | 2 | 3 | 4 | 5 |
| extremely resistant | very resistant | moderately resistant | slightly resistant | no resistance at all |

XV. How powerful did you perceived the robot to be (in terms of force exertion capability) compared to your arm/leg muscle strength?

1	2	3	4	5
extremely powerful	very powerful	moderately powerful	slightly powerful	not powerful at all

XVI.   How do you rate your motion accuracy while using the robot?

1	2	3	4	5
extremely accurate	very accurate	moderately accurate	slightly accurate	not accurate at all

Additional Comments:

Test Protocol on Healthy Subjects - Summer 2017

A. Run the VR
B. Assign an ID to the participant
C. Fill the information in Questionnaire
D. Attach the EMG sensors
E. Run Trigno Control Utility to see the active sensors
F. Run EMG_DataCollection_UDP_2017
G. Initialize and start the EMG sensors data transfer through UDP
H. Run the proper MATLAB code
I. Follow the instruction of the tests

| Sequence of attaching EMG sensors |
| --- |
| 1   Clean the skin with alcohol |
| 2   Follow the procedure on attaching the EMG sensors |
| 3   UE:

Bicep, EMG1 |

Triceps long head, EMG2
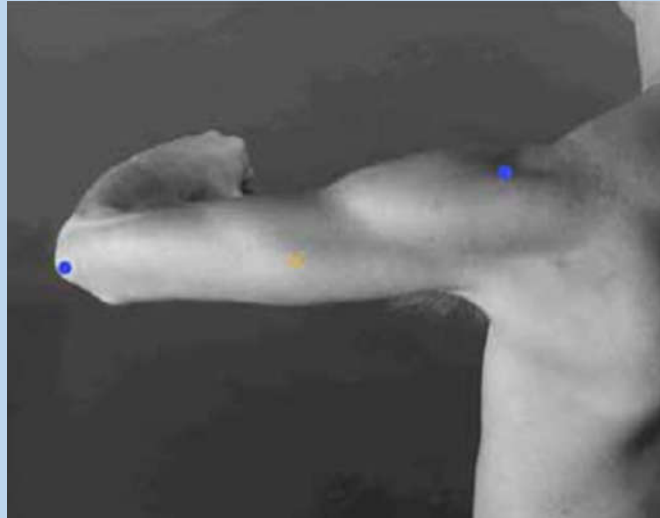
Triceps short head, EMG3

Movements of the wrist

| Movement	Joint	Muscle
Flexion	Midcarpal	Flexor carpi ulnaris, Flexor carpi radialis
Extension	Radio-carpal	Extensor carpi radialis longus & brevis, Extensor carpi ulnaris
Adduction	Radio-carpal	Flexor carpi ulnaris & extensor carpi ulnaris
Abduction	Midcarpal	Flexor carpi radialis & extensor carpi radialis

Flexor Carpi Ulnaris, EMG4
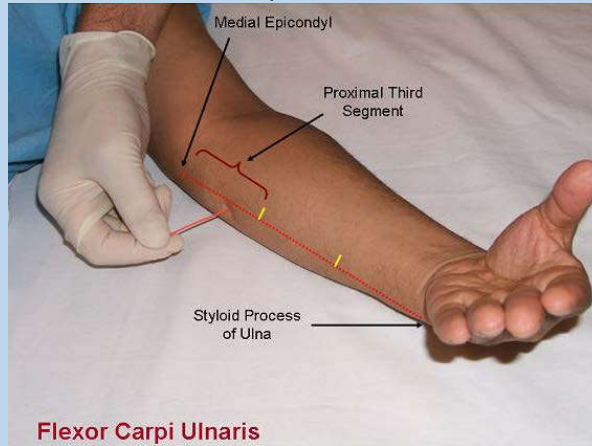
Flexor Carpi Radialis, EMG5
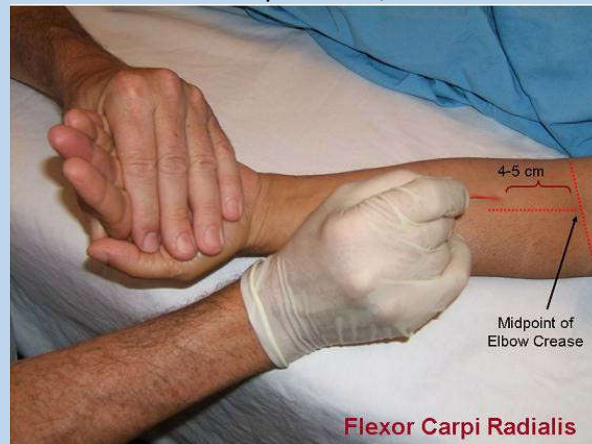
Extensor Carpi Radialis Longus, EMG6
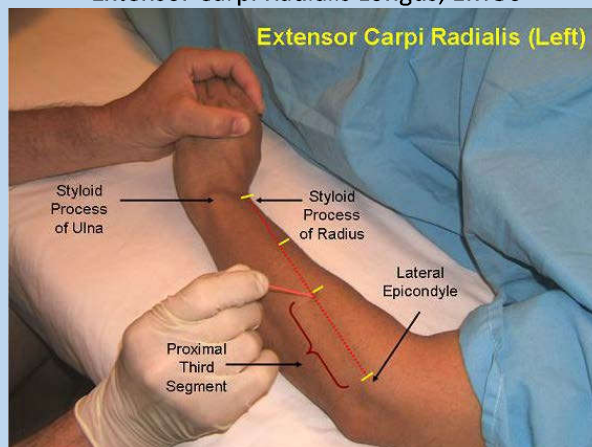
Extensor Digitorum Communis, EMG7
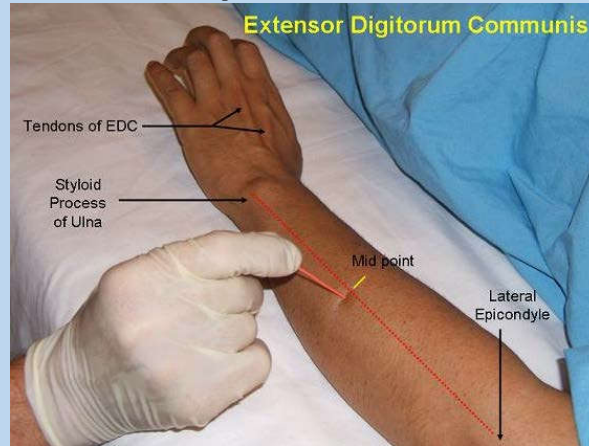
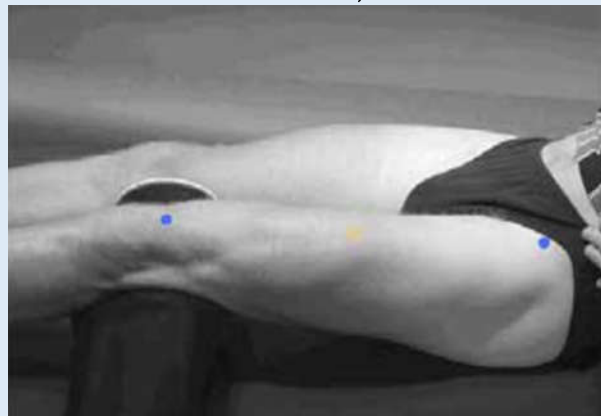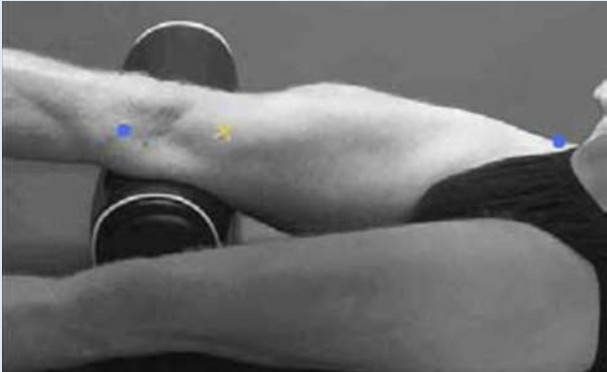### Flexor Digitorum Profundus , EMG8
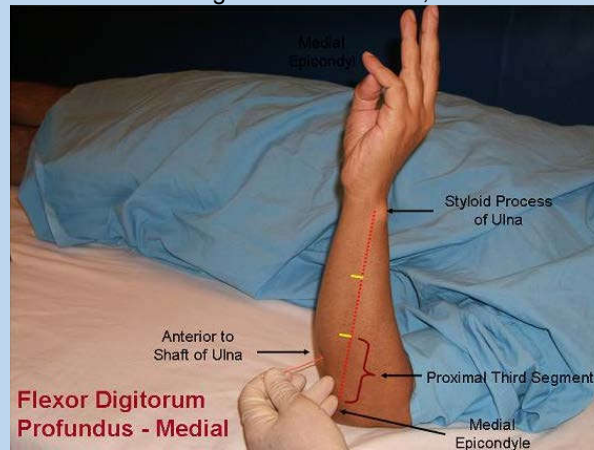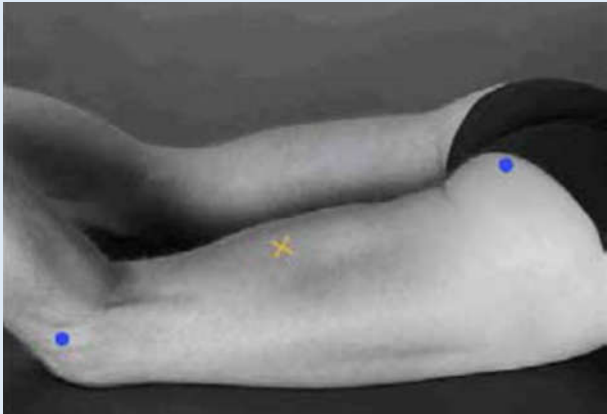

LE:
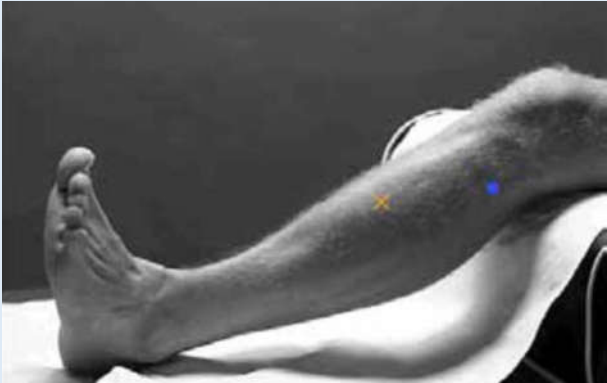### Rectus Femoris, EMG9

Vastus Medialis, EMG10

Vastus Lateralis, EMG11

Biceps Femoris, EMG12

Tibialis Anterior, EMG13

Soleus, EMG14

Gastrocnemius Medialis, EMG15

Gastrocnemius Lateralis EMG16

- Use the Trajectory MATLAB Code

Sequence of the Process for Task 1 (Following Trajectory)	
1	Make the subject familiar with the device
2	Explain the task (Try to move toward the green squares along the line)
3	Adjust the seat level so they can freely move the leg or arm
4	Place the feet on top of the robot and tighten the strap
5	Ask to follow the robot's move toward the green square (Apply as much voluntary motion as they want)

- Use the Assistive MATLAB Code

Sequence of the Process for Task 2 (Assistive Mode)	
1	Make the subject familiar with the device
2	Explain the task (Try to move toward the green squares along the line)
3	Ask them to move their leg toward the green square in a controlled way, as they are in charge of the motion. The robot will help them in performing the task by magnifying their applied force

Sequence of the Process for Task 3 (Idle Mode)	
1	Make the subject familiar with the device
2	Explain the task (Try to move toward the green squares along the line)
3	Ask them to move their leg toward the green square in a controlled way, as they are in charge of the motion. The robot will not help them as it is not actuated.

- Use the MATLAB Code Experiment A

Sequence of the Process for Task 4 (Resistive Mode A)	
1	Make the subject familiar with the device
2	Explain the task

	(Try to apply disturbance while the robot moves)
3	The robot will follow the motion to complete the tasks, They should try to resist in the direction of motion and apply disturbance in other directions.

- Use the MATLAB Code Experiment C

Sequence of the Process for Task 5 (Resistive Mode B)	
1	Make the subject familiar with the device
2	Explain the task (Try to move toward the green squares along the line)
3	Ask them to move their leg toward the green square in a controlled way, and resist the disturbance applied by the robot, as they oversee the tasks and providing the motion. The robot will prevent them in completing the tasks

VAHID MEHRABI

Education

M.Sc. Candidate, Biomedical Engineering   Western University · London, ON, Canada · **9/2015–present**

Thesis Project: "Design, Implementation and Control of a Robotic Platform for Post-Stroke Upper- and Lower-Limb Rehabilitation"

Supervisors: Prof. R.V. Patel and Prof. H.A. Talebi

B.Sc., Mechanical Engineering   Tehran Polytechnic · Tehran, Iran ·   **9/2005–4/2010**

Research Project: "Modeling and vibration analysis of unbalanced and misaligned rotor-ball bearing system"

Supervisor: Prof. A.R. Ohadi

Industry Experience

Co-Founder and Chief Mechanical Designer   Kaveh Robot Sanat Sharif Ltd. · Tehran, Iran ·   **7/2012–7/2015**

Multiple projects on automation process of glass production lines including a pick and place robot for painting various glass products and a paper box folding machine for the assembling section

Research Experience

Research Assistant, CSTAR   Western University · London, ON, Canada · **9/2015–present**

- Sensorization of the da Vinci surgical instrument for haptic force measurement

- Designing, dynamic analyzing, and manufacturing of 5 DOF mobile platform for lower- and upper-limb robotic rehabilitation

- Sensorizing joints for position measurement in the RAVEN surgical robot

- Modeling and FE analyzing of a magneto-rheological(MR) clutch for various haptic applications

- Research Ethics application for experimental trials of the novel robotic-assisted platform for physical rehabilitation on stroke patients

Research Assistant, Real-time systems Lab   Dept. of EE, Tehran Polytechnic · Iran · **5/2012–9/2014**

- Designing, dynamic analyzing, and manufacturing of a wrist rehabilitation module

- Designing, dynamic analyzing, and manufacturing of 9 DOF Beating Heart surgery module

- Designing and manufacturing a CanSat module for Eaglesat team, 8th International CanSat competition

Leader and Mechanical Designer, Parsian Robotic Lab   Tehran Polytechnic · Iran · **5/2011–9/2013**

- Designing, analyzing, and manufacturing a team of small-size soccer robots.

Honor and Awards

- Western Graduate Research Scholarship (WGRS),   **9/2015–present**

- Ranked **2nd** as a member of Eaglesat team at 8th International CanSat Competition Texas USA **6/2013**

- Ranked **1st** in Small Size Soccer League (technical challenge) RoboCup 2012 **7/2012**

- Ranked **4th** in Small Size Soccer League RoboCup 2012 **7/2012**

- Ranked **6th** in the nationwide university entrance exam in Mechanical Engineering, Iran **7/2010**

- Granted entry to M.Sc. program and 10% honor student in Mechanical Engineering, Tehran Polytechnic **9/2009**

Internships

Intern, Iran Khodro Powertrain Company(IPCO) · Tehran, Iran · **9/2009–1/2010**

- Learning and operating the ***Excite AVL workspace v4*** (a special software for designing Internal Combustion(IC) engines) with direct report to the powertrain design manager

Graduate Courses

Biomedical Engineering Program Western University · London, ON · **9/2015–6/2017**

- Advanced Medical Mechatronics
- Graduate Seminar
- Research Ethics and Bio-statistics
- Human and Animal Biomechanics
- Principles of Communication and Knowledge Transfer

Teaching Experience

Teaching Assistant Western University · London, ON · **9/2015–6/2017**

- Programming Fundamentals for Engineers - Computational Methods for Engineers
- Introductory Design and Innovation

Volunteer Experiences

Judge at First Robotic Competition   Western University · London, ON ·   **3/2017**

Volunteer at Science Olympics Competition   Western University · London, ON ·   **4/2017**